
This manuscript is a preprint and has been submitted for publication in **Paleoceanography and Paleoclimatology**. Please note that, despite having undergone peer review, the manuscript has yet to be formally accepted for publication. Subsequent versions of this manuscript may have slightly different content. If accepted, the final version of this manuscript will be available via the 'Peer-reviewed Publication DOI' link on the right-hand side of this webpage. Please feel free to contact any of the authors; we welcome feedback.

Paleoclimate Changes in the Pacific Northwest Over the Past 36,000 Years from Clumped Isotope Measurements and Isotope-Enabled Model Analysis

Ricardo Lopez-Maldonado^{1,2}, Jesse Bloom Bateman^{2,3}, Andre Ellis¹, Nicholas E. Bader⁴, Pedro Ramirez¹, Alexandra Arnold², Osinachi Ajoku⁵, Hung-I Lee^{2,6}, Gregory Jesmok^{2,7}, Deepshikha Upadhyay², Bryce Mitsunaga^{2,8}, Ben Elliott², Clay Tabor⁹, and Aradhna Tripathi^{2,10}

¹*Department of Geoscience and Environment, California State University, Los Angeles, CA, U.S.A.*

²*Department of Atmospheric and Oceanic Sciences, Department of Earth, Planetary, and Space Sciences, Institute of the Environment and Sustainability, Center for Diverse Leadership in Science, American Indian Studies Center, University of California, Los Angeles, CA, U.S.A.*

³*Department of Biology, SUNY Cortland, Cortland, NY, U.S.A.*

⁴*Department of Geology, Whitman College, Walla Walla, WA, U.S.A.*

⁵*National Center for Atmospheric Research, Boulder, CA, U.S.A.*

⁶*Department of Geophysical Sciences, University of Chicago, Chicago, IL, U.S.A.*

⁷*Department of Geology, California State University, Northridge, CA, U.S.A.*

⁸*Department of Geology, Brown University, Providence, RI, U.S.A.*

⁹*Department of Geography, University of Connecticut, Storrs, CT, U.S.A.*

¹⁰*UMR6538 Géosciences Océan, Institut Universitaire Européen de la Mer, Technopôle Brest-Iroise, Plouzané, 29280, France*

Corresponding authors: Ricardo Lopez-Maldonado and Aradhna Tripathi (ricardolopez9080@gmail.com and atripati@g.ucla.edu)

Key Points:

1. Warming and water isotope variations inferred from clumped isotopes are qualitatively similar to transient climate model simulations
2. Amount of warming was about three times the global average and is likely due to the proximity of site to ice margin during OIS 3 and LGM
3. Model analysis indicates $\delta^{18}\text{O}$ depletion in this location at the LGM is largely a result of the North American ice sheets

32 **Abstract**

33 Since the last glacial period, North America has experienced dramatic changes in regional
34 climate, including the collapse of ice sheets and changes in effective precipitation. We use
35 clumped isotopes and analysis of transient climate simulations to provide constraints on
36 hydroclimate changes in the Pacific Northwest. The coldest soil temperatures ($\sim 10.5 \pm 1.0^\circ\text{C}$ to
37 $14.9 \pm 1.2^\circ\text{C}$) occurred $\sim 34,000$ – $23,000$ years ago. Glacial warm average monthly temperatures
38 ($\sim 1^\circ\text{C}$) and mean annual air temperature ($\sim 9^\circ\text{C}$) indicate regional warming of $20.1 \pm 2.6^\circ\text{C}$ was
39 about three times the global average. Proxy data confirm the boundary of the cooler anticyclone
40 induced by LGM ice sheets, and the warmer cyclone in the Eastern Pacific Ocean. Model
41 analysis suggests regional amplification is due to the proximal location of the study area to the
42 Laurentide Ice Sheet margin and the impact of the glacial anticyclone on the region, as well as
43 local albedo. Isotope-enabled model experiments indicate variations in water $\delta^{18}\text{O}$ largely reflect
44 circulation changes, with westerly winds and associated storm tracks bringing more depleted
45 vapor to the region during the LGM.

46 **1 Introduction**

47 Proxy records and climate models show that variations in insolation, greenhouse gas
48 levels, the distribution of ice sheets, and other processes have driven changes in climate,
49 including glacial-interglacial cycles (COHMAP members, 1988; Weaver et al., 1998; Mix et al.,
50 2001; Lisiecki and Raymo, 2005). Studies examining sediments from different regions of North
51 America have shown that between the Last Glacial Maximum (LGM; $\sim 23,000$ – $19,000$ years ago
52 or ka) and the early Holocene (beginning 11 ka), there were dramatic environmental changes
53 including the collapse of the Cordilleran Ice Sheet (CIS) and Laurentide Ice Sheet (LIS), the
54 drying out of major lake systems in the southwestern US and Great Basin regions, and increased
55 effective precipitation in the Pacific Northwest (Lyle, et al., 2012; McDonald et al., 2012;
56 Whitlock et al., 1992). However, despite decades of study, our ability to quantify and understand
57 terrestrial climate variability in this region and other mid-latitude areas has been limited, largely
58 because of ambiguous reconstructions, and disagreement between reconstructions and
59 simulations.

60 Two promising tools for studying terrestrial hydroclimates are carbonate clumped isotope
61 thermometry and isotope-enabled climate models. Recent work has shown that carbonate

62 clumped isotope thermometry can constrain the growth temperatures of carbonate minerals
63 without a priori knowledge of other environmental factors such as water $\delta^{18}\text{O}$ (Passey et al.,
64 2010; Eiler, 2011; Eagle et al., 2013). Additionally, clumped isotope-derived growth
65 temperatures can be combined with carbonate oxygen isotope measurements to determine the
66 $\delta^{18}\text{O}$ of formation waters. Isotope-enabled climate model simulations offer the ability to track
67 processes impacting the water cycle via fractionations of oxygen and hydrogen isotopes
68 (LeGrande and Schmidt, 2008; Roberts et al., 2011; Zhu et al., 2017; Brady et al., 2019).

69 In this study, we use clumped isotope thermometry and $\delta^{18}\text{O}$ isotope measurements of
70 glacial and deglacial pedogenic carbonates from the Palouse loess with isotope-enabled
71 simulations to examine the evolution of temperature and precipitation in the Pacific Northwest.
72 The region examined is in the Columbia Basin province in eastern Washington. We chose this
73 region because it was directly affected by the Purcell lobe of the CIS during the Last Glacial
74 Maximum (LGM), and thus provides critical constraints on potential climate responses to
75 circulation changes induced by the collapse of the ice sheet (Lora et al., 2016).

76 Since soils form from parent material by pedogenic processes that depend on localized
77 terrestrial conditions (e.g., precipitation and heat flux) during the time of soil formation (Bader et
78 al., 2015; Sheldon and Tabor, 2009), paleosols have been used extensively to directly infer past
79 climates. In particular, different proxy measurements of pedogenic carbonates have extensively
80 been used as archives of paleoclimate data (Cerling, 1984; Breecker et al., 2009; Sheldon and
81 Tabor, 2009; Passey et al, 2010; Peters et al., 2012; Quade et al, 2012; Eagle et al., 2013).
82 Because calcic paleosols are characterized by the presence of a prominent Bk horizon, which
83 forms over hundreds to thousands of years, their chemical composition is a function of
84 equilibrium, and short-term climatic volatility does not overprint the long-term conditions (e.g.,

85 regional cooling due to volcanism; Peters et al., 2012; Sheldon and Tabor, 2009). With the
86 Palouse loess, we are able to build on prior work in this region examining controls on the stable
87 isotopic composition of paleosols (Passey et al., 2010; Takeuchi et al., 2009; Lechler et al.,
88 2018).

89 The chronology of the Palouse loess has been well constrained, and for this work, we
90 investigated the Washtucna paleosol that formed during the middle to late Wisconsin (~40 to 17
91 ka); and the Sand Hills Coulee that formed either during the Younger Dryas to early Holocene
92 (~13 to 11 ka) or the relatively warm and dry Holocene Climatic Optimum (HCO; ~11 to 7 ka)
93 (Berger and Busacca, 1995; Richardson et al., 1997; Blinnikov et al., 2002; Sweeney et al., 2005;
94 Spencer and Knapp, 2010). In addition to reconstructing past temperature and water isotope
95 changes, we utilize model simulations to investigate the likely factors influencing regional
96 climate variations.

97 Our study had several objectives: (i) to reconstruct carbonate formation temperatures
98 using carbonate clumped isotopes; (ii) to derive mean annual air temperatures (MAAT) and
99 warmest average monthly temperatures (WAMT) using air temperature transfer functions
100 developed by Quade et al. (2012) and compare these to modern and simulated regional MAAT
101 and WAMT; (iii) to use paleotemperature results obtained from the Sand Hills Coulee paleosol
102 to test if it formed during the Holocene Climatic Optimum (HCO); (iv) to compare reconstructed
103 climate parameters to climate model simulations, including those from the Paleoclimate
104 Modeling Intercomparison Project Phases 3 & 4 (PMIP3 & PMIP4) and the Transient Climate
105 Evolution of the Last 21,000 Years (TraCE-21k) project (Liu et al., 2009), in order to identify
106 unresolved model biases and a suitable model for the region; and (v) to track the source of local
107 precipitation using both proxy temperature and soil water $\delta^{18}\text{O}$ reconstructions and the stable

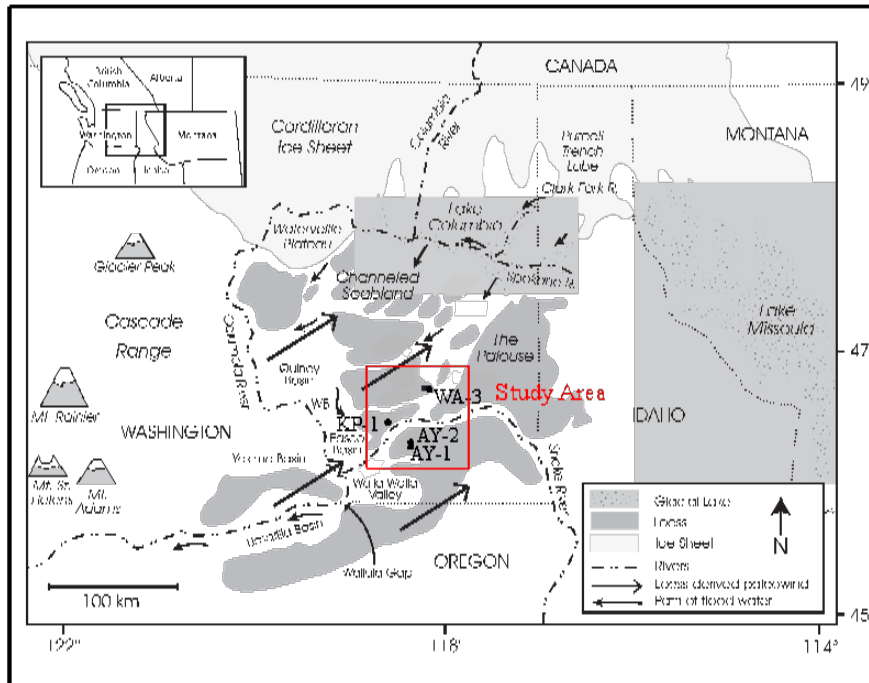
108 water isotope-enabled version of the Community Earth System Model (iCESM1.2; Brady et al.
109 2019).

110

111 **2. Background**

112 The study area is within an 80 km² region at 46 °N, 118 °W with an average elevation of
113 420 meters above average mean sea level in eastern Washington (Figure 1). The Palouse region
114 currently experiences a temperate climate with a mean annual temperature of 10.9 °C and a
115 summer average temperature of 21.2 °C; mean annual precipitation is 280 mm with the majority
116 occurring in winter (PRISM Climate Group, 2018). Paleosol sites include AY-1 (i.e. CLY-2 site
117 in Busacca and McDonald, 1994), AY-2 (i.e. CLY-1 site in Busacca and McDonald, 1994), KP1,
118 and WA-3 (i.e. Busacca's [1989] roadcut). Whitlock et al. (2000) and Blinnikov et al. (2002)
119 compiled a terrestrial climate record of the region using a pollen record from Carp Lake and a
120 phytolith record from the Palouse loess, which provide context for this work. In addition, Dyke
121 et al. (2002) describes the LIS and CIS margin advance and retreat. A composite ice sheet was
122 created for the Coupled Model Intercomparison Project Phase 5 experiments by combining
123 information from three reconstructions of the distribution of ice mass because direct evidence of
124 the distribution does not exist (ICE-6G v2.0: Argus and Peltier, 2010; GLAC -1a: Tarasov et
125 al., 2012; ANU: Lambeck et al., 2010).

126 Prior work has shown that the Palouse experienced cool, temperate, dry conditions during
127 the early-mid-Wisconsin (~42.9 to 30.9 ka), a point in time when the LIS margin was near the
128 boundary of the Canadian Shield and the CIS remained small (Dyke et al., 2002). Towards the
129 end of Oxygen Isotope Stage (OIS) 3 (36 to 27.6 ka) and the early stages of OIS 2 (beginning in
130 27.6 ka; Martinson et al., 1987), the LIS margin approximately followed the boundary of the
131 Canadian Shield and began its advance to its maximum extent (Dyke et al., 2002). The LIS
132 margin advanced to its late OIS 2 limit in the northwest, south, and northeast (i.e. south of the of
133 the Great Lakes) about 24-23 ka and in the southwest and far north about 21-20 ka (Dyke et al.,
134 2002). It remained near that limit until ~17 ka, while the CIS remained limited (Clark and Mix,
135 2002; Dyke et al., 2002).



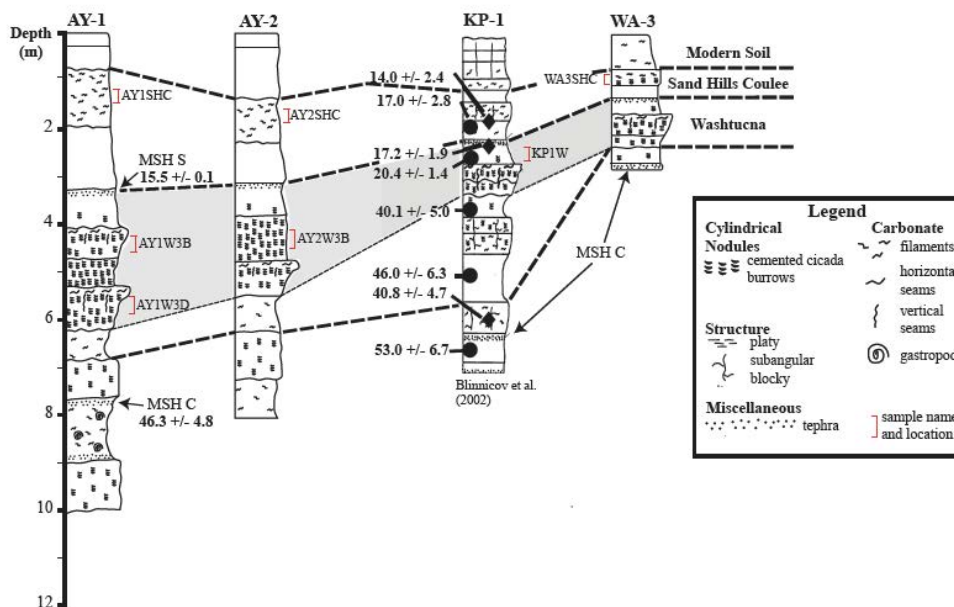
136

137 **Figure 1.** Locality map. Map of the Pacific Northwest showing the site locations within the
 138 context of glacial lake Missoula-Channeled Scabland system, the Cordilleran ice sheet at its Late
 139 Wisconsin maximum, loess deposits, prevailing winds, and generalized flow directions (as
 140 described in McDonald et al., 2012).

141 As the LIS retreated, the CIS advanced to its maximum extent at about 15-14 ka (Booth
 142 et al., 2003; Clark and Mix, 2002; Dyke et al., 2002; Whitlock, 1992). During this period (~30.9
 143 to 15 ka), the Palouse experienced cold, dry conditions; in addition, the late Wisconsin Glacial
 144 Lake Missoula (15.7-13.5 ka) was created by an ice dam formed by the Purcell Trench lobe of
 145 the CIS (Blinnikov et al., 2002; Booth et al., 2003; Whitlock et al., 2000). Near the end of OIS 2
 146 and the beginning of OIS 1 (14 ka; Martinson et al., 1987), the climate in the Palouse began to
 147 transition into a cooler and wetter climate that persisted throughout the late glacial period (~14 to
 148 11 ka; i.e., the Younger Dryas to early Holocene), progressing to a warmer and drier climate than
 149 the modern that persisted throughout the HCO (~11 to 7 ka).

150 The Palouse loess was likely sourced from slackwater sediments deposited during glacial
 151 outburst floods in basinal areas (i.e. Pasco Basin and Walla Walla Valley to the south and
 152 southwest, especially near Wallula Gap) (Bader et al., 2016; Sweeney et al., 2007; McDonald
 153 and Busacca, 1992; Spencer and Knapp, 2010). These floods were created from the rapid
 154 emptying of Glacial Lake Missoula by recurring hydraulic instability (Booth et al., 2003). After
 155 the deposition of slackwater sediments, prevailing southwesterly wind transported these deposits

156 from the basinal areas onto the surrounding Palouse hills (McDonald et al., 2012; Sweeney et al.,
 157 2007). Times of decreased eolian dust production may have allowed episodes of soil formation
 158 in the loess, which appear to have occurred primarily during full glacial conditions when the
 159 North American ice sheets produced a glacial anticyclone resulting in weakened westerly winds
 160 (Bartlein et al., 1998; Sweeney et al., 2004). The slowing loess transportation and deposition
 161 process promoted calcic soil formation in spite of a cold climate (Sweeney et al., 2004). Dust
 162 production decreased up to five-fold (~ 6 cm/yr) from 35 ka to 15 ka and increased afterwards to
 163 a rate greater than 20 cm/yr (Sweeney et al., 2004).
 164



174 **Figure 2.** Pedostratigraphic columns with sampled locations, and sedimentation rate estimates.
 175 Thermoluminescence loess ages are in thousands of years (circles from Berger and Busacca,
 176 1995 and diamonds from Richardson et al., 1997, 1999). The Mt. Saint Helens set S and C
 177 (MSH) tephra ages are in thousands of years. Sedimentation rate estimates from 35 ka to 15 ka
 178 (highlighted in gray) are estimated at approximately 6 cm per year, and before and after this
 179 interval, are estimated to be >20 cm per year (Sweeney and Busacca, 2004). KP-1 was modified
 180 from Blinnicov et al. (2002), and WA-3 was modified from Busacca (1989).

181 The entire Palouse loess spans the Pleistocene and Holocene (Busacca, 1989; Berger and
 182 Busacca, 1995; Blinnicov et al., 2002; Richardson et al., 1997; 1999; Spencer and Knapp, 2010).
 183 Table S1 summarizes chronologic constraints. Different sections of the Palouse loess have been
 184 dated using a range of techniques, including paleomagnetism, radiocarbon, and
 185 thermoluminescence. Two markers (i.e. Cascade-sourced tephras and distinct carbonate
 186 paleosols like the Washtucna and the Old Maid Coulee paleosols) were used in the field to

187 correlate horizons that have not been dated at sites being investigated in this study (McDonald et
188 al., 2012; Spencer and Knapp, 2010). In addition, estimated sedimentation rates from Sweeney et
189 al (2004) were applied between datums to estimate the age of horizons lacking an absolute age
190 date. In summary, (Figure 2), the main dated tephra layers for the sites being investigated include
191 the Mt. Saint Helens set C (MSH C; cal. 46.3 +/- 4.8 ka), and Mt. Saint Helens set S (MSH S;
192 cal. 15.4 +/- 0.1 ka; Sweeney et al. 2005; McDonald et al., 2012). Surrounding sites, not
193 investigated in this study, either contain the Glacier Peak tephra (cal. 11.6 +/- 0.05 ka), or the
194 Mazama Ash (cal. 7.6 +/- 0.1 ka; Sweeny et al. 2005; McDonald et al., 2012). Additional age
195 control is provided from thermoluminescence dating of quartz and feldspar grains (Berger and
196 Busacca, 1995; Richardson et al., 1997; 1999). Thermoluminescence age on the lower boundary
197 of the Washtucna paleosol is 40.1 +/- 3.7 ka, and an age for the upper boundary is 17.2 +/- 1.9 ka
198 (Richardson et al., 1997; 1999). A thermoluminescence age on the lower boundary of the Sand
199 Hills Coulee paleosol is 14.0 +/- 2.4 ka (Richardson et al., 1997); however, the upper boundary is
200 not well constrained, and appears to possibly extend into the HCO.

201

202 **2 Materials and Methods**

203 2.1 Field Methods

204 The sites were prepared for sampling by excavating all visibly weathered or modern
205 material from the surface of the soil profile in order to expose comparatively unaltered loess
206 (Bader et al., 2015). The sites are not described in this study because detailed descriptions
207 already exist from previously published literature (Busacca, 1989; McDonald and Busacca,
208 1992; Busacca and McDonald, 1994). Carbonate development in the field was assessed based on
209 visible calcic features and sample effervescence in 5% HCl. Micrite and microsparite field
210 samples were segregated from horizontal and vertical carbonate seams and used for clumped
211 isotope analysis (supplementary information). In addition, two supplemental analyses were used
212 to discriminate pedogenic carbonate from detrital carbonate (supporting information; Figure S1-
213 S6; Table S2).

214 2.2 Calculation of Isotopic Ratios and Temperatures

215 Detailed methods are in the supplementary information. Powdered paleosol samples were
216 measured on a modified MAT 253 gas-source IRMS mass spectrometer with both equilibrated

217 gas and carbonate standards measured, using methods described elsewhere (Defliese and Tripathi,
218 2020). 25 and 1000 °C gas standards were measured, along with ETH 1-4 standards, and a suite
219 of in-house carbonate standards. Data are reported using the Brand parameter set (Daeron et al.,
220 2016) and on the absolute reference frame (Dennis et al., 2010). An 0.082‰ acid fractionation
221 factor was added to samples (Defliese et al., 2015) which has been shown to yield accurate
222 results based on prior work in this lab (Defliese and Tripathi, 2020; Uphadhyay et al., in review).
223 The temperature calibration of Bernasconi et al. (2018) was used for calculating
224 paleotemperatures, and the carbonate-water oxygen-isotope calibration relationship of Kim and
225 O'Neil (1997) was used for reconstructing water $\delta^{18}\text{O}$. Calculated soil carbonate formation
226 temperatures (referred to as $T(\Delta_{\text{c}})$ or T_{c}) were then used to reconstruct MAAT and WAMT by
227 using the relationship published by Quade et al. (2012). Uncertainties in $T(\Delta_{\text{c}})$, MAAT, and
228 WAMT errors are reported as one standard error and represent propagated external errors,
229 following conventions from several studies (Passey et al., 2010; Eagle et al., 2013).

230 2.3 Model Simulations

231 We compared data to simulations from 9 PMIP3 models and 4 currently available PMIP4
232 models (Braconnot et al., 2012) to assess the regional climate in these simulations. We compared
233 reconstructed glacial to modern temperature changes to the changes in simulated temperatures
234 between LGM and pre-industrial simulations (LGM-PI). In addition, we compared MAAT and
235 WAMT derived from our samples to Pacific Northwest temperatures from the transient climate
236 simulation of the last 22 ka (TraCE-21k; He, 2011; Liu et al., 2009). To examine water isotopes
237 and gauge the impact of ice sheets on temperatures in the region of interest, we also performed
238 three simulations with the Community Earth System Model version 1.2 (CESM1.2) with water
239 isotope tracers (Brady et al., 2019). Isotopes of oxygen and hydrogen are included in the
240 dynamically coupled atmosphere (CAM5), ocean (POP2), land (CLM4), sea ice (CICE4), and
241 river runoff (RTM) components. For this work, the atmosphere and land are on a 1.9° latitude x
242 2.5° longitude finite-volume grid, and the ocean and sea ice use a ~1° rotated pole grid. Previous
243 studies show that the simulated isotopic distributions compare favorably with observation and
244 other models of similar complexity (Nusbaumer et al., 2017; Wong et al., 2017). We performed
245 three simulations: 1) a preindustrial control (PI) experiment, 2) a LGM experiment with period
246 appropriate boundary conditions, and 3) a LGM land-ice only (LGM-ice_only) experiment,
247 using the LGM ice sheet configuration with PI CO_2 and orbital conditions. Initial ocean oxygen

248 isotopic distributions came from the GISS interpolated ocean $\delta^{18}\text{O}$ dataset (LeGrande and
249 Schmidt, 2006). Ocean average $\delta^{18}\text{O}$ was increased by +1‰ for the LGM and LGM-ice_only
250 experiments to account for the large ice sheets (Duplessy et al. 2002). Ice volume and
251 topography came from the ICE-6G dataset (Peltier et al., 2015). All simulations were initialized
252 from previously equilibrated experiments and run for an additional 550 years with water isotope
253 tracers, allowing the atmosphere, land, and upper ocean to reach near equilibrium; data analyzed
254 is from the final 48 years of each simulation.

255 **3 Results**

256 3.1 Temperature and $\delta^{18}\text{O}$ changes: Proxy data

257 Measured stable isotope ratios of carbonates are in Table 3. The $\delta^{18}\text{O}$ of carbonates are
258 enriched (18.5‰–18.4‰) during the latter part of OIS (Oxygen Isotope Stage) 3 (36 to 27.6 ka)
259 as well as during OIS-2 (27.6 to 14 ka) (17.3‰–17.1‰) relative to modern values. OIS-1 (14
260 ka-present) carbonates have similar or enriched $\delta^{18}\text{O}$ values (19.2‰–16.8‰) relative to modern
261 values. Carbonate $\delta^{18}\text{O}$ values are consistent with two previous studies in the region (Stevenson,
262 1997; Takeuchi et al., 2009).

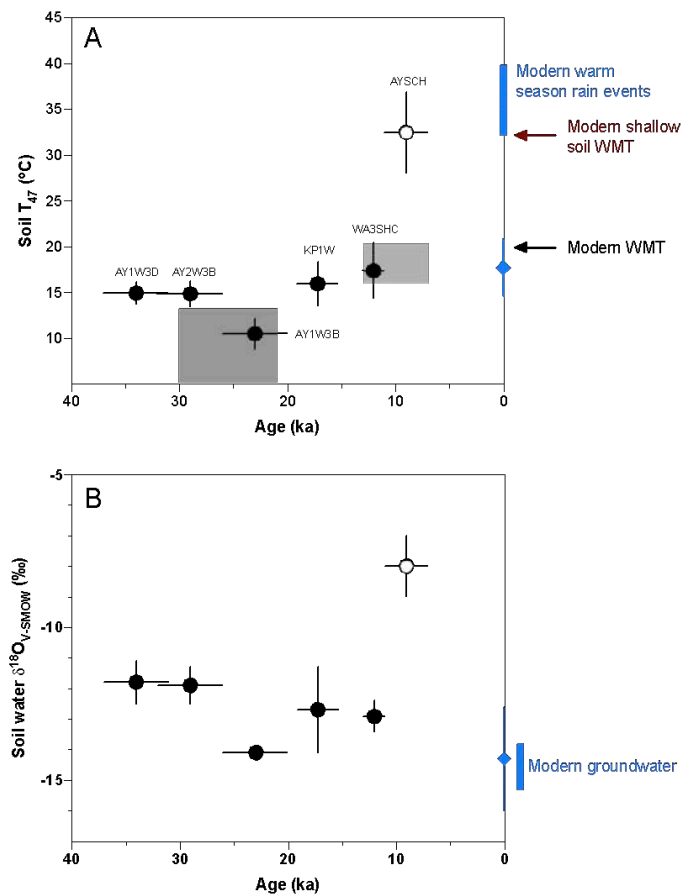
263 Clumped isotope data over the past 36,000 years reveal evidence for dynamic changes in
264 temperature, with soil temperatures warming by $21.9\text{ }^\circ\text{C} \pm 4.7\text{ }^\circ\text{C}$, mean annual air temperatures
265 warming by $26.3\text{ }^\circ\text{C}$, and warm month air temperatures warming by $24.8\text{ }^\circ\text{C}$ (Table 4; Figures 3
266 and 4). The LGM to present day warming in soil temperatures is $17.6\text{ }^\circ\text{C} \pm 4.6\text{ }^\circ\text{C}$, in MAAT is
267 $20.1\text{ }^\circ\text{C}$, and in WMAT is $20.2\text{ }^\circ\text{C}$.

268 The quantitative reconstruction of temperature from the clumped isotope data reveals a
269 pattern of change that is consistent with other non-thermodynamically derived proxy records for
270 the region. The data provide quantitative evidence to support the qualitative hydroclimate
271 reconstructions from pollen in nearby Carp Lake (Whitlock et al., 2000). The pattern also
272 matches the timing of changes in paleoclimate inferred from phytoliths in the Palouse loess
273 (Blinnikov et al., 2002). Data are also broadly consistent with inferences of temperature change
274 from proxies including chironomids and pollen (Meltzer and Holliday, 2010). The temperature
275 change we find is also consistent with what was inferred by Lechler et al. (2018) using clumped
276 isotopes, but provides further resolution on both the magnitude and timing of variations (Figure
277 3).

278

279

Figure 3. Estimates of soil carbonate formation temperatures from clumped isotopes (Soil T_{47}) and water $\delta^{18}\text{O}$ over the past 40,000 years (ka). (A) Soil carbonate formation temperatures with each paleosol labeled. Black circles indicate results from this work calculated using our measurements of Δ_{47} and the temperature calibration from Bernasconi et al. (2018). Open symbol indicates data from samples that formed during the Holocene Climatic Optimum, that could record formation during conditions similar to modern season rain events in shallow soils, after Lechler et al. (2018). Grey squares indicate temperatures reconstructed by Lechler et al. (2018). Blue diamond indicates modern soil temperature from Takeuchi et al. (2009). Black arrow indicates modern warm month mean temperatures, while blue vertical bar indicates temperatures during modern warm season rain events, and red arrow indicates modern shallow soil warm month mean temperatures, after Lechler et al. (2018). (B) Soil water $\delta^{18}\text{O}$. Black circles indicate results calculated using the temperature calibration from Bernasconi et al. (2018) and with the carbonate-water $\delta^{18}\text{O}$ calibration of Kim and O'Neil (1997). Blue diamond indicates modern soil water $\delta^{18}\text{O}$ and groundwater $\delta^{18}\text{O}$ from Takeuchi et al. (2009).



280

281

282

The coldest temperatures in the record occurred during the LGM ($\sim 23 \pm 3$ ka), with warming in the region occurring coeval with a decrease in a global benthic $\delta^{18}\text{O}$ stack (Lisiecki

283 and Stern, 2016) and synthesis of proxy data (Shakun et al., 2012) (Figure 4). Our data suggest
284 that temperatures during the Younger Dryas were warmer than LGM values, but cooler than at
285 present. A shift towards a warmer global climate (Diffenbaugh et al., 2010; Kaufman et al.,
286 2004; Mayewski et al., 2004; Shakun et al., 2012; Marcott et al., 2013), and regionally to a
287 warmer, wetter climate began to occur after a rapid loss of ice around 14 ka (Lora et al., 2016).
288 The loss of ice likely caused an abrupt reorganization of the circulation, during which time the
289 two branches of the westerly jet merged and shifted north by several degrees, leading to
290 moistening of the Pacific Northwest (Lora et al., 2016). This is consistent with the relationship
291 between thermal wind and baroclinic instability. A poleward retreat of land ice would likely
292 weaken equator-to-pole temperature gradients, thus migrating the jet stream further north. In
293 addition, northward shifts in baroclinic instability associated with a migrating jet brings
294 precipitation belts northerly, consistent with a moistening of the Pacific Northwest during
295 deglaciation. The weaker jets allow baroclinic waves to break, which in turn allows warm air to
296 leak into the Pacific Northwest. The warmest temperatures in our reconstruction occur during the
297 Holocene Climatic Optimum (HCO) at $\sim 9 \pm 2$ ka (Figure 4).

298 Soil water isotope values exhibit similar trends to the reconstruction of temperature, with
299 a total range of $6.2 \pm 0.5\text{‰}$ observed in the reconstruction (Figure 3). When a -1.2‰ global ice
300 volume correction is factored in, the most depleted water isotope values are reconstructed for the
301 LGM, with values $\sim 1\text{‰}$ less enriched than at present. The most enriched water isotope values
302 we reconstruct, $-6.7 \pm 0.9\text{‰}$, are observed during the HCO.

303

304 3.2 Regional amplification of warming

305 A global synthesis of terrestrial and marine proxy data combined with the ensemble of
306 PMIP2 climate models suggest global MAAT temperatures during the LGM were $\sim 4\text{ °C}$ cooler
307 than modern (Annan and Hargreaves, 2013; Bartlein et al., 2011; Braconnot et al., 2007; Shakun
308 et al., 2012) (Figure 4), while more recent proxy syntheses and model analysis suggests it may
309 have been $\sim 5\text{-}6.5\text{ °C}$ cooler (Friedrich et al., 2016; Tierney et al., 2020). The clumped isotope
310 data for the Palouse during the later part of OIS-3 (36 to 27.6 ka) and the beginning of OIS-2
311 (27.6 to 21 ka) would imply a much larger amplitude of regional temperature change ($\sim 20.1\text{ °C}$
312 cooler MAAT during the LGM) than either of these estimates for global surface temperatures.
313 These data, however, are broadly consistent with a range of qualitative proxies (see Section 3.1).

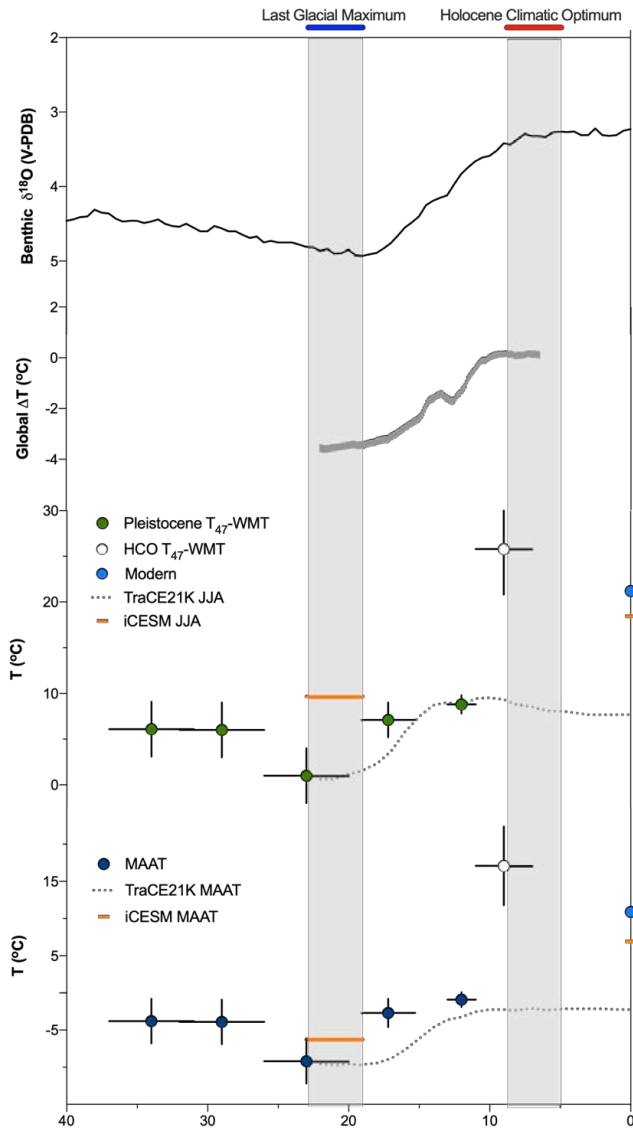


Figure 4. Estimates of warm month temperatures and mean annual air temperatures derived from clumped isotopes (T_{47}) compared to TraCE21K and iCESM temperature anomalies from simulations and benthic foraminiferal $\delta^{18}\text{O}$ over the past 40,000 years (ka). Last Glacial Maximum and Holocene Climatic Optimum (HCO) also marked. Benthic $\delta^{18}\text{O}$ is the Lisiecki and Stern (2016) stack. Global ΔT is from Shakun et al. (2012), with larger amplitude ($\sim 5\text{-}6.5$ $^{\circ}\text{C}$) changes estimated by Friedrich et al. (2016) and Tierney et al. (2020). TraCE21K anomalies are shown with dotted line (Liu et al., 2009). iCESM anomalies are shown with orange horizontal bars (Brady et al., 2019). Blue circles indicate modern values, and open symbols indicate HCO values.

314 The larger amplitude of cooling in the Palouse region during the latter part of OIS-3 and
 315 the beginning of OIS-2 coincides with a culmination of different events that would have strongly
 316 impacted regional climates. During the latter part of OIS-3 and the beginning of OIS-2, the last
 317 LIS buildup took place when the ice margin was at a proximal location to the study area
 318 (Bartlein et al., 1998; Dyke et al., 2002; Hostetler and Bartlein, 1999). During this time,
 319 anticyclonic circulation would have been produced by high atmospheric pressure over the ice
 320 sheet, and the westerly jet over the eastern portion of western North America would have been
 321 split (Bartlein et al., 1998; Hostetler and Bartlein, 1999; Manabe and Broccoli, 1985). Weakened
 322 westerlies due to the anticyclone decreased loess deposition rates at sites >150 km from the LIS

323 margin, extending as far south as the Washington and Oregon border from ~36 to 15 ka
324 (Sweeney et al, 2004). Moreover, dry conditions, inferred from pollen and phytoliths records,
325 would have resulted from the anticyclone deflecting moisture-bearing storms from the west and
326 southwest (Lora et al., 2017; Lora et al., 2016; Sweeney et al, 2004; Whitlock and Bartlein,
327 1997).

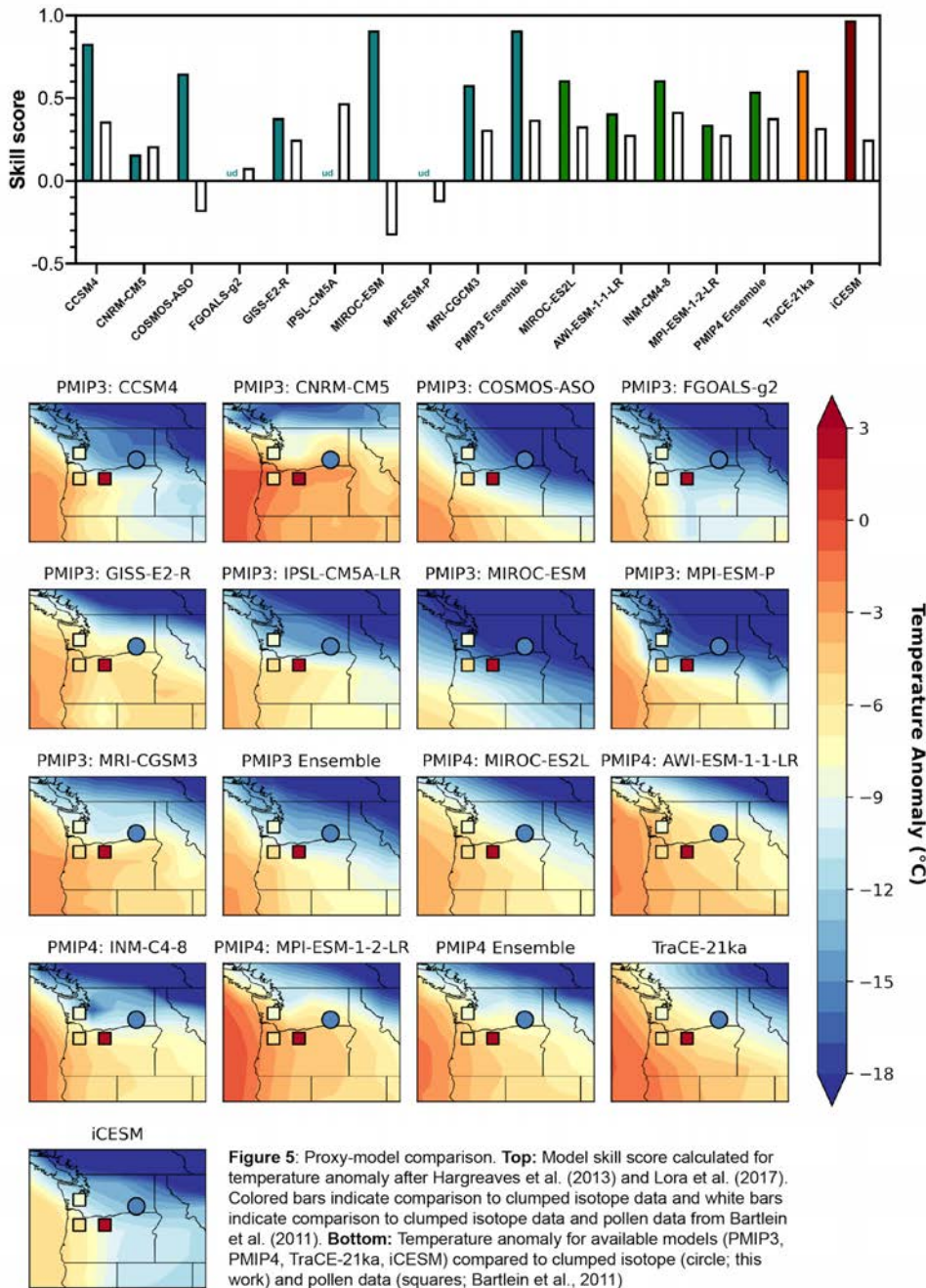
328 The Holocene Climatic Optimum temperatures that we reconstruct are similar to or
329 warmer than present, which is not dissimilar to the record of global temperatures (Figure 4). A
330 major factor associated with regional terrestrial hydroclimate changes during the early and mid-
331 Holocene is insolation driven by Earth's orbital variations (Diffenbaugh et al., 2010; Kaufman et
332 al., 2004; Mayewski et al., 2004; Skinner et al., 2020), and changes in atmospheric circulations
333 have been inferred from proxy and model analysis (Bartlein et al., 1989; Kaufman et al., 2004;
334 Skinner et al., 2020). A weakening of the Aleutian low in winter, identified by Lora et al (2016)
335 as beginning by 13.5 ka, and the strengthening of the eastern Pacific and Bermuda high-pressure
336 systems in summer, along with evidence for a poleward shift in atmospheric rivers in the mid-
337 Holocene (Skinner et al., 2020) associated with the northward movement of the jets, would have
338 created conditions that were less cloudy and drier than present in the region, which ultimately
339 caused hotter near-surface air temperatures (Bartlein et al., 1998). Furthermore, heat capacity
340 during this period of higher summer insolation increased as a result of more vegetated land
341 combined with ice sheet retreat (Gildor and Tziperman, 2001; Kaufman et al., 2004).

342

343 3.3 Proxy Temperatures Compared to Simulations

344 All climate model simulate Pacific Northwest MAAT depressions between their LGM
345 and Pre-Industrial (PI) simulations that exceed global average temperature changes, with six out
346 of nine models from the PMIP3 ensemble and iCESM simulating temperature changes in excess
347 of 10 °C, and two of the PMIP4 models showing changes of ~9 °C (Figure 5; Table S8). The
348 PMIP3 and PMIP4 multi-model ensemble mean LGM-PI MAAT difference for the region is
349 $13.2 \text{ °C} \pm 4.1 \text{ °C}$ (1 s.d.) and $8.0 \text{ °C} \pm 2.0 \text{ °C}$ (1 s.d.), respectively. Reconstructed PMIP4
350 temperature anomalies are warmer in comparison to PMIP3 models in extratropical North
351 America, which has been hypothesized to be due to change in North American Ice sheet
352 reconstructions within PMIP4 models (Kageyama et al., 2020). PMIP3 models are comparable to
353 but slightly lower in magnitude than the reconstructed change in MAAT of $20.1 \pm 4.6 \text{ °C}$, with

354 the difference not being statistically significant given the uncertainties. Five of the models that
 355 simulated the largest changes (i.e. PMIP3 CCSM4, FGOALS-g2, IPSL-CM5A-LR, MIROC-
 356 ESM, and MPI-ESM-P) all compare favorably to our result. The PMIP3 simulation results for
 357 changes in WAMT are similar, except that the inter-



358

359 model spread is greater. The LGM-PI WAMT anomaly in the multi-model average of PMIP4 is -
 360 7.2 ± 2.4 °C (1 s.d.), which is much smaller than the average anomaly in the PMIP3 multi-model
 361 average (-12.9 ± 9.0 °C (1 s.d.)) and our estimate of 20.2 ± 4.6 °C.

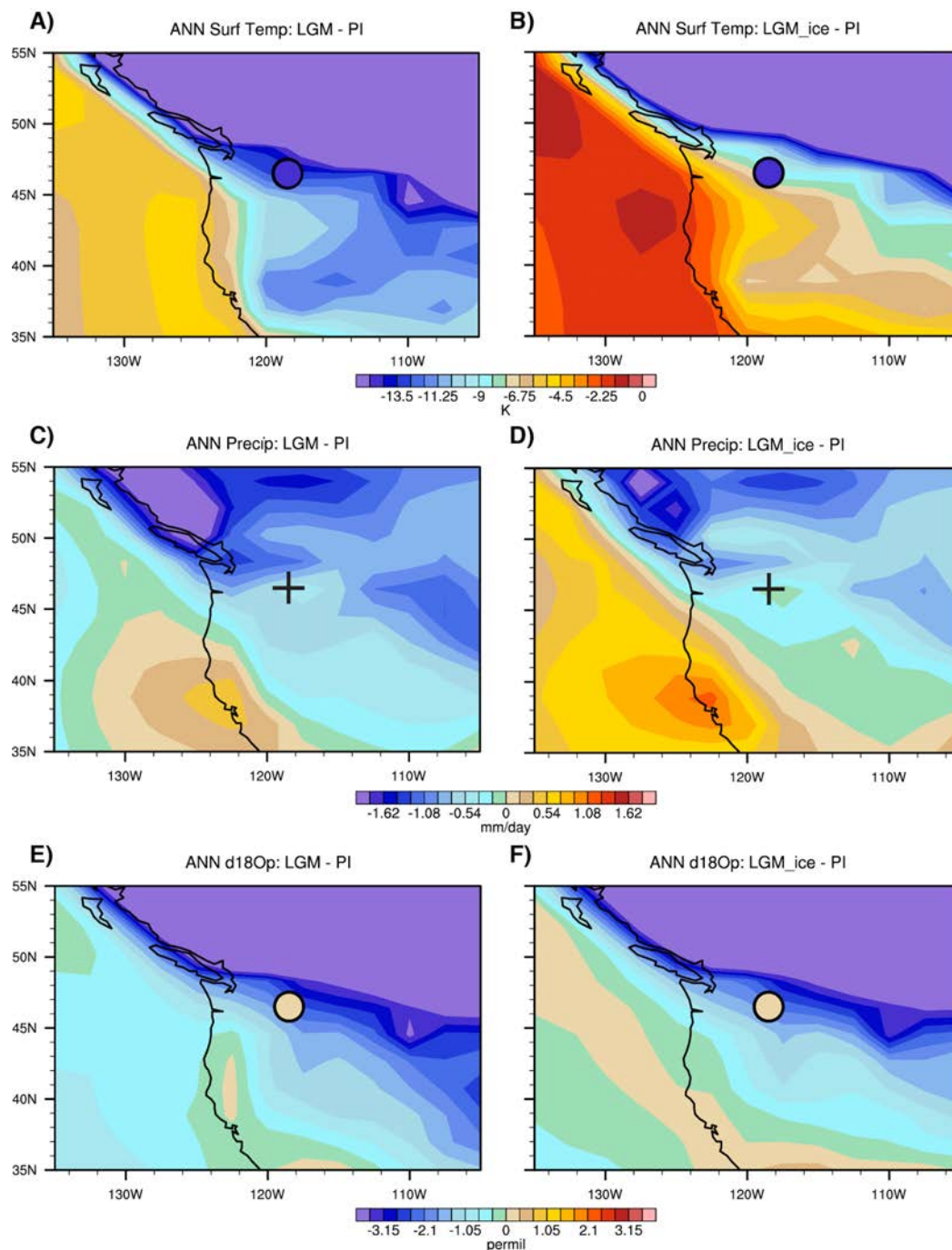
362 To quantitatively gauge climate model performance, we calculated the skill score for
 363 each of the models considered in this study using the equation:

$$364 \quad \text{Skill score (SS)} = 1 - \sqrt{\frac{\Sigma(m_i - o_i)^2 - \Sigma(e_i^2)}{\Sigma(n_i - o_i)^2 - \Sigma(e_i^2)}}$$

365 where m_i are the model results, n_i are the reference (in our case, $n_i=0$, with no change from the
 366 LGM to modern), o_i are the observations (clumped results), and e_i are the observation
 367 uncertainties (Hargreaves et al., 2013; Lora et al., 2017). A skill score of 1 represents a perfect
 368 model, where there is no disagreement between clumped and model estimates, a negative skill
 369 score demonstrates that the errors in the model are greater than the reconstructions and a skill
 370 score that is undefined would indicate that the model and clumped estimates are too close to
 371 evaluate within error of the observations.

372 Figure 5 shows the comparison of the LGM-PI MAAT anomaly for each model to our
 373 clumped-isotope derived estimates and pollen data from Bartlein et al. (2011). Overall, all
 374 models demonstrate positive skill with respect to the clumped-isotope reconstructed temperature
 375 change, with the PMIP3 multi-model average (SS = 0.91) having overall higher skill than the
 376 PMIP4 multi-model average (SS = 0.54) for clumped estimates (Figure XXb). With respect to
 377 both the clumped and pollen estimates of temperature anomalies, PMIP3 (SS = 0.37) and PMIP4
 378 (SS = 0.38) models perform similarly. Only three PMIP3 models (MIROC-ESM, MPI-ESM-P,
 379 and COSMOS-ASO) exhibit negative skill in capturing the temperature anomaly reflected in
 380 both the pollen and clumped isotope estimates.

381 We also compared our proxy data to the transient evolution of mean and warmest month
 382 temperatures from TraCE-21k and iCESM (Figure 4c, d). Our results follow the same broad
 383 pattern of temperature change as the TraCE simulation, with a warming trend through the last
 384 deglaciation, although the absolute proxy temperatures show larger-magnitude changes than the
 385 simulation, while the iCESM MAAT and WAMT reconstructs slightly higher temperatures.
 386 Within TraCE-21k, there is an overall similar amplitude of temperature change from the LGM to
 387 the Younger Dryas. However, temperature increase into the Holocene is more dramatic in the
 388 proxies than the model. Climate models struggle to capture the proxy-reconstructed warmth of



389

390 **Figure 6.** LGM iCESM 1.2 simulations. A. Annual average surface temperature anomalies
 391 (LGM minus pre-industrial). B. Annual average surface temperature anomalies (LGM_ice minus
 392 pre-industrial). C. Precipitation anomalies (LGM minus pre-industrial). D. Precipitation
 393 anomalies (LGM_ice minus pre-industrial). E. $\delta^{18}\text{O}_p$ anomalies (LGM minus pre-industrial). F.
 394 $\delta^{18}\text{O}_p$ anomalies (LGM_ice minus pre-industrial).

395 the Holocene (Liu et al., 2014; Kaufman et al., 2020), possibly due to an inability to accurately
396 simulate vegetation changes (Tabor et al., 2020). Nevertheless, the broad-scale agreement
397 between the transient simulation and our reconstruction supports the overall accuracy of the
398 regional climate changes simulated by TraCE-21k, despite disagreement in the absolute values of
399 temperature that may result from the model's low resolution or potentially point to unresolved
400 model and/or proxy biases.

401 To better understand the mechanisms responsible for the proxy signals, we compared our
402 measurements against outputs from LGM, LGM-ice_only, and PI iCESM model simulations (see
403 methods; Figure 6). For temperatures in the region, LGM-ice_only produces about 66% as much
404 cooling relative to PI as the full LGM simulation (Figure 5a and 5b), implying that a significant
405 portion of the LGM temperature signal is a consequence of topographic and albedo changes. We
406 suggest that the ice sheets alone only explain part of the local precipitation reduction at the LGM,
407 the regional pattern of precipitation response is quite similar between the LGM and LGM-
408 ice_only cases (Figures 6c and 6d), a consequence of similar Pacific circulation changes
409 (discussed above). Likewise, $\delta^{18}\text{O}$ from precipitation ($\delta^{18}\text{O}_p$) responses demonstrate that a large
410 portion of the LGM depletion signal relates to the presence of the ice sheets (Figures 6e and 6f).
411 The local $\delta^{18}\text{O}$ of column integrated vapor has a large depletion value relative to PI for both the
412 LGM and LGM-ice_only cases (-3.66 ‰ and -2.98 ‰, respectively), suggesting the ice sheets
413 play an important role bringing depleted moisture to the region. Although the specific causes of
414 isotopic change at the sample site are complex, it is clear that the North American ice sheets are
415 an important driver of the signal. Like the temperature response, the proximity of the site to the
416 ice edge leads to an amplified deglacial response in $\delta^{18}\text{O}$.

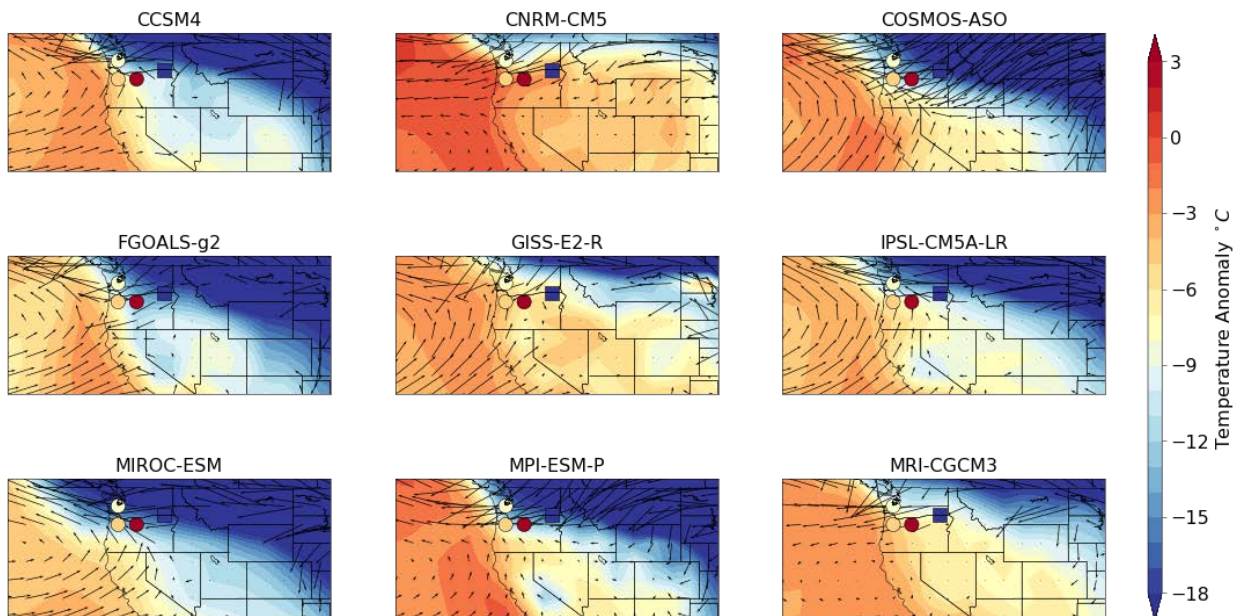
417

418 3.3 Implications for the boundary of the LGM anticyclone

419

420 Determining the regions that were influenced by the glacial anticyclone, given
421 disagreements between model simulations, remains a major essential challenge. Cyclonic wind
422 anomalies in the Eastern Pacific, driven by the decreasing sea level pressure (Lora et al., 2017),
423 bring warm air toward the west coast of the US. The warm air is mostly blocked by Pacific
424 coastal mountain ranges, and turns into the northwest US. The easterly wind anomalies, driven
425 by LGM ice, would have delivered cold air toward the west US, as observed in the PMIP3 model

426 ensemble 850 mbar anomalies (LGM-pre-industrial) shown in Figure 7. However, the Rocky
 427 Mountains, stretching from Idaho to Colorado, insulate most of the cold air.



428 **Figure 7** LGM minus Pre-Industrial MAAT anomalies for PMIP3 (colorful contours), pollen
 429 reconstruction (circle), and clumped isotope (square) with near surface (850mb) wind anomaly
 430 for PMIP3 (black arrows).
 431

431

432 Our study area, as it resides in a basin between the Pacific coastal ranges and the Rockies,
 433 provides constraints on the boundary of the glacial anticyclone induced by LGM ice sheets,
 434 between the cooler LGM anticyclone relative to the warmer cyclone in the Eastern Pacific
 435 Ocean. We compare the MAAT reconstruction derived from clumped isotopes to pollen data for
 436 three sites to the west (Figure 7). The weaker MAAT anomalies at pollen record sites indicate
 437 that these regions are mostly dominated by west to east flows of warmer air from the Eastern
 438 Pacific. However, the MAAT anomaly drops dramatically at our study site, consistent with
 439 evidence from the thick accumulation of loess in the region, suggesting coverage by the glacial
 440 anticyclone during the LGM. Given the dramatic difference between MAAT anomalies between
 441 the three pollen localities and our study area, it is very likely that the boundary of the LGM ice-
 442 dominated and Eastern Pacific-dominated regimes passed through central Oregon and
 443 Washington. These data would imply some climate models (e.g., FGOALS-g2) may
 444 overestimate the strength of glacial anticyclone driven by LGM ice, as they simulate cold air that
 445 flows into the entire Central Valley and Death Valley regions of California, while other models

446 (e.g. GISS-E2-R) may simulate the warm air from the Eastern Pacific penetrating too far. Further
447 investigation could help to shed light on the mechanisms that cause model disagreement.

448 **4 Conclusions**

449 This study provides novel paleoenvironmental constraints for the Pacific Northwest, a
450 region that was proximal to the ice sheet margin during the LGM, from clumped isotope analysis
451 and isotope-enabled simulations. We use clumped isotope measurements of paleosols to
452 reconstruct temperatures and water isotope values from soil carbonates ~36 to 9 ka in age. At the
453 LGM, when mean annual surface temperature changed globally by 4-6 °C, $T(\Delta_{17})$ suggests that
454 regional MAAT and WAMT changed by three to five times this amount in our study area.
455 Calculated soil carbonate formation temperatures, MAAT, and WAMT exhibit a pattern of
456 change from ~36 ka to modern that correlates with paleoenvironmental constraints from pollen
457 and phytoliths as well as with model simulations. Model-data comparison indicates the
458 magnitude of temperature change is likely explained by the proximity of the study area to the
459 LIS margin, the resulting influence of the glacial anticyclone on the region, and local albedo,
460 while changes in the isotopic composition of precipitation is likely due to large-scale
461 atmospheric circulation changes.

462 **Acknowledgments, Samples, and Data**

463 We thank Juan Lora, Alex Lechler, and Kate Huntington for discussions of this work. We thank
464 members of the Tripathi lab group for their support. RLM was partially supported by the NSF
465 CREST Center for Energy and Sustainability at Cal State LA (HRD-0932421). JBB was
466 supported by the postdoctoral fellowship: UPLIFT: UCLA Postdocs' Longitudinal Investment in
467 Faculty (Award # K12 GM106996) for a portion of this study. The work was supported by a
468 NSF CAREER award EAR-1352212 to AT. We also acknowledge support by the "Laboratoire
469 d'Excellence" LabexMER (ANR-10-LABX-19) and the French government ("Investissements
470 d'Avenir"). Development of the stable water isotope enabled version of the Community Earth
471 System Model was made possible by the National Science Foundation (NSF) grants AGS-
472 1401778, AGS-1401803, and AGS-1401802. Clay Tabor acknowledges funding from the
473 National Center for Atmosphere Research (NCAR) Advanced Study Program (ASP)
474 postdoctoral fellowship and the computational resources provided by the NCAR Strategic
475 Capability (NSC) project run by Computational and Information Systems Lab (CISL). All
476 simulations were carried out on the Yellowstone supercomputer managed by CISL and
477 sponsored by NSF, and are stored on the NCAR server and available upon request. All data
478 tables and supplementary tables included in the manuscript will be placed on the NOAA
479 Paleoclimatology database on acceptance.

480 **References**

481 Annan, J.D. and Hargreaves, J.C., 2013. A new global reconstruction of temperature changes at
482 the Last Glacial Maximum. *Clim. Past*, 9, 367-376.

- 483 Argus D.F. and Peltier W.R., 2010. Constraining models of postglacial rebound using space
484 geodesy: a detailed assessment of model ICE-5G (VM2) and its relatives. *Geophysical Journal*
485 *International*, 181, 697-723.
- 486 Bader, N. et al., 2015. Extensive middle Miocene weathering interpreted from a well-preserved
487 paleosol, Cricket, Oregon, USA. *Geoderma*, 239-240, 195-205.
- 488 Bader, N. et al., 2016. A loess record of pre-Late Wisconsin outburst flooding, Pleistocene
489 paleoenvironment, and Irvingtonian fauna from the Rulo site, southeastern Washington, USA.
490 *Palaeogeography, Palaeoclimatology, Palaeoecology*, 462, 57-69.
- 491 Bartlein, P.J. et al., 1998. Paleoclimate simulations for North America over the past 21,000 year:
492 Features of the simulated climate and comparisons with paleoenvironmental data. *Quaternary*
493 *Science*, 17, 549-585.
- 494 Bartlein, P.J. et al., 2011. Pollen-based continental climate reconstructions at 6 and 21 ka: a
495 global synthesis. *Clim. Dyn.*, 37, 775-802.
- 496 Barta, G., 2011. Secondary carbonates in loess-paleosol sequences: a general review. *Cent. Eur.*
497 *J. Geosci.*, 3(2), 129-146.
- 498 Bartlein, P.J. et al., 1998. Paleoclimate simulations for North America over the past 21,000
499 years: Features of the simulated climate and comparisons with paleoenvironmental data.
500 *Quaternary Science Reviews*, 17, 549-585.
- 501 Berger G.W. and Busacca A.J., 1995. Thermoluminescence dating of late Pleistocene loess and
502 tephra from eastern Washington and southern Oregon and implications for eruptive history of
503 Mount St. Helens. *Solid Earth*, 100, 11, 22361-22374.
- 504 Blinnikov M., et al., 2002. Reconstruction of the late Pleistocene grassland of the Columbia
505 basin, Washington, USA, based on phytoliths records in loess. *Palaeogeography,*
506 *Palaeoclimatology, Palaeoecology*, 177, 77-101.
- 507 Booth, D.B. et al., 2003. The cordilleran ice sheet. *Development in Quaternary Science*, 1, 17-43.
- 508 Braconnot, P. et al., 2007. Results of PMIP2 coupled simulations of the mid-Holocene and Last
509 Glacial Maximum - Part 1: experiments and large scale features. *Clim. Past.*, 3, 261-277.
- 510 Braconnot, P. et al., 2012. Evaluation of climate models using palaeoclimatic data. *Nature*
511 *Climate Change*, 2(6), 417-424.
- 512 Brady, E., Stevenson, S., Bailey, D., Liu, Z., Noone, D., Nusbaumer, J., Otto -Bliesner, B.L.,
513 Tabor, C., Tomas, R., Wong, T. and Zhang, J., 2019. The connected isotopic water cycle in the
514 Community Earth System Model version 1. *Journal of Advances in Modeling Earth*
515 *Systems*, 11(8), pp.2547-2566.
- 516 Breecker, D.O. et al., 2009. Seasonal bias in the formation and stable isotopic composition of
517 pedogenic carbonate in modern soils from central New Mexico. *GSA Bulletin*, v. 121. No. 3/4, p.
518 630-640.
- 519 Buggle, B. et al., 2011. An evolution of geochemical weathering indices in loess-paleosol
520 studies. *Quaternary International*, 240, 12-21.
- 521 Busacca, A.J., 1989. Long Quaternary record in Eastern Washington, U.S.A., interpreted from
522 multiple buried paleosols. *Geoderma*, 45, 105-122.

- 523 Busacca, A.J. and McDonald, E.V., 1994. Regional Sedimentation of the Late Quaternary loess
524 on the Columbia Plateau: sediment source areas and loess distribution patterns. *Bulletin-*
525 *Washington. Division of Geology and Earth Resources* 80, 181–203.
- 526 Cerling, T.E., 1984. The stable isotopic composition of modern soil carbonate and its
527 relationship to climate. *Earth and Planetary Science Letters*, 71, 229-240.
- 528 Clark, P.U. and Mix, A.C., 2002. Ice sheets and sea level of the Last Glacial Maximum.
529 *Quaternary Science Reviews*, 21, 1-7.
- 530 Defliese, W.F., et al., 2015. Compositional and temperature effects of phosphoric acid
531 fractionation on Δ_{47} analysis and implications for discrepant calibrations. *Chemical Geology*,
532 396, 51-60.
- 533 Dennis, K.J. et al., 2011. Defining an absolute reference frame for ‘clumped’ isotope studies of
534 CO₂. *Geochimica et Cosmochimica Acta*, 75, 7117-7131.
- 535 Dickson, J.A.D., 1966. Carbonate identification and genesis as revealed by staining. *Sedimentary*
536 *Petrology*, 36, 2, 491-505.
- 537 Diffenbaugh, N.S. et al., 2006. Summer aridity in the United States: Response to mid-Holocene
538 changes in insolation and sea surface temperature. *Geophysical Research Letters*, 33, L22712.
- 539 Duplessy, J.C., Labeyrie, L. and Waelbroeck, C., 2002. Constraints on the ocean oxygen isotopic
540 enrichment between the Last Glacial Maximum and the Holocene: Paleoceanographic
541 implications. *Quaternary Science Reviews*, 21(1), pp.315-330.
- 542 Durand N. et al., 2010. Interpretation of Micromorphological Features of Soils and Regolith.
543 *Elsevier*, 149.
- 544 Dyke, A.S., et al., 2002. The Laurentide and Innuitian ice sheets during the Last Glacial
545 Maximum. *Quaternary Science Reviews*, 21, 9-31.
- 546 Eagle, R.A. et al., 2013. High regional climate sensitivity over continental China constrained by
547 glacial-recent changes in temperature and the hydrologic cycle. *PNAS*, 110, 22, 8813-8818.
- 548 Eiler, J., 2011. Paleoclimate reconstruction using carbonate clumped isotope thermometry.
549 *Quaternary Science Reviews*, 30, 3575-3588.
- 550 Gildor, H. and Tziperman, E., 2001. A sea ice climate switch mechanism for the 100-kyr glacial
551 cycles. *Journal of Geophysical Research*, 106, 9117-9133.
- 552 Hostetler, S.W. and Bartlein, P.J., 1999. Simulation of the potential responses of regional climate
553 and surface processes in western North America to a Canonical Heinrich event. *Mechanisms of*
554 *Global Climate Change: American Geophysical Union Geophysical Monograph*, 12, 313-327.
- 555 He, F., 2011. Simulating transient climate evolution of the last deglaciation with CCSM3, *PhD*
556 *thesis*, Madison, Wisconsin.
- 557 Hurrell, J.W., Holland, M.M., Gent, P.R., Ghan, S., Kay, J.E., Kushner, P.J., Lamarque, J.F.,
558 Large, W.G., Lawrence, D., Lindsay, K. and Lipscomb, W.H., 2013. The community earth
559 system model: a framework for collaborative research. *Bulletin of the American Meteorological*
560 *Society*, 94(9), pp.1339-1360.

- 561 Kaufman, D.S. et al., 2004. Holocene thermal maximum in the western Arctic (0-180 W).
562 *Quaternary Science Reviews*, 23, 529-560.
- 563 Kim, S. and O'Neil, J.R., 1997. Equilibrium and nonequilibrium oxygen isotope effects in
564 synthetic carbonates. *Geochimica et Cosmochimica Acta*, 61, 16, 3461-3475.
- 565 Lambeck K. et al., 2010. The Scandinavian ice sheet sheet: from MIS 4 to the end of the last
566 glacial maximum. *Boreas*, 39, 410-435.
- 567 LeGrande, A.N. and Schmidt, G.A., 2006. Global gridded data set of the oxygen isotopic
568 composition in seawater. *Geophysical Research Letters*, 33(12).
- 569 LeGrande, A.N. and Schmidt, G.A., 2008. Ensemble, water isotope-enabled, coupled general
570 circulation modeling insights into the 8.2 ka event. *Paleoceanography*, 23(3).
- 571 Li, G. et al., 2013. Primary and secondary carbonate in Chinese loess discriminated by trace
572 element composition. *Geochimica et Cosmochimica Acta*, 103, 26-35.
- 573 Lisiecki, L. E., & Raymo, M. E. (2005). A Pliocene–Pleistocene stack of 57 globally distributed
574 benthic $\delta^{18}\text{O}$ records. *Paleoceanography*, 20(1).
- 575 Liu, Z. et al., 2009. Transient Simulation of Last Deglaciation with a New Mechanism for
576 Bølling-Allerød Warming, *Science*, 325, 310-314.
- 577 Lopez-Maldonado, R., 2017. Carbonate clumped isotope reconstruction of temperatures and
578 water $^{18}\text{O}/^{16}\text{O}$ ratios from Last Glacial Maximum and Holocene Climatic Optimum age calcic
579 paleosols in the Palouse Loess (Washington, USA). *M.S. Thesis*, California State University, Los
580 Angeles, 108 pages.
- 581 Lora, J.M., et al., 2016. Abrupt reorganization of the North Pacific and western North American
582 climate during the last deglaciation. *Geophysical Research Letters*, 43, 11,796-11,804.
- 583 Lora, J.M., et al., 2017. North Pacific atmospheric rivers and their influence on western North
584 America at the Last Glacial Maximum. *Geophysical Research Letters*, 44, 1051–1059.
- 585 Lyle, M. et al., 2012. Out of the tropics: The Pacific, Great Basins Lakes, and late Pleistocene
586 water cycle in the western United States. *Science*, 337, 1629-1633.
- 587 Manabe, S. and Broccoli, A.J., 1985. The influence of continental ice sheets on the climate of the
588 Ice Age. *J. Geophys. Res.*, 90, 2167-2190.
- 589 Marcott, S.A. et al., 2013. A reconstruction of regional and global temperature for the past
590 11,300 years. *Science*, 339, 1198-1201.
- 591 Martinson, D.G., 1987. Age dating and the orbital theory of the ice ages: Development of a high
592 resolution 0 to 300,000-year chronostratigraphy. *Quaternary Research*, 27, 1-29.
- 593 Mayewski, P.A. et al., 2004. Holocene climate variability. *Quaternary Research*, 62, 243-255.
- 594 McDonald, E.V. and Busacca A.J., 1992. Late quaternary stratigraphy of loess in the Channeled
595 Scabland and Palouse regions of Washington State. *Quaternary Research*, 38, 141-156.
- 596 McDonald, E.V. et al., 2012. Glacial outburst floods and loess sedimentation documented during
597 Oxygen Isotope Stage 4 on the Columbia Plateau, Washington State. *Quaternary Science-*
598 *Reviews*, 45, 18-30.

- 599 Meltzer, D.J. and Holliday, V.T., 2010. Would North America Paleoindians have noticed
600 Younger Dryas Age Climate Change?. *J. World Prehist*, 23:1–41.
- 601 Mix, A.C. et al., 2001. Environmental processes of the ice age: land, oceans, glaciers (EPILOG).
602 *Quaternary Science Reviews* 20, 627–657.
- 603 Nusbaumer, J., Wong, T.E., Bardeen, C. and Noone, D., 2017. Evaluating hydrological processes
604 in the Community Atmosphere Model Version 5 (CAM5) using stable isotope ratios of water.
605 *Journal of Advances in Modeling Earth Systems*.
- 606 Passey, B.H. et al., 2010. High-temperature environments of human evolution in East Africa
607 based on bond ordering in paleosol carbonates. *PNAS*, v. 107, no. 25, p. 11245–11249.
- 608 Peltier, W.R., Argus, D.F. and Drummond, R., 2015. Space geodesy constrains ice age terminal
609 deglaciation: The global ICE-6G_C (VM5a) model. *Journal of Geophysical Research: Solid
610 Earth*, 120(1), pp.450–487.
- 611 Peters, N.A. et al., 2012. Hot or not? Impact of seasonally variable soil carbonate formation on
612 paleotemperature and O-isotope records from clumped isotope thermometry. *Earth and
613 Planetary Science Letters*, 361, 208–218.
- 614 Quade, J. et al., 2012. The clumped isotope geothermometer in soil and paleosol carbonate.
615 *Geochimica et Cosmochimica Acta* 105, 92–107.
- 616 Richardson C.A. et al., 1997. Luminescence dating of loess from the northwest United States.
617 *Quaternary Science Reviews (Quaternary Geochronology)*, 16, 403–415.
- 618 Richardson C.A. et al., 1999. A luminescence chronology for loess deposition in Washington
619 state and Oregon, USA. *Zeitschrift fur Geomorphologie Supplementband*, 116, 77–95.
- 620 Roberts, C.D., LeGrande, A.N. and Tripathi, A.K., 2011. Sensitivity of seawater oxygen isotopes
621 to climatic and tectonic boundary conditions in an early Paleogene simulation with GISS
622 ModelE - R. *Paleoceanography*, 26(4).
- 623 Shakun, J.D. et al., 2012. Global warming preceded by increasing carbon dioxide concentrations
624 during the last deglaciation. *Nature*, 484, 49–55.
- 625 Sheldon, N.D. and Tabor, N.J., 2009. Quantitative paleoenvironmental and paleoclimatic
626 reconstruction using paleosols. *Earth-Science Reviews*, 95, 1–52.
- 627 Skinner, C. B., Lora, J. M., Payne, A. E., & Poulsen, C. J. (2020). Atmospheric river changes
628 shaped mid-latitude hydroclimate since the mid-Holocene. *Earth and Planetary Science Letters*,
629 541, 116293.
- 630 Spencer, P.K. and Knapp A.N., 2010. New stratigraphic markers in the late Pleistocene Palouse
631 loess: novel fossil gastropods, absolute age constraints and non-aeolian facies. *Sedimentology*,
632 57, 41–52.
- 633 Stevenson B.A., et al., 2010. Oxygen isotope ratios in Holocene carbonates across a climatic
634 gradient, eastern Washington state, USA: Evidence for seasonal effects on pedogenic mineral
635 isotopic composition. *The Holocene*, 204, 575–583.
- 636 Sweeney, M.R., Busacca, A.J., Richardson, C., Blinnikov, M., and McDonald, E., 2004, Glacial
637 anticyclone recorded in Palouse loess of northwestern United States: *Geology*, 32, 705–708.

- 638 Sweeney, M.R. et al., 2005. Topographic and climatic influences on accelerated loess
639 accumulation since the last glacial maximum in the Palouse, Pacific Northwest, USA.
640 *Quaternary Research*, 63, 261-273.
- 641 Sweeney, M.R., Gaylord, D.R., and Busacca, A.J., 2007, Evolution of Eureka Flat: A dust-
642 producing engine of the Palouse loess, USA: *Quaternary International*, 162, 76–96.
- 643 Takeuchi, A. et al., 2009. Isotopic evidence for temporal variation in proportion of seasonal
644 precipitation since the last glacial time in the inland Pacific Northwest of the USA. *Quaternary*
645 *Research*, 72, 198-206.
- 646 Tarasov L. et al., 2012. A data-calibrated distribution of deglacial chronologies for the North
647 American ice complex from glaciological modeling. *Earth and Planetary Science Letters*,
648 315-316: 30-40.
- 649 Tripathi, A.K., et al., 2015. Beyond temperature: Clumped isotope signatures in dissolved
650 inorganic carbon species and the influence of solution chemistry on carbonate mineral
651 composition. *Geochimica et Cosmochimica Acta*, 166, 344-371.
- 652 Wang Z., et al., 2004. Equilibrium thermodynamics of multiply-substituted isotopologues of
653 molecular gases. *Geochimica et Cosmochimica Acta*, 23, 4779-4797.
- 654 Weaver, P. P., Carter, L., & Neil, H. L. (1998). Response of surface water masses and circulation
655 to late Quaternary climate change east of New Zealand. *Paleoceanography*, 13(1), 70-83.
- 656 Whitlock, C., 1992. Vegetational and climatic history of the Pacific Northwest during the last
657 20,000 years: Implications for understanding present-day biodiversity. *The Northwest*
658 *Environmental Journal*, 8, 5-28.
- 659 Whitlock, C. and Bartlein, P.J., 1997. Vegetation and climate change in northwest America
660 during the past 125 kyr. *Nature*, 388, 57-61.
- 661 Whitlock, C., 2000. Environmental history and tephrostratigraphy at Carp Lake, southwestern
662 Columbia Basin, Washington, USA. *Palaeogeography, Palaeoclimatology, Palaeoecology*, 155,
663 7-29.
- 664 Wong, T.E., Nusbaumer, J. and Noone, D.C., 2017. Evaluation of modeled land-atmosphere
665 exchanges with a comprehensive water isotope fractionation scheme in version 4 of the
666 Community Land Model. *Journal of Advances in Modeling Earth Systems*, 9(2), 978-1001.
- 667 Zamanian K., et al., 2016. Pedogenic carbonates: Forms and formation processes. *Earth-Science*
668 *Reviews*, 157, 1-17.
- 669 Zhang, J., Liu, Z., Brady, E.C., Oppo, D.W., Clark, P.U., Jahn, A., Marcott, S.A. and Lindsay,
670 K., 2017. Asynchronous warming and $\delta^{18}\text{O}$ evolution of deep Atlantic water masses during the
671 last deglaciation. *Proceedings of the National Academy of Sciences*, 114(42), 11075-11080.
- 672 Zhu, J., Liu, Z., Brady, E., Otto-Bliesner, B., Zhang, J., Noone, D., Tomas, R., Nusbaumer, J.,
673 Wong, T., Jahn, A. and Tabor, C., 2017. Reduced ENSO Variability at the LGM Revealed by an
674 Isotope-enabled Earth System Model. *Geophysical Research Letters*, 44(13), 6984-6992.
- 675
- 676

677 **Table 1.** Field Localities.

678

Site	Paleosol Material	Elevation (amsl ft)	Latitude	Longitude
AY-1	Micritic Carbonate/Carbonate Seam	1255	46.312	-118.487
AY-2	Micritic Carbonate/Carbonate Seam	1186	46.315	-118.490
WA-3	Micritic Carbonate/Carbonate Seam	1583	46.767	-118.346
KP-1	Micritic Carbonate/Carbonate Seam	1383	46.569	-118.627

679

680

681 **Table 2:** Estimated sample ages. Geochronologic constraints in Table S2.

682

Paleosol Horizon and Sample ID	Age (ka)	uncertainty
Sand Hills Coulee Paleosol – Horizon Bkb1		
WA-3 WA3SHC	12	1
KP-1 KP1SHC	12	1.5
AY-1 AY1SHC	9	2
AY-2 AY2SHC	9	2
Washtucna Paleosol – Horizon Bwb2		
KP-1 KP1W	17.2	1.9
Washtucna Paleosol – Horizon Bkqmb2 (upper)		
AY-1 AY1W3B	23	3
WA-3 WA3W	34	3
Washtucna Paleosol – Horizon Bkqb2		
AY-2 AY2W3B	29	3
Washtucna Paleosol – Horizon Bkqmb2 (lower)		
AY-1 AY1W3D	34	3

683

684

685 **Table 3:** Stable isotope data summary. All units for isotope ratios in per mil. Errors are
 686 propagated. 1: Carbon dioxide equilibrated scale. 2: Likely impacted by detrital/dissolution
 687 based on petrography/ancillary geochemistry (Lopez-Maldonado, 2017).

Sample Name	# replicates	# acquisitions	$\delta^{13}\text{C}_c$ V-PDB	1 s.d.	$\delta^{18}\text{O}_c$ V-PDB	1 s.d.	Δ_{47} (CDES) ¹	1 s.e.
AY1SHC	4	36	-4.4	0.1	-12.2	0.1	0.638	0.009
AY1W3B	6	54	-6.3	0.0	-13.4	0.1	0.725	0.007
AY1W3D	9	81	-5.7	0.1	-12.0	0.2	0.708	0.005
AY2SHC	5	45	-4.4	0.1	-11.4	0.1	0.658	0.004
AY2W3B	3	27	-5.5	0.2	-12.2	0.1	0.708	0.005
AY2W3C ²	5	45	-4.5	0.2	-11.8	0.1	0.660	0.005
KP1SHC ²	3	27	-2.6	0.2	-12.3	0.2	0.595	0.007
KP1W	7	63	-4.5	0.2	-13.2	0.6	0.705	0.008
WA3SHC	2	18	-6.5	0.2	-13.7	0.4	0.699	0.011
WA3W ²	7	63	-4.6	0.1	-12.7	0.1	0.664	0.004

688

689

690

691 **Table 4:** Stable isotope-derived reconstructions. Errors are propagated. 1: Calculated using an
 692 equation from Bernasconi et al. (2018). 2: Calculated using an equation of Kim and O'Neil
 693 (1997). 3: Calculated using an equation from Quade et al. (2012).

694

Sample Name	Age (ka)	err	Δ_{47-T} [°C] ¹	1 s.e.	$\delta^{18}O_w$ V-SMOW ²	1 s.d.	MAAT [°C] ³	WMAT [°C] ³
AY1SHC	9	2	35.5	2.7	-7.8	1.1	20.9	29.3
AY2SHC	9	2	29.3	1.3	-8.1	0.6	13.4	22.2
<i>Average</i>	9	2	32.4	4.4	-8.0	0.2	17.1	25.8
WA3SHC	12	1	17.4	3.0	-12.9	0.5	-0.9	8.8
KP1W	17.2	1.9	15.9	2.4	-12.7	1.4	-2.7	7.1
AY1W3B	23	3	10.5	1.7	-14.1	0.4	-9.2	1.0
AY2W3B	29	3	14.8	1.4	-11.9	0.6	-3.9	6.0
AY1W3D	34	3	14.9	1.2	-11.8	0.7	-3.8	6.1

695

696

Paleoclimate Changes in the Pacific Northwest Over the Past 36,000 Years from Clumped Isotope Measurements and Isotope-Enabled Model Analysis

Ricardo Lopez-Maldonado^{1,2}, Jesse Bloom Bateman^{2,3}, Andre Ellis¹, Nicholas E. Bader⁴, Pedro Ramirez¹, Alexandra Arnold², Osinachi Ajoku⁵, Hung-I Lee^{2,6}, Gregory Jesmok^{2,7}, Deepshikha Upadhyay², Bryce Mitsunaga^{2,8}, Ben Elliott², Clay Tabor⁹, and Aradhna Tripathi^{2,10}

¹*Department of Geoscience and Environment, California State University, Los Angeles, CA, U.S.A.*

²*Department of Atmospheric and Oceanic Sciences, Department of Earth, Planetary, and Space Sciences, Institute of the Environment and Sustainability, Center for Diverse Leadership in Science, American Indian Studies Center, University of California, Los Angeles, CA, U.S.A.*

³*Department of Biology, SUNY Cortland, Cortland, NY, U.S.A.*

⁴*Department of Geology, Whitman College, Walla Walla, WA, U.S.A.*

⁵*National Center for Atmospheric Research, Boulder, CA, U.S.A.*

⁶*Department of Geophysical Sciences, University of Chicago, Chicago, IL, U.S.A.*

⁷*Department of Geology, California State University, Northridge, CA, U.S.A.*

⁸*Department of Geology, Brown University, Providence, RI, U.S.A.*

⁹*Department of Geography, University of Connecticut, Storrs, CT, U.S.A.*

¹⁰*UMR6538 Géosciences Océan, Institut Universitaire Européen de la Mer, Technopôle Brest-Iroise, Plouzané, 29280, France*

Text S1
Figures S1 to S6
Tables S1 to S7

Additional Supporting Information (Files uploaded separately)

Captions for Tables S1 to S7

Introduction

We provide supporting information including a discussion of the materials and methods and analysis of results, six supporting figures, and seven supporting tables.

Text S1.

A. Materials and Methods

A1. Microscale pedogenic carbonate

For this study, we analyzed microscale pedogenic carbonates from the rhizosphere (Barta, 2011), specifically hypocotings, which are thought to form on the order of weeks to months (Zamanian et al., 2016). Other microscale pedogenic carbonates that we identified in our samples and at our sites were carbonate coatings and calcite laminar caps (i.e. petrocalcic horizons). We did not use either the carbonate coatings or the calcite laminar caps in our analyses because these carbonates are believed to form on the order of 10^2 to 10^3 y. In the Sand Hills Coulee samples, we only found hypocotings, whereas in the Washtucna paleosol we found both hypocotings and carbonate coatings and observed a calcite laminar cap in the soil profile. Additional details are in the M.S. thesis of the lead author (Lopez-Maldonado, 2017).

A2. Detrital and pedogenic carbonate discrimination

We used two approaches to identify and differentiate between pedogenic carbonates and detrital carbonate in our samples to ensure that our results reflect the environment at the time of formation (pedogenic carbonates) and not subsequent alteration (detrital carbonates). A detailed description is in the M.S. thesis of the lead author (Lopez-Maldonado, 2017). First, we analyzed the Manganese:Calcium (Mn:Ca) and Magnesium:Calcium (Mg:Ca) ratios of samples to determine the purity of secondary carbonates (Li et al., 2013). Next, we examined the samples' micromorphology using thin sections of horizon samples. Both analyses were performed at California State University, Los Angeles (Cal State LA).

To analyze the samples Mn:Ca and Mg:Ca ratios, we digested samples in 0.2 M acetic acid for 24 h. After digestion we centrifuged the samples, and then collected the supernatant for analysis on a Perkin-Elmer ICP-OES Optima 5300. A calibrated blank and a 5 M Sigma-Aldrich multi-element standard solution were run to verify the accuracy and precision of the analysis. Analytical standard errors were <5%.

To analyze micromorphology, we sent samples to Quality Thin Sections (Tucson, AZ) for thin section preparation. Quality Thin Sections impregnated disturbed samples with epoxy, cut them into thin sections, and stained the thin sections with alizarin red-S and potassium ferricyanide. After thin section preparation, we analyzed the samples using standard petrographic microscope techniques.

A3. Stable isotope analysis

A detailed description is in the M.S. thesis of the lead author (Lopez-Maldonado, 2017). Prior to isotope analysis, we cleaned samples by soaking them in 3% H₂O₂ for 4 h to remove trace amounts of organic material (Eagle et al., 2013). After cleaning, we rinsed samples with deionized water, and then oven-dried them at 40 °C. We homogenized samples with an agate mortar and pestle that was cleaned with 10% HCl between samples. Between oven-drying and analysis on the mass spectrometer, samples were stored in desiccators to prevent isotopic exchange with ambient water vapor.

To obtain pure CO₂ gas for analysis, the homogenized samples first go through an automated sampling process comprised of a Costech Zero Blank Autosampler and common acid bath coupled with a gas purification system and gas chromatograph (either from Thermo or Agilent). Acid temperature is kept at 90 ± 2 °C, and is checked daily whilst the machine is in operation. The gas purification system uses a series of cryotrap to remove water vapor from the gas released upon reaction with the acid and a silver wool filter to remove SO₄⁻ compounds. Samples are then automatically transferred to the mass spectrometer for analysis. We ran the samples on either a Nu Perspective IS mass spectrometer or a Thermo Finnigan MAT 253 gas source mass spectrometer specially configured to make precise clumped isotope measurements of mass-47 CO₂. Isotope analyses were performed in the Tripathi lab at UCLA.

A4. Calculations to derive stable isotope values and their errors

A detailed description is in the M.S. thesis of the lead author (Lopez-Maldonado, 2017). All data are reported on the absolute reference frame (Dennis et al., 2011), with equilibrated gases and carbonate standards analyzed daily. Gas standards were equilibrated at either 1000 °C or 25 °C, and consisted of an isotopically depleted gas or an enriched gas standard. Our working gas is a high-purity Oztech brand CO₂ reference gas (i.e. δ¹³C = -3.60 ‰ VPDB and δ¹⁸O = 25.03 ‰ V-SMOW). Every sample run also included carbonate standards of known isotopic compositions that were analyzed between every 2-3 samples. Between 3 and 12 replicates were run of each sample.

A5. iCESM simulations

We performed three simulations with the isotope-enabled version of the Community Earth System Model version 1.2 (CESM1.2): 1) A preindustrial control (PI) experiment, 2) a LGM experiment with period appropriate boundary conditions, and 3) a LGM land-ice only (LGM-ice_only) experiment, using the LGM ice sheet configuration with PI CO₂ and orbital conditions.

Isotopes of oxygen and hydrogen are included in the dynamically coupled atmosphere (CAM5), ocean (POP2), land (CLM4), sea ice (CICE4), and river runoff (RTM) components. For this work, the atmosphere and land were run on a 1.9° latitude x 2.5° longitude finite-volume grid, and the ocean and sea ice used a ~1° rotated pole grid. Previous studies have shown that the simulated isotopic distributions compare favorably with observations and other models of similar complexity (Nusbaumer et al., 2017; Wong et al., 2017; Zhang et al., 2017; Zhu et al., 2017). Initial ocean oxygen isotopic distributions were taken from the GISS interpolated ocean $\delta^{18}\text{O}$ dataset (LeGrande and Schmidt, 2006). Ocean average $\delta^{18}\text{O}$ was increased by +1 ‰ for the LGM and LGM-ice only experiments, to account for the large ice sheets (Duplessy et al. 2002). Ice volume and topography came from the ICE-6G dataset (Peltier et al., 2015). All simulations were initialized from previously equilibrated experiments and run for an additional 550 years with water isotope tracers, allowing the atmosphere, land, and upper ocean to reach near equilibrium; analyses were performed on the final 48 years of each simulation.

B. Analysis of Results

B1. Analysis of Mg/Ca and Mn/Ca ratios

A detailed description is in the M.S. thesis of the lead author (Lopez-Maldonado, 2017). Pure pedogenic carbonates are characterized by low Mg/Ca and Mn/Ca ratios. Mg/Ca and Mn/Ca in the carbonates from our samples ranged from 0.02 to 0.06 mol/mol and 0.03 to 0.15 mmol/mol, respectively (Figure S1-S2). Table S1 shows a summary of the Mg/Ca and Mn/Ca ratio data.

B2. Analysis of Micromorphology

A detailed description is in the M.S. thesis of the lead author (Lopez-Maldonado, 2017). The thin sections in plane-polarized light mainly show a pale structureless pink stain and a pseudofabric in the groundmass formed from non-calcareous silt (Figures S3. C, D, and Figure S4. A, E, and F). Dickson (1966) states that the pale pink stain covering the entire thin section results from the “floods” of carbon dioxide bubbles during the carbonate staining, and indicates that calcite is the only carbonate mineral present. The structureless appearance and pseudofabric suggest a micritic and microsparite carbonate groundmass, which coincides with the dominant pedogenic calcite form in the region (Busacca, 1989; Durand et al., 2010; McDonald and Busacca, 1992). Dissolution voids are not present, and re-precipitated carbonate cannot be distinguished in any of the thin sections.

Thin sections reveal that detrital carbonate grains exist in some of the horizons characterized as pure pedogenic carbonate by the Mg/Ca and Mn/Ca ratios in trace amounts. Under cross-polarized light the Sand Hills Coulee paleosol thin sections—excluding the WA-3 calcic horizon—produced second and third order reds, blues, and yellows (Figure S5.). These colors are the result of the etching process, and are indicative of the presence of detrital limestone or marble grains (Dickson, 1966). Visual inspection of the Washtucna paleosol thin sections in cross-polarized light also showed evidence of very few detrital carbonate grains (Figure S6. A, B, and D), and pedogenic carbonate coatings, which represent carbonate recrystallization, within and around mineral grains in the KP-1 cambic horizon (Figure S6. D).

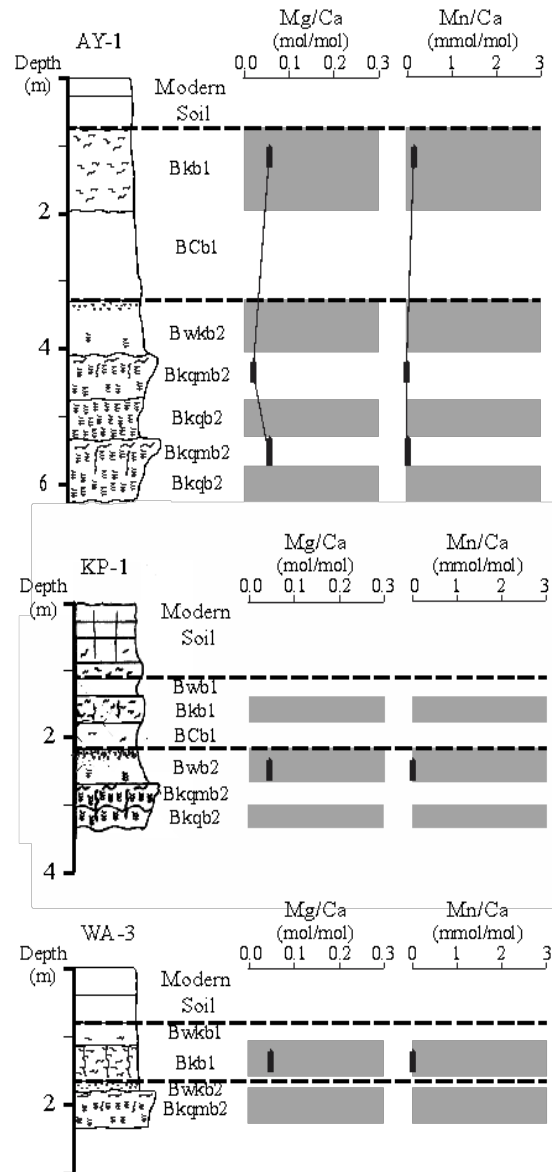


Figure S1. Mg/Ca and Mn/Ca ratios at AY-1, KP-1, and WA-3.

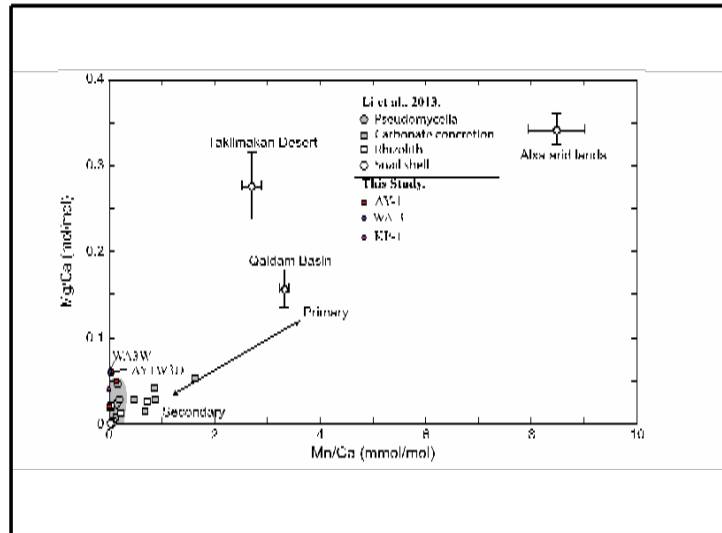


Figure S2. Mg/Ca and Mn/Ca ratios of pedogenic carbonates (modified from Li et al., 2013).

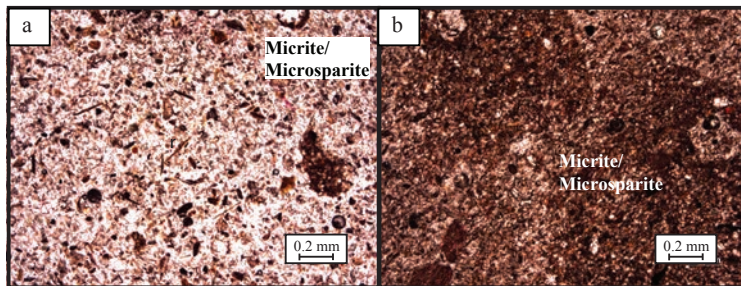


Figure S3. Examples of Sand Hills Coulee paleosol thin sections in plane polarized light. Thin sections are carbonate stained with alizarin red-s and potassium ferricyanide, and depict the entire area containing micrite.

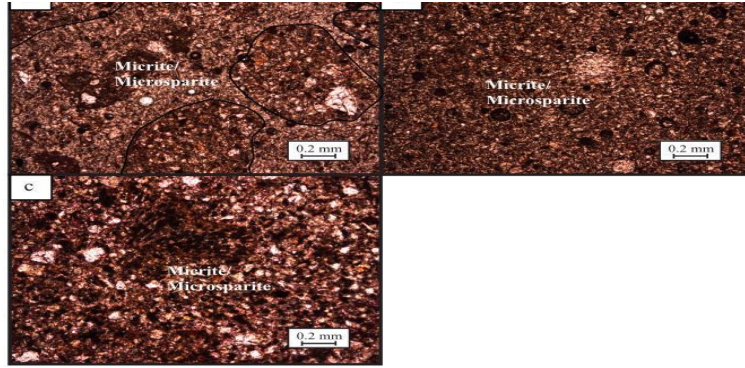


Figure S4. Examples of Washtucna paleosol thin sections in plane polarized light. Thin sections are carbonate stained with alizarin red-s and potassium ferricyanide, and show the area containing micrite.

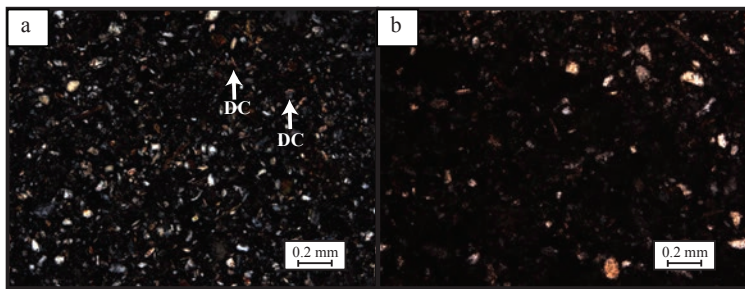


Figure S5. Examples of Sand Hills Coulee paleosol thin sections in cross-polarized light. White arrows are pointing to detrital limestone or marble (DC) giving second and third order red, blues and yellows.

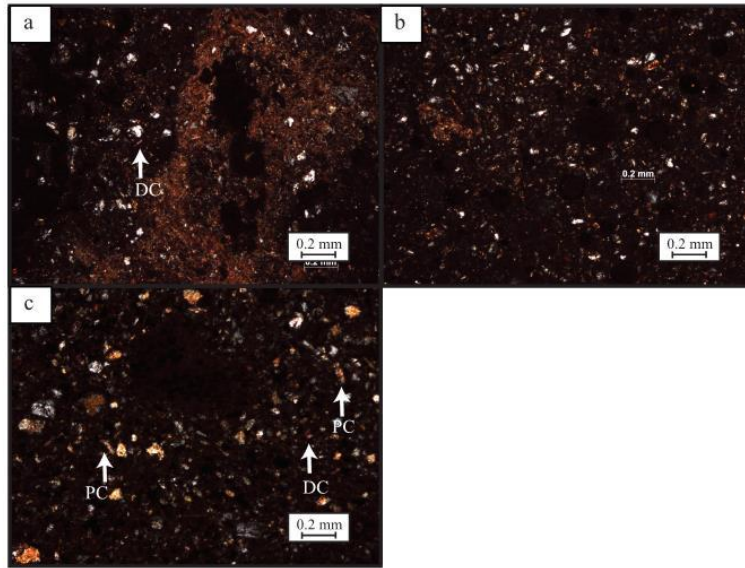


Figure S6. Examples of Washtucna paleosol thin sections in cross-polarized light. White arrows are pointing to detrital limestone or marble (DC) or pedogenic carbonate coatings (PC) within and around a mineral grain in second and third order red, blues, and yellows.

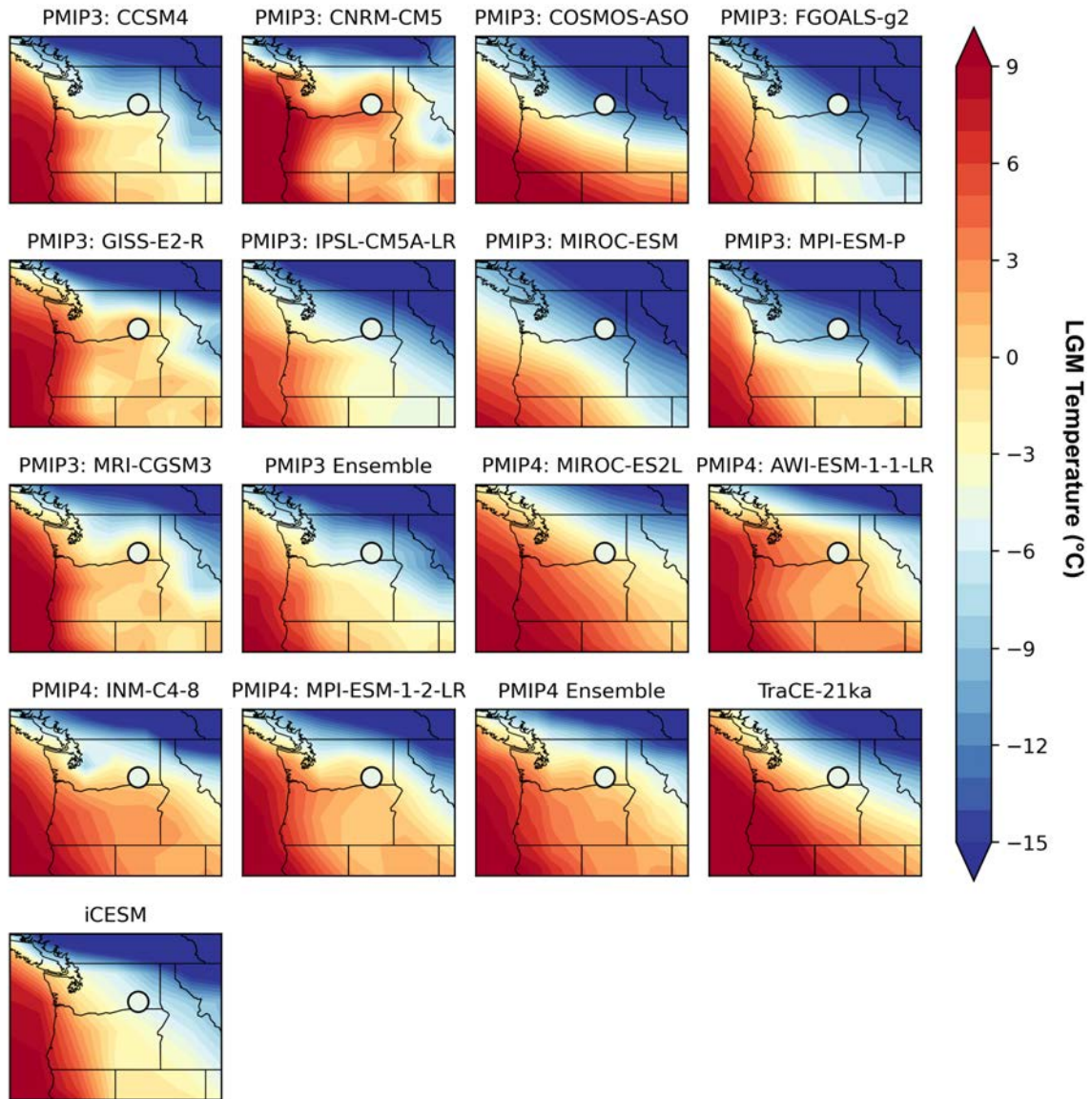


Figure S6: LGM temperatures for available models (PMIP3, PMIP4, TraCE-21ka, iCESM) compared to clumped isotope (circle; this work).

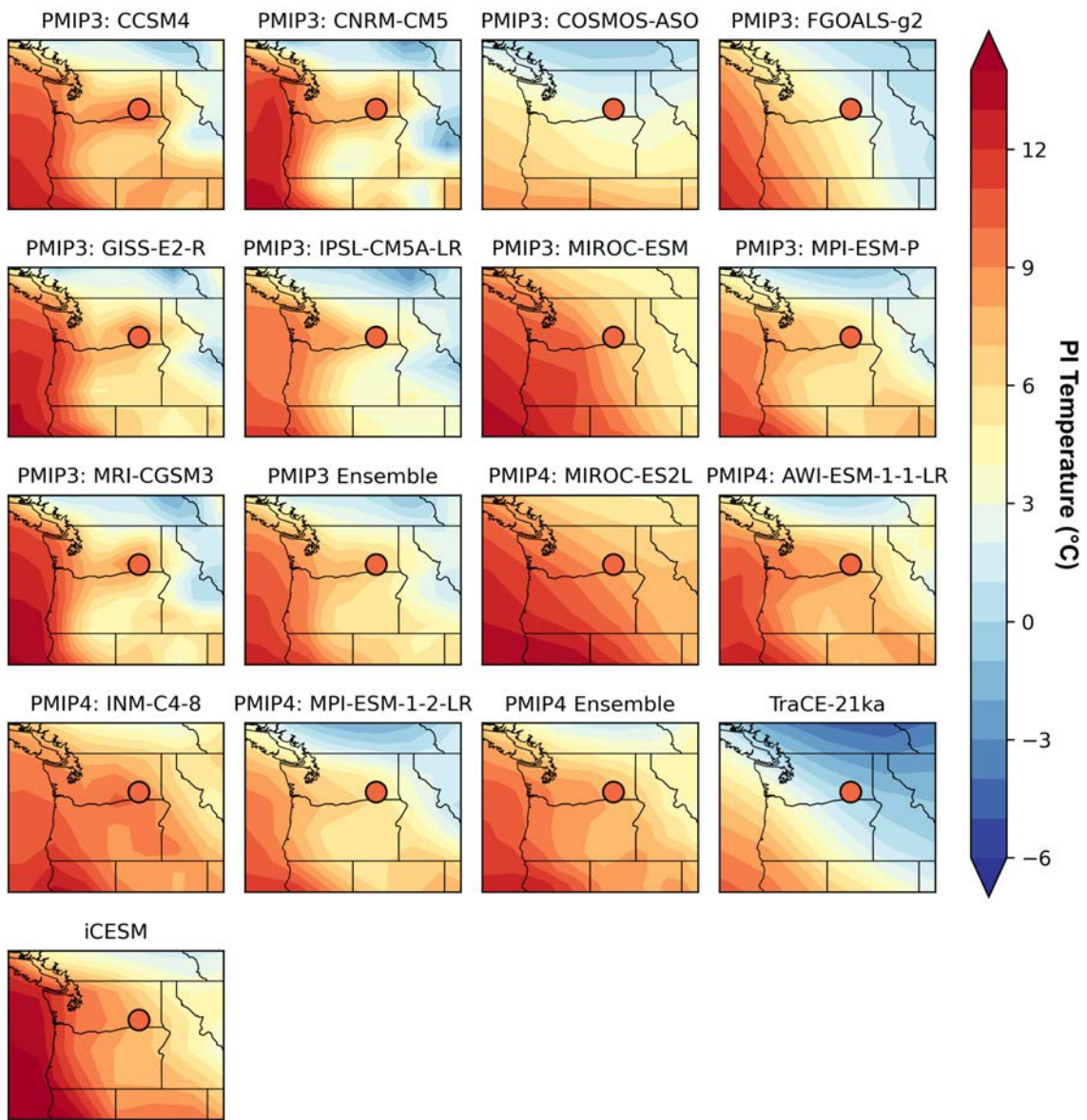


Figure S7: Pre-industrial temperatures for available models (PMIP3, PMIP4, TraCE-21ka, iCESM) compared to modern values (PRISM Climate Group, 2018).

Supporting Tables are in a separate excel file.

Table S1. Mg/Ca and Mn/Ca Ratios of Bulk Carbonate.

Sample I.D.	Sample Type	Horizon	Bulk Carbonate Major Elements			Bulk Carbonate Ratios	
			Ca (mmol)	Mg (mmol)	Mn (micro mol)	Mg/Ca (mol/mol)	Mn/Ca (mmol/mol)
AY-1							
AY1SHC	Micritic Carbonate	Bkb1	0.29 +/- 0.01	0.02 +/- 0.00	0.04 +/- 0.00	0.05 +/- 0.03	0.13 +/- 0.03
AY1W3B	Micritic Carbonate/Carbonate Seam	Bkqmb2	0.73 +/- 0.01	0.02 +/- 0.00	0.02 +/- 0.00	0.02 +/- 0.01	0.03 +/- 0.01
AY1W3D	Micritic Carbonate/Carbonate Seam	Bkqmb2/Bkqb2	0.29 +/- 0.00	0.02 +/- 0.00	0.02 +/- 0.00	0.06 +/- 0.01	0.07 +/- 0.00
KP-1							
KP1W	Micritic Carbonate	Bwb2	0.31 +/- 0.01	0.01 +/- 0.00	0.01 +/- 0.00	0.04 +/- 0.02	0.03 +/- 0.02
WA-3							
WA3SHC	Micritic Carbonate	Bkb1	0.37 +/- 0.01	0.02 +/- 0.00	0.01 +/- 0.00	0.05 +/- 0.03	0.04 +/- 0.03

Table S2: Age Constraints. TL = thermoluminescence; ¹⁴C AMS = radiocarbon

Site	Unit	Material Dated	Age Estimate (ka)	Uncertainty	Method	Stratigraphic Context
KP-1	Sand Hills Coulee	Loess	14.0	+/- 2.4	TL	Straddling above MSH S tephra, slightly above Berger and Busacca, 1995.
KP-1	Sand Hills Coulee	Loess	17.0	+/- 2.6	TL	Straddling above MSH S tephra.
CHR-1	Sand Hills Coulee	Loess	8.2	+/- 1.6	TL	Located 77 cm above the cap of the Washtucna soil.
McFeely	Sand Hills Coulee	Gastropod	12.48	+/- 0.06	14C AMS	Above MSH S tephra and below Glacier Peak Tephra (lengths are not provided by the authors).
KP-1	Washtucna	Loess	20.4	+/- 1.4	TL	Straddling below MSH S tephra.
KP-1	Washtucna	Loess	17.2	+/- 1.9	TL	Straddling below MSH S tephra, slightly above Berger and Busacca, 1995.
CON-1	Washtucna	Loess	20.5	+/- 1.8	TL	Straddling below MSH S tephra.
CHR-1	Washtucna	Loess	33.2	+/- 3.4	TL	Located 58 cm below the base of the Sand Hills Coulee.
CLY-2	Washtucna	Loess	23.7	+/- 2.0	TL	Located approximately 160 cm below the MSH S Tephra.
CLY-2	Washtucna	Loess	36.1	+/- 4.3	TL	Located approximately 270 cm below the MSH S Tephra.
CLY-2	Washtucna	Loess	40.1	+/- 3.7	TL	Located approximately 370 cm below the MSH S Tephra.
Marias Pass	Glacier Peak Tephra	Twig Fragments	11.6 Cal.	+/- 0.05	14C AMS	Located below the cap of the Sand Hills Coulee soil.
NA	MSH S Tephra	NA	15.4 Cal.	+/- 0.1	14C AMS	Separates the Sand Hills Coulee soil and Washtucna soil, overlain by L1 loess and underlain by L2 loess.

Table S3. AY-1 and AY-2 Field Descriptions.

Site	Unit	Depth (cm)	Horizon	Dry Color
AY-1	Sand Hills Coulee	81	Bkb1	2.5Y6/3
		190	BCb1	2.5Y6/3
	Washtucna	331	Bwkb2	2.5Y6/3
		421	Bkqmb2	2.5Y7/2
		479	Bkqb2	2.5Y6/3
		544	Bkqmb2	2.5Y7/2
		580	Bkqb2	2.5Y6/3
		630	BCb2	2.5Y6/3
AY-2	Sand Hills Coulee	140	Bkb1	2.5Y5/3
		230	BCb1	2.5Y6/3
	Washtucna	320	Bwkb2	2.5Y5/4
		390	Bkqb2	2.5Y6/3
		480	Bkqmb2	2.5Y7/2
		520	Bkqb2	2.5Y6/3
		553	BCb2	2.5Y6/3

Table S4. Air Temperature Transfer Functions and modern climate data (monthly air temperatures from PRISM Climate Group, 2017, and modern carbonate formation temperatures from Takeuchi et al., 2009).

Air Temperature Interval	Equation	R ₂	Source
Mean Annual	MAAT = 1.20*TC(D47) - 21.72	0.92	Quade et al., 2012
June-August	WAMT = 1.13*TC(D47) - 10.81	0.89	Quade et al., 2012

Month	Monthly Mean Air Temperatures	MAT Modern	WAMT Modern	Carbonate Formation Temperatures
Jan	0.6	10.9	21.2	14.6 °C to 20.7 °C
Feb	2.8			
March	6.7			
Apr	10.3			
May	14.4			
Jun	18.3			
Jul	22.6			
Aug	22.6			
Sep	17.7			
Oct	11.1			
Nov	4.6			
Dec	-0.3			

Table S5: PMIP3 simulation results used for this work. All data regridded and output to 46.5 °N, 118.5 °W. Model and simulation descriptions are in Bracconot et al. (2012).

Time (ka)	Temperature		Change in T	
	MAT (K)	JJA Temp (K)	MAT (C)	JJA Temp (C)
22	266.6	276.7	-6.55	3.55
21	266.5	276.7	-6.65	3.55
20	266.6	277.3	-6.55	4.15
19	266.5	277.6	-6.65	4.45
18	266.7	278.3	-6.45	5.15
17	267.3	279.6	-5.85	6.45
16	268.5	281.7	-4.65	8.55
15	270	283.3	-3.15	10.15
14	271.5	284.5	-1.65	11.35
13	272.5	284.8	-0.65	11.65
12	272.9	284.5	-0.25	11.35
11	273.6	285.2	0.45	12.05
10	273.9	285.3	0.75	12.15
9	273.9	285.1	0.75	11.95
8	273.9	284.6	0.75	11.45
7	274.1	284.4	0.95	11.25
6	273.9	284	0.75	10.85
5	274	283.9	0.85	10.75
4	274	283.7	0.85	10.55
3	274	283.5	0.85	10.35
2	274	283.5	0.85	10.35
1	273.9	283.5	0.75	10.35
0	273.9	283.5	0.75	10.35

Table S6: TraCE21k simulation results used for this work. Data for 46.4 °N,240 °E was averaged over 100 years around age. Model and simulation descriptions are in Liu et al. (2009).

PMIP3 MODELS: (46.5N,118.5W)

Model	PI MAT (C)	LGM MAT (C)	Temperature Anomaly (C)
CCSM4	9.07	-6.14	-15.21
CNRM-CM5	8.35	3.24	-5.11
COSMOS-ASO	3.05	-12.81	-15.86
FGOALS-g2	3.34	-11.72	-15.06
GISS-E2-R	9.48	2.09	-7.39
IPSL-CM5A-LR	7.92	-6.19	-14.11
MIROC-ESM	6.70	-10.88	-17.58
MPI-ESM-P	6.16	-10.33	-16.49
MRI-CGCM3	8.74	0.21	-8.54
PMIP3 Ensemble	6.98	-5.92	-12.90

PMIP4 MODELS: (46.5N,118.5W)

Model	PI MAT (C)	LGM MAT (K)	Temperature Anomaly (C)
MIROC-ES2L	7.97	-1.07	-9.05
AWI-ESM-1-1-LR	7.85	1.72	-6.13
INM-CM4-8	9.79	0.77	-9.02
MPI-ESM-1-2-LR	5.61	0.54	-5.07
PMIP4 Ensemble	7.67	-0.35	-8.02
iCESM	6.97	-6.28	-13.25
TraCE	0.75	-6.60	-7.35

Table S7: Stable isotope data for samples and standards.

ID	Identifier_1	Mass Spec	Easotope Name	Acid Temp	Acquisitions	abled	Acquisiti	3C VPDB	(RaC	VPDB	(Raw/C	VPDB	(Raw/	80 VPDB	(RaO	VPDB	(Raw/O	VPDB	(Raw)	O VSMOW	(Ri	VSMOW	(Ra
R1	2015-11-02 11:21 PST	Bonedry 5.90mb UH RD+MG 4/14	Chewbacca	Unheated gas	9	9	-37.89	0.01	0	-25.06	0.01	0	5.02	0.01									
R2	2015-11-04 11:17 PST	Evap DI+CM 5.85mb UH MG 11/13	Chewbacca	Unheated gas	8	8	2.48	0.01	0	17.68	0.01	0.01	49.08	0.01									
R1	2015-11-04 17:25 PST	50 B1 AY2W3B 1/2	Chewbacca	AY2W3B	90	9	-5.46	0.01	0	-4.43	0.01	0	26.29	0.01									
R3	2015-11-04 23:40 PST	4 A3 carrera marble	Chewbacca	Carrara Marble	90	9	1.97	0.01	0	6.43	0.01	0	37.49	0.01									
R4	2015-11-05 01:47 PST	5 B12 carmel chalk	Chewbacca	Carmel Chalk	90	9	-2.32	0.01	0	4.01	0.02	0.01	34.99	0.02									
R2	2015-11-05 16:35 PST	11 C9 AY2W3B-1-3-14 (1/3)	Chewbacca	AY2W3B	90	9	-5.26	0.01	0	-4.49	0.01	0	26.23	0.01									
R5	2015-11-06 02:57 PST	22 D5 ETH-4	Chewbacca	ETH-4-1	90	9	-10.14	0.01	0	-10.88	0.01	0	19.65	0.01									
R6	2015-11-06 05:04 PST	23 A4 CARRERA MARBLE	Chewbacca	Carrara Marble	90	9	1.95	0.01	0	6.28	0.01	0	37.33	0.01									
R7	2015-11-07 01:56 PST	40 A3 SET 2 VEINSTROM	Chewbacca	Veinstrom	90	9	-6.09	0.01	0	-4.67	0.01	0	26.04	0.01									
R3	2015-11-07 16:45 PST	45 C4 AYLW3B-1-3-24 (1/3)	Chewbacca	AY2W3B	90	9	-6.06	0.01	0	-5.23	0.01	0	25.47	0.01									
R8	2015-11-09 15:37 PST	21 C1 ETH-3	Chewbacca	ETH-3-1	90	9	1.68	0.01	0	6.07	0.01	0	37.12	0.01									
R9	2015-11-09 17:43 PST	22 D1 ETH-4	Chewbacca	ETH-4-1	90	9	-10.11	0	0	-10.92	0.01	0	19.61	0.01									
R10	2015-11-10 11:41 PST	Bonedry 5.54mb 01/08 RD	Chewbacca	Unheated gas	9	9	-37.54	0.01	0	-26.04	0.01	0	4.01	0.01									
R11	2015-11-11 21:59 PST	42 A5 VEINSTROM	Chewbacca	Veinstrom	90	9	-6.19	0.01	0	-4.76	0.01	0	25.95	0.02									
R12	2015-11-12 11:44 PST	Evap DI+CM H 5.79mb 1/20 RD	Chewbacca	Heated Gas	9	9	2.36	0.01	0	8.75	0.01	0	39.88	0.01									
R13	2015-11-13 00:36 PST	5 A8 CARRERA MARBLE	Chewbacca	Carrara Marble	90	9	2.04	0.01	0	6.41	0.01	0	37.47	0.01									
R14	2015-11-13 04:52 PST	7 C2 CARMEL CHALK	Chewbacca	Carmel Chalk	90	9	-2.26	0.01	0	3.85	0.01	0	34.83	0.01									
R1	2015-11-13 11:27 PST	8 B9 AY1SHC-1-5-14 (1/5)	Chewbacca	AY1SHC	90	9	-4.43	0	0	-4.54	0.01	0	26.18	0.01									
R2	2015-11-13 13:28 PST	13 C2 AY1SHC-1-5-24 (1/5)	Chewbacca	AY1SHC	90	9	-4.43	0	0	-4.45	0.01	0	26.27	0.01									
R3	2015-11-13 15:34 PST	18 C7 AY1SHC-1-5-34 (1/5)	Chewbacca	AY1SHC	90	9	-4.39	0.01	0	-4.49	0.01	0	26.23	0.01									
R15	2015-11-13 19:42 PST	24 A3 ETH-1	Chewbacca	ETH-1-1	90	9	1.81	0.01	0	5.54	0.01	0	36.57	0.01									
R16	2015-11-15 12:44 PST	31 Cararra A11	Chewbacca	Carrara Marble	90	9	2.01	0	0	6.39	0.01	0	37.45	0.01									
R17	2015-11-15 14:55 PST	32 A8 Veinstrom	Chewbacca	Veinstrom	90	9	-6.16	0	0	-4.75	0.01	0	25.96	0.01									
R18	2015-11-15 23:32 PST	36 D3 ETH-4	Chewbacca	ETH-4-1	90	9	-10.26	0	0	-11	0.01	0	19.52	0.01									
R19	2015-11-17 13:29 PST	Evap DI+CM6.33mb WD 10/30/2014	Chewbacca	Unheated gas	9	9	-8.83	0.01	0	14.07	0.02	0.01	45.37	0.02									
R4	2015-11-17 15:39 PST	48 C12 AYLSHC-1-5-44(1/5)	Chewbacca	AY1SHC	90	10	-4.14	0	0	-4.41	0.01	0	26.31	0.01									
R20	2015-11-18 12:53 PST	Bonedry UH 5.63 mbar MG 6/24	Chewbacca	Unheated gas	9	9	-37.87	0.01	0	-25.49	0.01	0	4.58	0.01									
R21	2015-11-19 14:16 PST	19 B1 CARRERA MARBLE	Chewbacca	Carrara Marble	90	9	2.06	0	0	6.37	0.01	0	37.42	0.01									
R22	2015-11-20 23:22 PST	32 C10 carmel chalk	Chewbacca	Carmel Chalk	90	9	-2.23	0.01	0	3.93	0.01	0	34.91	0.01									
R23	2015-11-23 11:08 PST	Bonedry 5.65mb H 4/8 RD	Chewbacca	Heated Gas	9	9	-38.08	0.01	0	-23.54	0.01	0	6.59	0.01									
R24	2015-11-23 15:19 PST	46 G3 ETH-3	Chewbacca	ETH-3-1	90	9	1.71	0.01	0	6.14	0.01	0	37.19	0.01									
R25	2015-11-23 23:40 PST	50 H2 ETH-4	Chewbacca	ETH-4-1	90	9	-10.14	0.01	0	-10.94	0.01	0	19.58	0.01									
R26	2015-11-24 11:37 PST	Evap DI+CM 5.51 mb H 6/26 MG	Chewbacca	Heated Gas	9	9	1.57	0.01	0	4.36	0.01	0	35.36	0.01									
R27	2015-11-25 05:34 PST	9 E4 ETH-1	Chewbacca	ETH-1-1	90	9	2	0.01	0	5.71	0.01	0	36.75	0.01									
R28	2015-11-27 20:01 PST	34 Carmel Chalk D1	Chewbacca	Carmel Chalk	90	9	-2.22	0.01	0	3.87	0.01	0	34.85	0.01									
R29	2015-11-28 14:39 PST	39 Veinstrom B3	Chewbacca	Veinstrom	90	9	-6.08	0.01	0	-4.88	0.02	0.01	25.83	0.02									
R30	2015-11-28 17:50 PST	41 Carmel Chalk	Chewbacca	Carmel Chalk	90	9	-2.17	0.01	0	3.75	0.01	0	34.72	0.01									
R31	2015-11-30 12:38 PST	Evap Bonedry UH 6.03 mb	Chewbacca	Unheated gas	9	9	-37.57	0.01	0	-2.79	0.01	0	27.98	0.01									
R32	2015-12-01 13:03 PST	Evap DI+CM 5.73MB H	Chewbacca	Unheated gas	9	9	2.9	0.01	0	12.14	0.01	0	43.38	0.01									
R33	2016-06-13 17:09 PDT		R2D2-SarlaccBel	Heated Gas	4	4	-38.18	0	0	-3.3	0	0	27.45	0									
R34	2016-06-13 18:48 PDT		R2D2-SarlaccBel	Unheated gas	4	4	-37.25	0	0	-0.51	0	0	30.34	0									
R35	2016-06-14 01:24 PDT		R2D2-SarlaccBel	ETH-4-1	90	4	-10.13	0	0	-10.61	0	0	19.93	0									
R36	2016-06-14 11:22 PDT		R2D2-SarlaccBel	Carmel Chalk	90	4	-2.32	0	0	4.15	0	0	35.14	0									
R37	2016-06-14 13:01 PDT		R2D2-SarlaccBel	TV03	90	4	2.51	0	0	-0.22	0	0	30.63	0									
R38	2016-06-14 14:40 PDT		R2D2-SarlaccBel	Carrara Marble	90	4	2.05	0	0	6.64	0	0	37.71	0									
R39	2016-06-14 16:19 PDT		R2D2-SarlaccBel	Veinstrom	90	4	-6.17	0	0	-4.55	0	0	26.17	0									
R40	2016-06-15 11:51 PDT		R2D2-SarlaccBel	Unheated gas	4	4	1.98	0	0	29.72	0	0	61.49	0									
R41	2016-06-15 13:29 PDT		R2D2-SarlaccBel	Unheated gas	4	4	-37.55	0	0	-0.38	0	0	30.46	0									
R42	2016-06-15 15:09 PDT		R2D2-SarlaccBel	Heated Gas	4	4	1.9	0	0	22.7	0	0	54.26	0									
R43	2016-06-15 16:49 PDT		R2D2-SarlaccBel	Heated Gas	4	4	-37.34	0	0	-2.17	0	0	28.63	0									
R44	2016-06-16 14:29 PDT		R2D2-SarlaccBel	Unheated gas	4	4	1.9	0	0	29.42	0	0	61.18	0									
R45	2016-06-16 18:09 PDT		R2D2-SarlaccBel	ETH-4-1	90	4	-10.12	0	0	-10.5	0	0	20.04	0									
R46	2016-06-17 11:54 PDT		R2D2-SarlaccBel	Unheated gas	4	4	-38.2	0	0	-1.62	0	0	29.2	0									
R47	2016-06-18 15:47 PDT		R2D2-SarlaccBel	TV03	90	4	2.48	0	0	-0.21	0	0	30.64	0									
R48	2016-06-20 18:53 PDT		R2D2-SarlaccBel	Veinstrom	90	4	-6.01	0	0	-4.09	0	0	26.65	0									
R49	2016-06-21 01:56 PDT		R2D2-SarlaccBel	Carrara Marble	90	4	1.98	0	0	6.88	0	0	37.95	0									
R50	2016-06-23 16:44 PDT		R2D2-SarlaccBel	Unheated gas	4	4	1.97	0	0	24.23	0	0	55.84	0									
R51	2016-06-23 18:23 PDT		R2D2-SarlaccBel	Carrara Marble	90	4	1.98	0	0	6.64	0	0	37.7	0									
R52	2016-06-25 00:44 PDT		R2D2-SarlaccBel	ETH-2-1	90	4	-10.11	0	0	-10.51	0	0	20.02	0									
R53	2016-06-25 11:01 PDT		R2D2-SarlaccBel	Heated Gas	4	4	2.45	0	0	7.25	0	0	38.33	0									
R54	2016-06-27 18:56 PDT		R2D2-SarlaccBel	Unheated gas	4	4	2.04	0	0	29.51	0	0	61.28	0									
R55	2016-06-27 20:35 PDT		R2D2-SarlaccBel	Veinstrom	90	4	-6.21	0	0	-4.51	0	0	26.22	0									
R56	2016-06-28 16:54 PDT		R2D2-SarlaccBel	Unheated gas	4	4	-37.24	0.55	0.27	-0.27	0.09	0.04	30.58	0.09									
R57	2016-06-29 14:33 PDT		R2D2-SarlaccBel	ETH-1-1	90	4	1.99	0	0	6.21	0	0	37.26	0									
R58	2016-06-30 14:50 PDT		R2D2-SarlaccBel	Unheated gas	4	4	-37.69	0	0	-2.88	0	0	27.89	0									

R59	2016-06-30 16:29 PDT	R2D2-SarlaccBel	Veinstrom	90	4	4	-6.18	0	0	-4.31	0	0	26.42	0
R60	2016-06-30 23:07 PDT	R2D2-SarlaccBel	TV03	90	4	4	2.51	0	0	0.13	0	0	31	0
R61	2016-07-06 20:55 PDT	R2D2-SarlaccBel	ETH-2-1	90	4	4	-10.11	0	0	-10.73	0	0	19.8	0
R62	2016-07-07 15:57 PDT	R2D2-SarlaccBel	Veinstrom	90	4	4	-6.16	0	0	-4.59	0	0	26.13	0
R63	2016-07-08 12:59 PDT	R2D2-SarlaccBel	Unheated gas	90	4	4	-37.36	0	0	-0.46	0	0	30.38	0
R64	2016-07-08 17:59 PDT	R2D2-SarlaccBel	Carrara Marble	90	4	4	2.01	0	0	6.66	0	0	37.73	0
R65	2016-07-09 00:37 PDT	R2D2-SarlaccBel	Carmel Chalk	90	4	4	-2.25	0	0	4.24	0	0	35.23	0
R66	2016-07-12 00:40 PDT	R2D2-SarlaccBel	ETH-4-1	90	4	4	-10.17	0	0	-10.63	0	0	19.9	0
R67	2016-07-12 16:05 PDT	R2D2-SarlaccBel	Heated Gas	90	4	4	2.59	0	0	14.51	0	0	45.81	0
R68	2016-07-12 17:45 PDT	R2D2-SarlaccBel	Heated Gas	90	4	4	-37.98	0	0	-6.26	0	0	24.41	0
R69	2016-07-13 12:25 PDT	R2D2-SarlaccBel	Unheated gas	90	4	4	2.04	0	0	28.93	0	0	60.68	0
R1	2016-07-13 14:05 PDT	R2D2-SarlaccBel	KP1W	90	4	4	-4.19	0	0	-4.98	0.01	0	25.73	0.01
R70	2016-07-14 15:58 PDT	R2D2-SarlaccBel	Carmel Chalk	90	4	4	-2.18	0	0	4.23	0	0	35.22	0
R2	2016-07-14 17:38 PDT	R2D2-SarlaccBel	KP1W	90	4	4	-4.05	0	0	-4.62	0	0	26.1	0
R4	2016-07-14 19:18 PDT	R2D2-SarlaccBel	AY2W3B	90	4	4	-5.51	0	0	-3.77	0	0	26.97	0
R71	2016-07-14 20:58 PDT	R2D2-SarlaccBel	ETH-1-1	90	4	4	2.06	0	0	5.97	0	0	37.02	0
R72	2016-07-15 12:55 PDT	R2D2-SarlaccBel	Unheated gas	90	4	4	-37.83	0	0	-1.19	0	0	29.64	0
R73	2016-07-15 14:35 PDT	R2D2-SarlaccBel	ETH-2-1	90	4	4	-10.1	0	0	-10.67	0	0	19.86	0
R3	2016-07-15 18:29 PDT	R2D2-SarlaccBel	KP1W	90	4	4	-4.11	0	0	-4.78	0	0	25.93	0
R5	2016-07-15 20:08 PDT	R2D2-SarlaccBel	AY2W3B	90	4	4	-5.55	0	0	-3.94	0	0	26.8	0
R1	2016-07-15 21:57 PDT	R2D2-SarlaccBel	AY2SHC	90	4	4	-4.4	0	0	-3.33	0	0	27.43	0
R74	2016-07-19 16:12 PDT	R2D2-SarlaccBel	Heated Gas	90	4	4	-37.31	0.01	0.01	-5.28	0.01	0.01	25.42	0.01
R75	2016-07-19 17:52 PDT	R2D2-SarlaccBel	Veinstrom	90	4	4	-6.14	0	0	-4.65	0	0	26.06	0
R76	2016-07-20 00:33 PDT	R2D2-SarlaccBel	Carmel Chalk	90	4	4	-2.36	0	0	4.2	0	0	35.19	0
R77	2016-07-20 17:42 PDT	R2D2-SarlaccBel	Carmel Chalk	90	4	4	-2.26	0	0	4.14	0	0	35.13	0
R2	2016-07-20 19:21 PDT	R2D2-SarlaccBel	AY2SHC	90	4	4	-4.14	0	0	-3.07	0	0	27.7	0
R6	2016-07-21 16:44 PDT	R2D2-SarlaccBel	AY2W3B	90	4	4	-5.54	0	0	-3.49	0	0	27.26	0
R1	2016-07-21 18:28 PDT	R2D2-SarlaccBel	WA3SHC	90	4	4	-6.72	0	0	-5.34	0	0	25.36	0
R3	2016-07-21 20:08 PDT	R2D2-SarlaccBel	AY2SHC	90	4	4	-4.74	0	0	-3.45	0	0	27.3	0
R78	2016-07-22 16:32 PDT	R2D2-SarlaccBel	Veinstrom	90	4	4	-6.03	0.02	0.01	-4.6	0.01	0.01	26.12	0.01
R2	2016-07-22 21:32 PDT	R2D2-SarlaccBel	WA3SHC	90	4	4	-6.47	0	0	-5.43	0	0	25.26	0
R79	2016-07-22 23:11 PDT	R2D2-SarlaccBel	Carmel Chalk	90	4	4	-2.13	0	0	4.12	0	0	35.11	0
R3	2016-07-23 00:51 PDT	R2D2-SarlaccBel	WA3SHC	90	4	4	-6.56	0	0	-5.57	0	0	25.12	0
R80	2016-07-23 14:36 PDT	R2D2-SarlaccBel	Unheated gas	90	4	4	-37.43	0	0	-0.51	0	0	30.33	0
R81	2016-07-23 16:16 PDT	R2D2-SarlaccBel	TV03	90	4	4	2.61	0	0	-0.26	0	0	30.59	0
R82	2016-07-24 13:49 PDT	R2D2-SarlaccBel	Unheated gas	90	4	4	2.15	0	0	29.89	0	0	61.67	0
R1	2016-07-25 19:35 PDT	R2D2-SarlaccBel	KP1SHC	90	4	4	-2.46	0	0	-4.38	0	0	26.34	0
R83	2016-07-25 22:53 PDT	R2D2-SarlaccBel	Carmel Chalk	90	4	4	-2.18	0	0	4.17	0	0	35.16	0
R2	2016-07-26 03:51 PDT	R2D2-SarlaccBel	KP1SHC	90	4	4	-2.57	0	0	-4.45	0	0	26.28	0
R84	2016-07-27 14:44 PDT	R2D2-SarlaccBel	Heated Gas	90	4	4	2.46	0	0	7.85	0	0	38.95	0
R85	2016-07-27 18:05 PDT	R2D2-SarlaccBel	Unheated gas	90	4	4	2.05	0	0	9.74	0	0	40.9	0
R86	2016-07-28 02:38 PDT	R2D2-SarlaccBel	TV03	70	4	4	2.5	0	0	0	0	0	30.86	0
R87	2016-07-28 15:03 PDT	R2D2-SarlaccBel	Unheated gas	90	4	4	-37.33	0	0	-2.16	0	0	28.63	0
R88	2016-07-28 16:43 PDT	R2D2-SarlaccBel	Unheated gas	90	4	4	2.34	0	0	10.7	0	0	41.9	0
R89	2016-07-29 10:57 PDT	R2D2-SarlaccBel	Heated Gas	90	4	4	-37.63	0	0	-7.52	0	0	23.1	0
R3	2016-07-29 12:36 PDT	R2D2-SarlaccBel	KP1SHC	90	4	4	-2.69	0	0	-4.43	0	0	26.29	0
R4	2016-07-29 14:16 PDT	R2D2-SarlaccBel	AY2SHC	90	4	4	-4.28	0	0	-3.13	0	0	27.64	0
R90	2016-07-29 17:04 PDT	R2D2-SarlaccBel	Heated Gas	90	4	4	2.34	0	0	3.43	0	0	34.39	0
R91	2016-07-29 18:42 PDT	R2D2-SarlaccBel	ETH-3-1	90	4	4	1.75	0	0	6.52	0	0	37.58	0
R92	2016-07-30 01:47 PDT	R2D2-SarlaccBel	Veinstrom	90	4	4	-6.15	0	0	-4.48	0	0	26.24	0
R93	2016-07-30 13:59 PDT	R2D2-SarlaccBel	ETH-4-1	90	4	4	-10.16	0	0	-10.72	0	0	19.81	0
R94	2016-07-30 22:47 PDT	R2D2-SarlaccBel	Carrara Marble	90	4	4	2.07	0	0	6.63	0	0	37.69	0
R95	2016-07-31 21:41 PDT	R2D2-SarlaccBel	ETH-1-1	90	4	4	2.08	0	0	6.14	0	0	37.19	0
R96	2016-08-01 12:33 PDT	R2D2-SarlaccBel	Unheated gas	90	4	4	2.41	0	0	10.7	0	0	41.89	0
R97	2016-08-01 14:12 PDT	R2D2-SarlaccBel	Unheated gas	90	4	4	-37.28	0	0	-0.21	0	0	30.65	0
R98	2016-08-01 18:53 PDT	R2D2-SarlaccBel	Carmel Chalk	90	4	4	-2.15	0	0	4.09	0	0	35.08	0
R99	2016-08-01 20:33 PDT	R2D2-SarlaccBel	TV03	90	4	4	2.62	0	0	-0.41	0	0	30.43	0
R100	2016-08-01 23:53 PDT	R2D2-SarlaccBel	Carrara Marble	90	4	4	2.08	0	0	6.55	0	0	37.61	0
R101	2016-08-02 01:33 PDT	R2D2-SarlaccBel	Carmel Chalk	90	4	4	-2.12	0.01	0.01	4.12	0.07	0.04	35.11	0.07
R102	2016-08-02 10:51 PDT	R2D2-SarlaccBel	Heated Gas	90	4	4	2.43	0	0	7.34	0	0	38.42	0
R103	2016-08-02 12:31 PDT	R2D2-SarlaccBel	Heated Gas	90	4	4	-37.57	0	0	-4.52	0	0	26.2	0
R104	2016-08-02 22:20 PDT	R2D2-SarlaccBel	ETH-2-1	90	4	4	-10.2	0	0	-10.69	0	0	19.84	0
R105	2016-08-03 13:48 PDT	R2D2-SarlaccBel	Unheated gas	90	4	4	2.35	0	0	10.42	0	0	41.6	0
R106	2016-08-03 15:27 PDT	R2D2-SarlaccBel	Unheated gas	90	4	4	-37.56	0	0	-0.69	0	0	30.15	0
R107	2016-08-03 17:06 PDT	R2D2-SarlaccBel	ETH-4-1	90	4	4	-10.17	0	0	-10.73	0	0	19.8	0
R108	2016-08-03 23:49 PDT	R2D2-SarlaccBel	ETH-3-1	90	4	4	1.7	0	0	6.5	0	0	37.56	0
R109	2016-08-04 17:54 PDT	R2D2-SarlaccBel	Unheated gas	90	4	4	2.78	0	0	10.64	0	0	41.82	0
R110	2016-08-04 19:33 PDT	R2D2-SarlaccBel	Carmel Chalk	90	4	4	-2.21	0	0	4.17	0	0	35.15	0

R111	2016-08-04 22:54 PDT	R2D2-SarlaccBel	Veinstrom	90	4	4	-6.18	0.01	0	-4.61	0	0	26.11	0
R112	2016-08-05 16:10 PDT	R2D2-SarlaccBel	Unheated gas		4	4	2.47	0	0	10.36	0	0	41.54	0
R113	2016-08-05 17:50 PDT	R2D2-SarlaccBel	Carrara Marble	90	4	4	2.08	0	0	6.63	0	0	37.7	0
R114	2016-08-05 19:29 PDT	R2D2-SarlaccBel	Carmel Chalk	90	4	4	-2.22	0	0	4.21	0	0	35.2	0
R115	2016-08-05 21:10 PDT	R2D2-SarlaccBel	Veinstrom	90	4	4	-6.09	0	0	-4.53	0	0	26.19	0
R116	2016-08-05 22:50 PDT	R2D2-SarlaccBel	Carrara Marble	90	4	4	2.06	0	0	6.61	0	0	37.67	0
R117	2016-08-08 13:48 PDT	R2D2-SarlaccBel	Unheated gas		4	4	2.72	0	0	10.62	0	0	41.8	0
R118	2016-08-08 16:53 PDT	R2D2-SarlaccBel	Unheated gas		4	4	2.95	0	0	10.72	0	0	41.91	0
R119	2016-08-08 20:14 PDT	R2D2-SarlaccBel	ETH-2-1	90	4	4	-10.1	0.1	0.05	-10.71	0.08	0.04	19.82	0.08
R120	2016-08-08 21:56 PDT	R2D2-SarlaccBel	TV03	90	4	4	2.53	0	0	-0.33	0	0	30.52	0
R121	2016-08-08 23:37 PDT	R2D2-SarlaccBel	Carrara Marble	90	4	4	2.27	0.05	0.03	6.34	0.11	0.05	37.4	0.11
R122	2016-08-09 17:54 PDT	R2D2-SarlaccBel	Heated Gas		4	4	-37.38	0	0	-23.58	0	0	6.55	0
R123	2016-08-10 10:21 PDT	R2D2-SarlaccBel	Heated Gas		4	4	2.46	0	0	5.78	0	0	36.81	0
R124	2016-08-10 13:51 PDT	R2D2-SarlaccBel	Carrara Marble	90	4	4	2.08	0	0	6.61	0	0	37.67	0
R125	2016-08-10 17:56 PDT	R2D2-SarlaccBel	Unheated gas		4	4	-38.12	0	0	-1.57	0.03	0.01	29.24	0.03
R126	2016-08-10 19:37 PDT	R2D2-SarlaccBel	Carmel Chalk	90	4	4	-2.19	0	0	4.17	0	0	35.16	0
R127	2016-08-11 16:58 PDT	R2D2-SarlaccBel	Heated Gas		4	4	2.42	0	0	7.09	0	0	38.17	0
R128	2016-08-11 18:37 PDT	R2D2-SarlaccBel	Carmel Chalk	90	4	4	-2.14	0	0	4.24	0	0	35.23	0
R129	2016-08-11 20:17 PDT	R2D2-SarlaccBel	Carrara Marble	90	4	4	2.33	0	0	6.47	0	0	37.53	0
R130	2016-08-11 21:59 PDT	R2D2-SarlaccBel	Carmel Chalk	90	4	4	-2.25	0	0	4.25	0	0	35.24	0
R131	2016-08-11 23:39 PDT	R2D2-SarlaccBel	Carrara Marble	90	4	4	2.31	0	0	6.46	0	0	37.52	0
R132	2016-08-12 14:16 PDT	R2D2-SarlaccBel	Unheated gas		4	4	-38.08	0	0	-1.46	0	0	29.35	0
R133	2016-08-15 16:18 PDT	R2D2-SarlaccBel	Heated Gas		4	4	2.57	0	0	7.79	0	0	38.89	0
R134	2016-08-15 23:10 PDT	R2D2-SarlaccBel	Veinstrom	90	4	4	-6.08	0	0	-4.47	0	0	26.26	0
R135	2016-09-25 12:04 PDT	EVAP DI+CM H	Chewbacca		9	9	0.51	0	0	20.82	0.01	0	52.32	0.01
R136	2016-09-26 14:10 PDT	ETH-4	ETH-4-1	90	9	9	-10.18	0	0	-10.95	0.01	0	19.58	0.01
R137	2016-10-06 14:26 PDT	Boneory+DI 9-28-16 NH CW	Chewbacca		9	9	-36.81	0.01	0	0.02	0.01	0	30.88	0.01
R138	2016-10-07 12:44 PDT	Evap DI+CM H 9-19-16	Chewbacca		9	9	1.1	0	0	18.02	0	0	49.44	0
R139	2016-10-09 01:33 PDT	TV03	TV03	90	9	9	2.54	0	0	-0.49	0.01	0	30.36	0.01
R140	2016-10-11 11:49 PDT	Bonedry DI U CW 9-23	Chewbacca		9	9	-37.64	0	0	-0.98	0.01	0	29.85	0.01
R141	2016-10-11 13:59 PDT	TV03	TV03	90	9	9	2.41	0	0	-0.55	0.01	0	30.3	0.01
R142	2016-10-13 14:26 PDT	VeinStrom	Chewbacca		9	9	-6.17	0	0	-4.9	0	0	25.81	0.01
R143	2016-10-14 12:35 PDT	Bonedry DI H CW 9-23	Chewbacca		9	9	-37.42	0.01	0	-6.22	0.01	0	24.45	0.01
R144	2016-10-14 14:45 PDT	ETH-2	Chewbacca		90	9	-10.22	0	0	-11.11	0.01	0	19.41	0.01
R145	2016-10-14 23:21 PDT	ETH-4	Chewbacca		90	9	-10.17	0	0	-11.11	0.01	0	19.41	0.01
R146	2016-10-15 12:31 PDT	Evap DI+CM H 9-19 DU	Chewbacca		9	9	1.84	0	0	2.68	0.01	0	33.62	0.01
R147	2016-10-15 23:22 PDT	Carmel Chalk	Chewbacca		90	9	-2.24	0	0	3.51	0.01	0	34.48	0.01
R148	2016-10-17 00:00 PDT	TV03	Chewbacca		90	9	2.5	0	0	-0.84	0.01	0	30	0.01
R149	2016-10-19 12:09 PDT	Bonedry DI H CW 9-23	Chewbacca		9	9	-37.95	0.01	0	-6.54	0	0	24.12	0
R150	2016-10-19 14:17 PDT	ETH-2	Chewbacca		90	9	-10.23	0	0	-10.97	0.01	0	19.56	0.01
R151	2016-10-19 23:00 PDT	ETH-3	Chewbacca		90	9	1.61	0	0	5.83	0	0	36.86	0
R152	2016-10-20 12:05 PDT	Bonedry DI U NH 10-17	Chewbacca		9	9	-37.54	0.01	0	10.43	0.01	0	41.61	0.01
R153	2016-10-20 14:15 PDT	ETH-4	Chewbacca		90	9	-10.21	0	0	-11	0.01	0	19.52	0.01
R1	2016-10-20 16:25 PDT	AY1W3D_mc	Chewbacca		90	9	-5.81	0	0	-4.65	0.01	0	26.07	0.01
R154	2016-10-20 22:53 PDT	TV03	Chewbacca		90	9	2.49	0	0	-0.78	0.01	0	30.05	0.01
R2	2016-10-21 01:05 PDT	AY1W3D_mc	Chewbacca		90	9	-5.74	0	0	-4.58	0.01	0	26.14	0.01
R3	2016-10-21 03:19 PDT	AY1W3D_mc	Chewbacca		90	9	-5.74	0	0	-4.58	0.01	0	26.14	0.01
R155	2016-10-21 14:32 PDT	Carrera Marble	Chewbacca		90	9	1.95	0	0	6.12	0.01	0	37.17	0.01
R4	2016-10-21 18:47 PDT	AY1W3D_mc	Chewbacca		90	9	-5.84	0	0	-4.08	0.01	0	26.66	0.01
R5	2016-10-21 21:01 PDT	AY1W3D_mc	Chewbacca		90	9	-5.77	0	0	-4.32	0.01	0	26.41	0.01
R156	2016-10-21 23:15 PDT	Veinstrom-01	Chewbacca		90	9	-6.14	0	0	-4.94	0	0	25.77	0
R157	2016-10-22 16:39 PDT	Bonedry DI UH	Chewbacca		9	9	-37.59	0.01	0	10.29	0.01	0	41.47	0.01
R158	2016-10-22 18:50 PDT	47 ETH-1	Chewbacca		90	9	1.89	0	0	5.33	0.01	0	36.35	0.01
R159	2016-10-23 05:58 PDT	2 ETH-2	Chewbacca		90	9	-10.19	0	0	-11.09	0.01	0	19.43	0.01
R160	2016-10-24 15:35 PDT	Carmel Chalk	Chewbacca		90	9	-2.24	0	0	3.48	0.01	0	34.45	0.01
R161	2016-10-25 00:24 PDT	TV03	Chewbacca		90	9	2.57	0	0	-0.7	0.01	0	30.13	0.01
R162	2016-10-25 14:11 PDT	ETH-3	Chewbacca		90	9	1.64	0	0	5.8	0.01	0	36.84	0.01
R163	2016-10-26 14:41 PDT	Carrera Marble-UCLA	Chewbacca		90	9	1.93	0	0	6.03	0	0	37.08	0
R164	2016-10-27 01:40 PDT	VeinStrom-01	Chewbacca		90	9	-6.19	0	0	-5.11	0.01	0	25.59	0.01
R165	2016-10-28 18:20 PDT	ETH-3	Chewbacca		90	9	1.6	0	0	5.85	0.01	0	36.68	0.01
R166	2016-10-29 12:41 PDT	Bonedry DI UH 10/17 NH	Chewbacca		9	9	-37.46	0.01	0	10.54	0.01	0	41.72	0.01
R167	2016-10-29 14:50 PDT	Veinstrom-01	Chewbacca		90	9	-6.2	0	0	-4.84	0	0	25.87	0
R168	2016-10-29 23:25 PDT	TV03	Chewbacca		90	9	2.34	0	0	-0.85	0.01	0	29.98	0.01
R6	2016-10-30 01:35 PDT	AY1W3D_mc	Chewbacca		90	9	-5.65	0	0	-4.5	0.01	0	26.22	0.01
R169	2016-10-30 13:04 PDT	Carrera Marble	Chewbacca		90	9	2.18	0	0	5.86	0.01	0	36.9	0.01
R5	2016-10-30 22:03 PDT	AY2SHC	Chewbacca		90	9	-3.87	0	0	-3.17	0.01	0	27.6	0.01
R4	2016-10-31 04:40 PDT	WA3SHC	Chewbacca		90	9	-6.38	0	0	-5.88	0.01	0	24.8	0.01
R4	2016-10-31 06:56 PDT	KP1SHC	Chewbacca		90	9	-2.42	0	0	-4.59	0.01	0	26.12	0.01

R170	2016-10-31 13:19 PDT	BonedryDI UH DU 10-14	Chewbacca	Unheated gas	9	9	-37.59	0	0	-1.68	0.01	0	29.13	0.01
R171	2016-10-31 15:28 PDT	ETH-4	Chewbacca	ETH-4-1	90	9	-10.16	0	0	-10.96	0.01	0	19.56	0.01
R7	2016-10-31 17:40 PDT	AY1W3D_mc	Chewbacca	AY1W3D	90	9	-5.69	0	0	-4.52	0.01	0	26.2	0.01
R8	2016-10-31 19:50 PDT	AY1W3D_mc	Chewbacca	AY1W3D	90	9	-5.68	0	0	-4.58	0.01	0	26.14	0.01
R9	2016-10-31 22:01 PDT	AY1W3D_mc	Chewbacca	AY1W3D	90	9	-5.59	0	0	-4.47	0.01	0	26.26	0.01
R172	2016-11-01 00:13 PDT	TV03	Chewbacca	TV03	90	9	2.56	0	0	-0.67	0.01	0	30.17	0.01
R10	2016-11-01 02:38 PDT	AY1W3D_mc	Chewbacca	AY1W3D	90	9	-5.71	0	0	-4.48	0.01	0	26.25	0.01
R173	2016-11-01 16:44 PDT	Carmel Chalk	Chewbacca	Carmel Chalk	90	9	-2.25	0	0	3.47	0	0	34.43	0
R11	2016-11-01 18:52 PDT	AY1W3D_mc	Chewbacca	AY1W3D	90	9	-5.67	0	0	-4.59	0.01	0	26.13	0.01
R12	2016-11-01 21:03 PDT	AY1W3D_mc	Chewbacca	AY1W3D	90	9	-5.76	0	0	-4.61	0.01	0	26.1	0.01
R174	2016-11-02 01:34 PDT	ETH-2	Chewbacca	ETH-2-1	90	9	-10.15	0	0	-10.86	0.01	0	19.67	0.01
R175	2016-11-02 12:49 PDT	BonedryDI H DU 10-28	Chewbacca	Heated Gas	9	9	-36.93	0.01	0	-3.02	0.01	0	27.75	0.01
R176	2016-11-03 17:25 PDT	TV03	Chewbacca	TV03	90	9	2.57	0	0	-0.69	0	0	30.15	0
R177	2016-11-03 22:48 PDT	Carmel Chalk	Chewbacca	Carmel Chalk	90	9	-2.18	0	0	3.73	0	0	34.71	0
R178	2016-11-04 00:57 PDT	ETH-4	Chewbacca	ETH-4-1	90	9	-10.17	0	0	-11.21	0.01	0	19.31	0.01
R179	2016-11-04 14:59 PDT	ETH-2	Chewbacca	ETH-2-1	90	9	-10.2	0	0	-10.94	0.01	0	19.58	0.01
R180	2016-11-06 21:58 PST	Veinstrom	Chewbacca	Veinstrom	90	9	-6.23	0	0	-5.07	0	0	25.64	0
R181	2016-11-07 14:53 PST	ETH-1	Chewbacca	ETH-1-1	90	9	1.99	0	0	5.4	0.01	0	36.42	0.01
R182	2016-11-07 23:34 PST	ETH-3	Chewbacca	ETH-3-1	90	9	1.63	0	0	5.84	0.01	0	36.88	0.01
R183	2016-11-08 15:32 PST	Carmel Chalk	Chewbacca	Carmel Chalk	90	9	-2.2	0	0	3.46	0.01	0	34.42	0.01
R184	2016-11-09 00:13 PST	TV03	Chewbacca	TV03	90	9	2.62	0	0	-0.96	0.01	0	29.87	0.01
R185	2016-11-09 14:39 PST	Vein strom UCLA-1	Chewbacca	Veinstrom	90	9	-6.26	0	0	-4.98	0.01	0	25.72	0.01
R186	2016-11-10 16:32 PST	Carrera Marble	Chewbacca	Carrera Marble	90	9	1.94	0	0	6.02	0.01	0	37.07	0.01
R187	2016-11-11 14:45 PST	ETH-1	Chewbacca	ETH-1-1	90	9	1.97	0	0	5.43	0.01	0	36.46	0.01
R188	2016-11-12 00:40 PST	ETH-4	Chewbacca	ETH-4-1	90	9	-10.15	0	0	-10.95	0.01	0	19.57	0.01
R189	2016-11-12 15:32 PST	TV03	Chewbacca	TV03	90	9	2.5	0	0	-0.7	0.01	0	30.14	0.01
R190	2016-11-13 00:19 PST	VeinStrom	Chewbacca	Veinstrom	90	9	-6.13	0	0	-4.88	0.01	0	25.83	0.01
R191	2016-11-14 15:02 PST	ETH-2	Chewbacca	ETH-2-1	90	9	-10.27	0	0	-11	0.01	0	19.52	0.01
R192	2016-11-15 00:23 PST	ETH-3	Chewbacca	ETH-3-1	90	9	1.54	0	0	5.56	0	0	36.59	0
R193	2016-11-15 14:34 PST	ETH-3	Chewbacca	ETH-3-1	90	9	1.57	0	0	5.79	0.01	0	36.83	0.01
R194	2016-11-16 23:19 PST	TV03	Chewbacca	TV03	90	9	2.59	0	0	-0.84	0	0	30	0
R195	2016-11-17 15:53 PST	Carmel Chalk	Chewbacca	Carmel Chalk	90	9	-2.14	0	0	3.61	0	0	34.58	0
R196	2016-11-18 00:39 PST	Carrera Marble	Chewbacca	Carrera Marble	90	9	1.95	0	0	6.05	0	0	37.1	0.01
R197	2016-11-18 16:02 PST	Veinstrom-01	Chewbacca	Veinstrom	90	9	-6.19	0	0	-4.93	0.01	0	25.78	0.01
R198	2016-11-19 14:17 PST	BonedryDI H DU	Chewbacca	Heated Gas	9	9	-36.96	0.01	0	-3.79	0	0	26.96	0
R199	2016-11-19 22:51 PST	ETH-4	Chewbacca	ETH-4-1	90	9	-10.17	0	0	-10.96	0.01	0	19.56	0.01
R200	2016-11-20 21:54 PST	TV03	Chewbacca	TV03	90	9	2.54	0	0	-0.75	0.01	0	30.09	0.01
R201	2016-11-21 23:43 PST	Carmel Chalk	Chewbacca	Carmel Chalk	90	9	-2.12	0	0	3.7	0.01	0	34.67	0.01
R202	2016-11-22 15:57 PST	ETH-1	Chewbacca	ETH-1-1	90	9	1.96	0	0	5.43	0.01	0	36.46	0.01
R203	2016-11-23 15:04 PST	Carrera Marble-UCLA	Chewbacca	Carrera Marble	90	9	1.96	0	0	6.08	0.01	0	37.12	0.01
R204	2016-11-28 22:54 PST	ETH-3	Chewbacca	ETH-3-1	90	9	1.61	0	0	5.78	0	0	36.82	0
R205	2016-11-29 15:26 PST	Carmel Chalk	Chewbacca	Carmel Chalk	90	9	-2.26	0	0	3.57	0.01	0	34.54	0.01
R206	2016-11-30 04:20 PST	Veinstrom	Chewbacca	Veinstrom	90	9	-6.2	0	0	-4.97	0	0	25.73	0
R207	2016-11-30 13:03 PST	BonedryDI UH GJ 10-14-16	Chewbacca	Unheated gas	9	9	-37.57	0.01	0	-1.82	0.01	0	28.98	0.01
R208	2016-11-30 15:15 PST	ETH-3	Chewbacca	ETH-3-1	90	9	1.58	0	0	5.73	0	0	36.77	0
R209	2016-11-30 21:31 PST	Veinstrom UCLA-2	Chewbacca	Veinstrom	90	9	-6.16	0	0	-5	0	0	25.71	0
R210	2016-12-01 15:15 PST	Carrera Marble	Chewbacca	Carrera Marble	90	9	1.95	0	0	6.08	0.01	0	37.12	0.01
R211	2016-12-01 23:56 PST	TV03	Chewbacca	TV03	90	9	2.5	0	0	-0.72	0.01	0	30.12	0.01
R212	2016-12-05 23:34 PST	ETH-3	Chewbacca	ETH-3-1	90	9	1.48	0	0	5.58	0	0	36.61	0
R213	2016-12-09 16:30 PST	BonedryDI UH DU 10-14	Chewbacca	Unheated gas	9	9	-37.66	0	0	-1.94	0.01	0	28.86	0.01
R214	2016-12-09 18:38 PST	Carrera Marble	Chewbacca	Carrera Marble	90	9	1.93	0	0	6.02	0	0	37.06	0
R215	2016-12-09 20:47 PST	TV03	Chewbacca	TV03	90	9	2.59	0	0	-0.86	0	0	29.97	0
R216	2016-12-09 22:54 PST	Carmel Chalk	Chewbacca	Carmel Chalk	90	9	-2.21	0	0	3.52	0.01	0	34.49	0.01
R217	2016-12-10 01:03 PST	Veinstrom	Chewbacca	Veinstrom	90	9	-6.19	0	0	-5.06	0.01	0	25.65	0.01
R218	2016-12-13 15:21 PST	ETH-1	Chewbacca	ETH-1-1	90	9	1.93	0	0	5.32	0.01	0	36.34	0.01
R219	2016-12-14 12:54 PST	BonedryDI UH CW 12-5-16	Chewbacca	Unheated gas	9	9	-37.48	0	0	10.8	0.01	0	41.99	0.01
R220	2016-12-16 13:40 PST	BonedryDI H CW 12-5-16	Chewbacca	Heated Gas	9	9	-37.61	0	0	0.9	0	0	31.79	0.01
R221	2016-12-18 11:05 PST	BonedryDI UH DH 11-3-16	Chewbacca	Unheated gas	9	9	-37.57	0	0	10.55	0.01	0	41.74	0.01
R222	2016-12-19 11:38 PST	Bonedry + DI UH NH 10.17.16	Chewbacca	Unheated gas	9	9	-37.53	0	0	10.58	0	0	41.76	0
R223	2016-12-19 22:16 PST	TV03	Chewbacca	TV03	90	9	2.43	0	0	-0.92	0	0	29.91	0
R224	2016-12-20 11:34 PST	Bonedry + DI UH CW 9.23.16	Chewbacca	Unheated gas	9	9	-37.02	0	0	-0.09	0	0	30.76	0
R225	2016-12-20 21:00 PST	ETH-3	Chewbacca	ETH-3-1	90	9	1.58	0	0	5.55	0	0	36.58	0
R226	2016-12-21 12:05 PST	Bonedry + DI UH GJ 11.3.16	Chewbacca	Unheated gas	9	9	-37.24	0	0	11.1	0	0	42.3	0
R227	2016-12-21 14:13 PST	Carmel Marble	Chewbacca	Carrera Marble	90	9	2.26	0	0	5.76	0.01	0	36.8	0.01
R228	2016-12-22 11:50 PST	Evap DI + CM UH WD 12.21.16	Chewbacca	Unheated gas	9	9	1.95	0	0	17.49	0.01	0	48.89	0.01
R229	2016-12-22 14:00 PST	ETH-1	Chewbacca	ETH-1-1	90	9	1.93	0	0	5.18	0	0	36.2	0
R230	2016-12-23 14:04 PST	Evap DI+CM H WD 12-21-16	Chewbacca	Unheated gas	9	9	1.98	0	0	18.7	0	0	50.13	0
R231	2016-12-23 16:12 PST	ETH-3	Chewbacca	ETH-3-1	90	10	1.68	0	0	5.68	0	0	36.71	0

R232	2016-12-26 11:42 PST	Evap DI + CM UH WD 12.21.16	Chewbacca	Unheated gas	9	9	2.09	0	0	19.13	0.01	0	50.58	0.01
R233	2016-12-27 17:07 PST	Evap DI+CM H WD 12-21-16	Chewbacca	Heated Gas	9	9	2.09	0	0	13.23	0	0	44.49	0.01
R234	2016-12-27 19:14 PST	ETH-3	Chewbacca	ETH-3-1	90	9	1.7	0	0	5.58	0	0	36.81	0
R235	2016-12-28 11:24 PST	Evap DI+CM 12/21/16 UH WD	Chewbacca	Unheated gas	9	9	1.91	0	0	17.58	0.01	0	48.98	0.01
R236	2016-12-30 12:13 PST	Evap DI+CM H WD 12-21-16	Chewbacca	Heated Gas	9	9	2.39	0	0	16.03	0	0	47.38	0
R237	2017-02-23 10:13 PST	Bonedry DI UH ND 1-24	Chewbacca	Unheated gas	9	9	-37.57	0	0	10.1	0	0	41.28	0
R4	2017-02-23 14:31 PST	KP1W	Chewbacca	KP1W	90	9	-4.63	0	0	-6.47	0.03	0.01	24.19	0.03
R5	2017-02-23 16:59 PST	KP1W	Chewbacca	KP1W	90	10	-4.62	0.01	0	-6.43	0.02	0.01	24.23	0.02
R6	2017-02-23 19:24 PST	KP1W	Chewbacca	KP1W	90	9	-4.65	0	0	-6.64	0.01	0	24.02	0.01
R238	2017-02-23 21:28 PST	ETH-4	Chewbacca	ETH-4-1	90	9	-10.07	0	0	-11.5	0.01	0	19	0.01
R5	2017-02-23 23:42 PST	KP1SHC	Chewbacca	KP1SHC	90	9	-2.4	0	0	-4.94	0	0	25.77	0.01
R239	2017-02-24 12:05 PST	Bonedry DI H DU 2/3/17	Chewbacca	Heated Gas	9	9	-38.28	0.01	0	-7.01	0	0	23.63	0
R240	2017-02-24 23:00 PST	Carrera Marble	Chewbacca	Carrera Marble	90	9	2.11	0	0	5.94	0	0	36.98	0
R241	2017-02-25 13:48 PST	Evap DI + CM UH DU 2/24/17	Chewbacca	Unheated gas	9	9	-37.09	0	0	-0.21	0	0	30.64	0
R242	2017-02-25 15:54 PST	TV03	Chewbacca	TV03	90	9	2.77	0	0	-1.09	0	0	29.74	0.01
R243	2017-02-27 11:30 PST	Bonedry DI H ND 1/24/17	Chewbacca	Heated Gas	9	9	-37.26	0	0	4.47	0.01	0	35.46	0.01
R244	2017-02-28 12:33 PST	Bonedry DI H ND 1/24	Chewbacca	Heated Gas	9	9	-37.51	0	0	5.72	0	0	36.75	0
R245	2017-03-01 13:47 PST	Evap DI + CM UH DU 2/24/2017	Chewbacca	Unheated gas	9	9	-37.02	0	0	-0.13	0.01	0	30.73	0.01
R246	2017-03-04 13:31 PST	Bone Dry DI H ND 1/4	Chewbacca	Heated Gas	9	9	-37.44	0	0	5.25	0.01	0	36.27	0.01
R247	2017-03-04 15:44 PST	ETH-4	Chewbacca	ETH-4-1	90	9	-10.17	0	0	-11.32	0	0	19.19	0
R248	2017-03-05 14:25 PST	Evap DI + CM H GJ 2/24/2017	Chewbacca	Heated Gas	9	9	-37.78	0	0	-3.23	0	0	27.53	0
R249	2017-03-05 16:31 PST	TV03	Chewbacca	TV03	90	9	2.53	0	0	-0.88	0.01	0	29.96	0.01
R250	2017-03-05 22:54 PST	Veinstrom	Chewbacca	Veinstrom	90	9	-6.1	0	0	-5.03	0	0	25.67	0
R251	2017-03-06 13:04 PST	Bonedry DI H ND 1/24/2017	Chewbacca	Heated Gas	9	9	-37.89	0.01	0	5.22	0.01	0	36.24	0.01
R252	2017-03-06 15:10 PST	Carrera Marble	Chewbacca	Carrera Marble	90	9	1.96	0	0	5.88	0	0	36.92	0
R253	2017-03-07 13:31 PST	ETH-2	Chewbacca	ETH-2-1	90	9	-10.17	0	0	-11.28	0	0	19.23	0.01
R254	2017-03-07 21:56 PST	ETH-3	Chewbacca	ETH-3-1	90	9	1.72	0	0	5.9	0	0	36.94	0
R255	2017-03-08 12:46 PST	Bonedry DI H DU	Chewbacca	Heated Gas	9	9	-37.18	0.01	0	-4.9	0	0	25.81	0
R256	2017-03-08 14:57 PST	ETH-1	Chewbacca	ETH-1-1	90	9	2.06	0	0	5.4	0	0	36.43	0.01
R257	2017-03-08 23:41 PST	ETH-4	Chewbacca	ETH-4-1	90	9	-10.13	0	0	-11.25	0	0	19.26	0.01
R258	2017-03-09 12:37 PST	Bonedry DI UH DU	Chewbacca	Unheated gas	9	9	-38.51	0	0	-2.69	0	0	28.09	0
R259	2017-03-09 14:48 PST	Veinstrom	Chewbacca	Veinstrom	90	9	-6.22	0	0	-5.26	0	0	25.44	0
R260	2017-03-09 23:07 PST	TV03	Chewbacca	TV03	90	9	2.58	0	0	-0.86	0	0	29.98	0
R261	2017-03-10 13:31 PST	Bonedry DI H DU 2/3/2017	Chewbacca	Heated Gas	9	9	-38.29	0	0	-6.25	0	0	24.42	0
R262	2017-03-10 15:41 PST	ETH-4	Chewbacca	ETH-4-1	90	9	-10.16	0	0	-11.33	0	0	19.18	0
R263	2017-03-11 14:26 PST	Evap DI + CM UH DU 3.10.17	Chewbacca	Unheated gas	9	9	2.16	0	0	19.66	0	0	51.13	0
R264	2017-03-11 16:31 PST	Carrera Marble	Chewbacca	Carrera Marble	90	9	2.06	0	0	6.13	0	0	37.18	0
R265	2017-03-12 01:17 PST	Carmel Chalk	Chewbacca	Carmel Chalk	90	9	-2.21	0	0	3.63	0	0	34.6	0
R266	2017-03-13 10:42 PDT	Bonedry + DI H ND	Chewbacca	Heated Gas	9	9	-37.41	0	0	4.74	0.01	0	35.75	0.01
R267	2017-03-13 13:32 PDT	Veinstrom	Chewbacca	Veinstrom	90	9	-6.06	0	0	-4.99	0.01	0	25.72	0.01
R268	2017-03-13 21:52 PDT	TV03	Chewbacca	TV03	90	9	2.68	0	0	-0.66	0	0	30.18	0
R269	2017-03-14 14:29 PDT	Carmel Chalk	Chewbacca	Carmel Chalk	90	9	-2.13	0	0	3.67	0	0	34.64	0
R270	2017-03-14 20:58 PDT	Carrera Marble	Chewbacca	Carrera Marble	90	9	2.1	0	0	6.19	0	0	37.24	0
R271	2017-03-15 13:31 PDT	Bonedry DI UH WD 3.13.17	Chewbacca	Unheated gas	9	9	-37.55	0	0	10.86	0	0	42.05	0
R272	2017-03-15 15:38 PDT	Veinstrom	Chewbacca	Veinstrom	90	9	-6.14	0	0	-5.04	0.01	0	25.66	0.01
R273	2017-03-16 00:32 PDT	TV03	Chewbacca	TV03	90	9	2.63	0	0	-0.71	0.01	0	30.13	0.01
R274	2017-03-16 12:17 PDT	Evap DI + CM UH GJ 3.10.17	Chewbacca	Unheated gas	9	9	1.59	0	0	18.62	0	0	50.05	0
R275	2017-03-16 14:28 PDT	ETH-2	Chewbacca	ETH-2-1	90	9	-10.13	0	0	-11.23	0	0	19.28	0
R276	2017-03-16 22:55 PDT	ETH-3	Chewbacca	ETH-3-1	90	9	1.77	0	0	5.86	0	0	36.9	0
R277	2017-03-18 14:07 PDT	Bonedry + DI H 12/5 CW	Chewbacca	Heated Gas	9	9	-37.41	0	0	2.17	0.01	0	33.1	0.01
R278	2017-03-18 16:23 PDT	ETH-1	Chewbacca	ETH-1-1	90	9	2.05	0	0	5.39	0	0	36.42	0
R279	2017-03-20 13:27 PDT	Evap DI+CM H GJ 3/10/17	Chewbacca	Heated Gas	9	9	3.5	0	0	20.13	0	0	51.61	0
R280	2017-03-20 15:31 PDT	Carrera Marble	Chewbacca	Carrera Marble	90	9	2.01	0	0	5.91	0.01	0	36.95	0.01
R281	2017-03-20 21:58 PDT	Carmel Chalk	Chewbacca	Carmel Chalk	90	9	-2.21	0	0	3.49	0.01	0	34.46	0.01
R282	2017-03-21 15:02 PDT	TV03	Chewbacca	TV03	90	9	2.71	0	0	-0.68	0	0	30.15	0
R283	2017-03-21 21:28 PDT	ETH 4	Chewbacca	ETH-4-1	90	9	-10.12	0	0	-11.22	0	0	19.29	0
R284	2017-03-22 12:07 PDT	Bonedry DI UH WD 3.13.17	Chewbacca	Unheated gas	9	9	-37.49	0	0	10.37	0	0	41.54	0
R285	2017-03-22 14:19 PDT	ETH-2	Chewbacca	ETH-2-1	90	9	-10.14	0	0	-11.08	0.01	0	19.44	0.01
R286	2017-03-23 15:58 PDT	Bonedry DI H CW 12.5.16	Chewbacca	Heated Gas	9	9	-37.34	0	0	2.38	0	0	33.31	0
R287	2017-03-24 12:30 PDT	Evap DI+CM UH DU 3/23/17	Chewbacca	Unheated gas	9	9	1.09	0	0	7.95	0	0	39.05	0
R288	2017-03-24 14:36 PDT	ETH-1	Chewbacca	ETH-1-1	90	9	2	0	0	5.28	0	0	36.3	0
R289	2017-03-24 21:11 PDT	Carrera Marble	Chewbacca	Carrera Marble	90	9	2.05	0	0	6.14	0.01	0	37.19	0.01
R290	2017-03-25 16:24 PDT	Evap DI+CM H DU 3/23/17	Chewbacca	Heated Gas	9	9	1.38	0	0	5.85	0	0	36.89	0
R291	2017-03-25 18:31 PDT	ETH-4	Chewbacca	ETH-4-1	90	9	-10.14	0	0	-11.27	0.01	0	19.24	0.01
R292	2017-03-26 13:27 PDT	Veinstrom	Chewbacca	Veinstrom	90	9	-6.07	0	0	-4.93	0	0	25.78	0
R293	2017-03-27 12:44 PDT	Bonedry DI UH NH 3/24/17	Chewbacca	Unheated gas	9	9	-37.37	0	0	10.36	0	0	41.54	0
R294	2017-03-27 14:50 PDT	TV03	Chewbacca	TV03	90	9	2.7	0	0	-0.77	0	0	30.06	0
R295	2017-03-27 21:07 PDT	Carmel Chalk	Chewbacca	Carmel Chalk	90	9	-2.16	0	0	3.62	0	0	34.59	0

R296	2017-03-28 12:55 PDT	Evap DI+CM UH DU 3/23/17	Chewbacca	Unheated gas	9	9	9	1.31	0	0	8.4	0	0	39.52	0
R297	2017-03-28 15:05 PDT	ETH-2	Chewbacca	ETH-2-1	90	9	9	-10.1	0	0	-11.26	0.01	0	19.25	0.01
R298	2017-03-29 15:57 PDT	ETH-1	Chewbacca	ETH-1-1	90	9	9	2.02	0	0	5.34	0.01	0	36.37	0.01
R299	2017-03-30 12:17 PDT	EVAP DI+CM UH DU 3/23/17	Chewbacca	Unheated gas	9	9	9	1.33	0	0	8.47	0	0	39.59	0
R300	2017-03-31 10:50 PDT	Bonedry DI H DU 3-24-17	Chewbacca	Heated Gas	90	9	9	-38.4	0	0	-3.29	0.01	0	27.47	0.01
R5	2017-03-31 15:09 PDT	WA3SHC	Chewbacca	WA3SHC	90	9	9	-6.56	0	0	-6.64	0.01	0	24.01	0.01
R5	2017-03-31 17:10 PDT	AY1SHC	Chewbacca	AY1SHC	90	9	9	-3.57	0	0	-5.05	0.01	0	25.65	0.01
R301	2017-03-31 19:19 PDT	ETH-2	Chewbacca	ETH-2-1	90	9	9	-10.2	0	0	-11.42	0.01	0	19.09	0.01
R6	2017-03-31 21:29 PDT	AY1SHC	Chewbacca	AY1SHC	90	9	9	-3.54	0	0	-5.02	0.01	0	25.69	0.01
R7	2017-03-31 23:35 PDT	AY1SHC	Chewbacca	AY1SHC	90	9	9	-3.57	0	0	-5.05	0.01	0	25.65	0.01
R302	2017-04-01 13:18 PDT	Evap DI+CM H DU 3-23-17	Chewbacca	Heated Gas	9	9	9	1.33	0	0	5.51	0	0	36.54	0
R303	2017-04-03 13:01 PDT	Bonedry DI UH DU 3/24/17	Chewbacca	Unheated gas	9	9	9	-38.12	0	0	-1.87	0.01	0	28.93	0.01
R304	2017-04-03 15:11 PDT	Veinstrom	Chewbacca	Veinstrom	90	9	9	-6.17	0	0	-5.15	0.01	0	25.55	0.01
R305	2017-04-04 13:16 PDT	Evap DI+CM UH NH 3/30/17	Chewbacca	Unheated gas	9	9	9	2.05	0	0	-3.27	0	0	27.49	0
R306	2017-04-05 12:31 PDT	Bonedry DI H DU 3/24/17	Chewbacca	Heated Gas	9	9	9	-38.6	0	0	-3.33	0	0	27.43	0
R307	2017-04-05 21:01 PDT	TV03	Chewbacca	TV03	90	9	9	2.33	0	0	-1.27	0	0	29.55	0
R308	2017-04-06 12:53 PDT	Evap DI+CM UH	Chewbacca	Unheated gas	9	9	9	2.06	0	0	-3.15	0.01	0	27.62	0.01
R309	2017-04-06 15:08 PDT	Eth-1	Chewbacca	ETH-1-1	90	9	9	2.08	0	0	5.46	0.01	0	36.49	0.01
R310	2017-04-07 12:17 PDT	Bonedry DI UH DU 3.24.17	Chewbacca	Unheated gas	9	9	9	-38.17	0	0	-1.56	0.01	0	29.26	0.01
R311	2017-04-07 14:24 PDT	ETH-3	Chewbacca	ETH-3-1	90	9	9	1.72	0	0	5.74	0.01	0	36.77	0.01
R312	2017-04-10 11:57 PDT	Evap DI+CM UH NH 4.1.17	Chewbacca	Unheated gas	9	9	9	2	0	0	-3.57	0.01	0	27.18	0.01
R313	2017-05-14 13:16 PDT	Bonedry DI UH DU 5/10/2017	Chewbacca	Unheated gas	9	9	9	-36.79	0.01	0	-2.79	0.01	0	27.98	0.01
R314	2017-05-14 15:21 PDT	ETH-1	Chewbacca	ETH-1-1	90	9	9	2.07	0	0	5.45	0.01	0	36.48	0.01
R315	2017-05-14 21:40 PDT	VeinStrom	Chewbacca	Veinstrom	90	9	9	-6.04	0	0	-4.82	0	0	25.89	0
R316	2017-05-15 12:07 PDT	Evap DI+CM UH GJ 4/24/17	Chewbacca	Unheated gas	9	9	9	0.97	0	0	3.31	0	0	34.27	0
R317	2017-05-16 13:42 PDT	Evap DI+CM H NH 4/1/17	Chewbacca	Heated Gas	9	9	9	2.17	0	0	-5.84	0	0	24.84	0
R318	2017-05-16 15:53 PDT	Carrara Marble	Chewbacca	Carrara Marble	90	9	9	2.09	0	0	6.1	0	0	37.14	0
R319	2017-05-16 22:17 PDT	Carmel Chalk	Chewbacca	Carmel Chalk	90	9	9	-2.14	0	0	3.7	0	0	34.68	0
R320	2017-05-17 11:45 PDT	Bonedry DI H DU 5/6/17	Chewbacca	Heated Gas	9	9	9	-38.26	0	0	-6.04	0	0	24.63	0
R321	2017-05-17 13:56 PDT	VeinStrom	Chewbacca	Veinstrom	90	9	9	-6.06	0	0	-4.94	0.01	0	25.77	0.01
R322	2017-05-17 20:17 PDT	88B Dolomitic Limestone	Chewbacca	SRM 88B	90	9	9	1.97	0	0	1.29	0	0	32.19	0
R323	2017-05-18 09:31 PDT	Bonedry DI uH GJ 5/10/17	Chewbacca	Unheated gas	9	9	9	-37.25	0	0	-3.5	0	0	27.25	0
R324	2017-05-19 20:53 PDT	ETH-3	Chewbacca	ETH-3-1	90	9	9	1.66	0	0	5.68	0.01	0	36.72	0.01
R325	2017-05-20 13:18 PDT	Evap DI+CM H GJ 5/8/17	Chewbacca	Heated Gas	9	9	9	1.87	0	0	2.65	0.01	0	33.59	0.01
R326	2017-05-20 15:32 PDT	ETH-4	Chewbacca	ETH-4-1	90	9	9	-10.09	0	0	-11.12	0	0	19.39	0
R327	2017-05-20 22:04 PDT	Carrara Marble	Chewbacca	Carrara Marble	90	9	9	2.07	0	0	6.14	0	0	37.19	0
R328	2017-05-22 11:49 PDT	Bonedry DI UH DU 5/6/17	Chewbacca	Unheated gas	9	9	9	-38.46	0	0	-5.54	0	0	25.15	0
R329	2017-05-22 16:08 PDT	Carmel Chalk	Chewbacca	Carmel Chalk	90	9	9	-2.1	0	0	3.67	0.01	0	34.65	0.01
R330	2017-05-22 23:56 PDT	SRM 88B	Chewbacca	SRM 88B	90	9	9	1.85	0	0	1.36	0	0	32.26	0
R331	2017-05-23 12:33 PDT	Bonedry DI H GJ 5/10/17	Chewbacca	Heated Gas	9	9	9	-38.17	0	0	-6.22	0	0	24.45	0
R332	2017-05-23 14:50 PDT	88B Dolomitic Limestone	Chewbacca	SRM 88B	90	9	9	2.05	0	0	1.11	0.01	0	32.01	0.01
R333	2017-05-23 21:17 PDT	ETH-1	Chewbacca	ETH-1-1	90	9	9	2.11	0	0	5.51	0	0	36.54	0
R334	2017-05-24 11:52 PDT	Evap DI + CM UH NH 3-30-17	Chewbacca	Unheated gas	9	9	9	2.02	0	0	-3.05	0	0	27.72	0
R335	2017-05-24 14:04 PDT	Carrara Marble	Chewbacca	Carrara Marble	90	9	9	2.1	0	0	6.09	0	0	37.14	0
R336	2017-05-24 20:51 PDT	ETH-2	Chewbacca	ETH-2-1	90	9	9	-10.03	0	0	-11.02	0	0	19.5	0
R337	2017-05-25 11:47 PDT	Evap DI + CM H DU 5/17/17	Chewbacca	Heated Gas	9	9	9	1.88	0	0	3.06	0.01	0	34.01	0.01
R338	2017-05-25 13:53 PDT	ETH-3	Chewbacca	ETH-3-1	90	9	9	1.69	0	0	5.7	0	0	36.73	0
R339	2017-05-25 20:18 PDT	ETH-4	Chewbacca	ETH-4-1	90	9	9	-10.12	0	0	-11.22	0	0	19.29	0
R340	2017-05-26 11:24 PDT	Bonedry DI UH DU 5/22/17	Chewbacca	Unheated gas	9	9	9	-37.85	0	0	1.57	0	0	32.48	0
R341	2017-05-26 13:32 PDT	Veinstrom	Chewbacca	Veinstrom	90	9	9	-6.05	0	0	-4.95	0	0	25.75	0
R342	2017-05-26 19:50 PDT	Carmel Chalk	Chewbacca	Carmel Chalk	90	9	9	-2.13	0	0	3.72	0	0	34.7	0
R343	2017-05-27 16:10 PDT	ETH-1	Chewbacca	ETH-1-1	90	9	9	2.09	0	0	5.4	0	0	36.42	0
R344	2017-05-27 22:31 PDT	Carrara Marble	Chewbacca	Carrara Marble	90	9	9	2.15	0	0	6.02	0	0	37.06	0
R345	2017-05-28 13:41 PDT	EvapDI+CM U GJ4-24	Chewbacca	Unheated gas	9	9	9	1.17	0	0	3.5	0	0	34.46	0
R346	2017-05-28 15:52 PDT	SRM 88B	Chewbacca	SRM 88B	90	9	9	2.17	0	0	1.24	0	0	32.14	0
R347	2017-05-29 00:18 PDT	ETH-2	Chewbacca	ETH-2-1	90	9	9	-10	0	0	-10.99	0	0	19.53	0
R348	2017-05-29 12:56 PDT	EvapDI+CM H GJ 5/8/17	Chewbacca	Heated Gas	9	9	9	1.81	0	0	2.58	0	0	33.51	0
R349	2017-05-30 12:41 PDT	bonedry DI UH GJ 5/22/17	Chewbacca	Unheated gas	9	9	9	-38.26	0	0	0.72	0	0	31.61	0
R350	2017-05-30 14:52 PDT	Veinstrom	Chewbacca	Veinstrom	90	9	9	-6.12	0	0	-5.06	0	0	25.65	0
R351	2017-05-30 21:10 PDT	Carmel Chalk	Chewbacca	Carmel Chalk	90	9	9	-2.11	0	0	3.73	0	0	34.71	0.01
R352	2017-05-31 12:14 PDT	bonedry DI H GJ 5/10/17	Chewbacca	Heated Gas	9	9	9	-38.01	0.01	0	-5.38	0	0	25.32	0.01
R353	2017-05-31 14:19 PDT	ETH-1	Chewbacca	ETH-1-1	90	9	9	2.02	0	0	5.39	0	0	36.42	0
R354	2017-05-31 20:43 PDT	ETH-2	Chewbacca	ETH-2-1	90	9	9	-10.08	0	0	-11.1	0	0	19.41	0
R355	2017-06-04 13:36 PDT	Bonedry DI UH 5/22/17 GJ	Chewbacca	Unheated gas	9	9	9	-38.26	0	0	0.75	0	0	31.64	0
R356	2017-06-04 15:46 PDT	Carmel Chalk	Chewbacca	Carmel Chalk	90	9	9	-2.25	0	0	3.52	0	0	34.49	0
R357	2017-06-04 17:51 PDT	Eth-1	Chewbacca	ETH-1-1	90	9	9	2.09	0	0	5.49	0	0	36.52	0.01
R358	2017-06-04 19:57 PDT	Eth-2	Chewbacca	ETH-2-1	90	9	9	-10.11	0	0	-11.14	0	0	19.38	0
R359	2017-06-05 00:09 PDT	88B dolomitic limestone	Chewbacca	SRM 88B	90	9	9	2.17	0	0	1.27	0.01	0	32.17	0.01

R360	2017-06-05 13:28 PDT	Evap DI+CM H 4/24/17 GJ	Chewbacca	Heated Gas	9	9	9	0.96	0	0	1.05	0.01	0	31.94	0.01
R361	2017-06-05 15:37 PDT	ETH-3	Chewbacca	ETH-3-1	90	9	9	1.73	0	0	5.78	0	0	36.82	0
R362	2017-06-05 21:57 PDT	ETH-4	Chewbacca	ETH-4-1	90	9	9	-10.1	0	0	-11.19	0.01	0	19.33	0.01
R363	2017-06-06 13:10 PDT	Evap DI+CM UH 6/11/17 DU	Chewbacca	Unheated gas	9	9	9	0.31	0	0	-3.95	0.01	0	26.79	0.01
R364	2017-06-06 15:13 PDT	Carrara Marble	Chewbacca	Carrara Marble	90	9	9	2.14	0	0	6.18	0	0	37.23	0
R365	2017-06-10 12:02 PDT	Bonedry DI UH 6.7.17 DU	Chewbacca	Unheated gas	9	9	9	-37.37	0	0	2.29	0.05	0.02	33.22	0.05
R366	2017-06-10 14:05 PDT	88b dolomitic limestone	Chewbacca	SRM 88B	90	9	9	1.88	0	0	1.1	0.01	0	31.99	0.01
R367	2017-06-10 19:17 PDT	ETH-1	Chewbacca	ETH-1-1	90	9	9	1.83	0	0	5.49	0.01	0	36.52	0.01
R368	2017-06-11 04:12 PDT	VeinStrom	Chewbacca	Veinstrom	90	9	9	-6.1	0	0	-4.82	0.01	0	25.89	0.01
R369	2017-06-11 14:48 PDT	BondryDI H DU5-6	Chewbacca	Heated Gas	9	9	9	-37.84	0	0	-5.57	0.01	0	25.12	0.01
R370	2017-06-11 16:52 PDT	Carmel Chalk	Chewbacca	Carmel Chalk	90	9	9	-2.29	0	0	3.63	0.01	0	34.6	0.01
R371	2017-06-12 12:01 PDT	Evap DI+CM H 6/11/17 DU	Chewbacca	Heated Gas	9	9	9	1.06	0	0	-3.05	0.01	0	27.71	0.01
R372	2017-06-12 14:12 PDT	Carrara Marble	Chewbacca	Carrara Marble	90	9	9	1.99	0	0	6.11	0.01	0	37.16	0.01
R373	2017-06-12 20:22 PDT	SRM 88B	Chewbacca	SRM 88B	90	9	9	1.95	0	0	1.17	0.01	0	32.07	0.01
R374	2017-06-13 12:19 PDT	Evap DI+CM UH 6/7/17 DU	Chewbacca	Unheated gas	9	9	9	-38.12	0	0	1.34	0.01	0	32.25	0.01
R375	2017-06-13 14:28 PDT	ETH-1	Chewbacca	ETH-1-1	90	9	9	1.99	0	0	5.41	0.01	0	36.44	0.01
R376	2017-06-13 20:49 PDT	ETH-2	Chewbacca	ETH-2-1	90	9	9	-10.07	0	0	-10.93	0.01	0	19.59	0.01
R377	2017-06-14 11:40 PDT	Bonedry DI UH 5/10/17 GJ	Chewbacca	Unheated gas	9	9	9	-37.58	0	0	-3.98	0.01	0	26.76	0.01
R378	2017-06-14 13:45 PDT	ETH-3	Chewbacca	ETH-3-1	90	9	9	1.65	0	0	5.77	0.01	0	36.81	0.01
R379	2017-06-14 20:08 PDT	ETH-4	Chewbacca	ETH-4-1	90	9	9	-10.18	0	0	-11.15	0.01	0	19.36	0.01
R380	2017-06-15 11:57 PDT	Bonedry DI H 3.24.17 DU	Chewbacca	Heated Gas	9	9	9	-38.44	0	0	-3.03	0.01	0	27.74	0.01
R381	2017-06-15 14:00 PDT	Veinstrom	Chewbacca	Veinstrom	90	9	9	-6.16	0	0	-5.03	0	0	25.68	0
R382	2017-06-15 20:25 PDT	Carmel Chalk	Chewbacca	Carmel Chalk	90	9	9	-2.23	0	0	3.61	0	0	34.58	0.01
R383	2017-06-16 11:27 PDT	Evap DI+CM H 6-13-17 DU	Chewbacca	Heated Gas	9	9	9	2.95	0	0	-3.76	0	0	26.99	0
R384	2017-06-16 13:30 PDT	Carrara Marble	Chewbacca	Carrara Marble	90	9	9	1.95	0	0	6.03	0	0	37.08	0
R385	2017-06-16 22:05 PDT	SRM 88B	Chewbacca	SRM 88B	90	9	9	1.78	0	0	1.5	0.04	0.01	32.4	0.04
R386	2017-06-17 11:47 PDT	Evap DI+CM UH 6.15.17 GJ	Chewbacca	Unheated gas	9	9	9	1.66	0	0	-5.62	0.01	0	25.06	0.01
R387	2017-06-17 13:54 PDT	ETH-1	Chewbacca	ETH-1-1	90	9	9	1.98	0	0	5.44	0.01	0	36.46	0.01
R388	2017-06-17 22:23 PDT	ETH-2	Chewbacca	ETH-2-1	90	9	9	-10.2	0	0	-11.15	0.01	0	19.36	0.01
R389	2017-06-18 12:37 PDT	Bonedry DI UH 6-6-17 GJ	Chewbacca	Unheated gas	9	9	9	-37.44	0	0	2.31	0	0	33.25	0
R390	2017-06-18 14:44 PDT	ETH-3	Chewbacca	ETH-3-1	90	9	9	1.64	0	0	5.81	0	0	36.85	0
R391	2017-06-18 23:17 PDT	ETH-4	Chewbacca	ETH-4-1	90	9	9	-10.19	0	0	-11.17	0.01	0	19.34	0.01
R392	2017-06-19 12:20 PDT	Bonedry DI H 4.4.17 NH	Chewbacca	Heated Gas	9	9	9	-37.43	0	0	-6.48	0.01	0	24.18	0.01
R393	2017-06-19 14:24 PDT	TV03	Chewbacca	TV03	90	9	9	2.5	0	0	-0.71	0	0	30.13	0
R394	2017-06-19 21:00 PDT	Veinstrom	Chewbacca	Veinstrom	90	9	9	-6.2	0	0	-4.96	0	0	25.75	0
R395	2017-06-20 12:29 PDT	Evap DI + CM H 6.13.17 GJ	Chewbacca	Heated Gas	9	9	9	3.34	0	0	-2.96	0.01	0	27.81	0.01
R396	2017-06-20 14:31 PDT	Carmel Chalk	Chewbacca	Carmel Chalk	90	9	9	-2.23	0	0	3.62	0	0	34.6	0
R397	2017-06-21 12:32 PDT	Evap DI + CM UH 6.15.17 GJ	Chewbacca	Unheated gas	9	9	9	1.9	0	0	-5.21	0	0	25.48	0
R398	2017-06-21 14:42 PDT	8544 NBS19 Limestone	Chewbacca	NBS 19	90	9	9	1.88	0	0	5.45	0	0	36.47	0
R399	2017-06-22 12:37 PDT	Bonedry DI UH 6.6.17 GJ	Chewbacca	Unheated gas	9	9	9	-37.55	0	0	2.06	0.01	0	32.99	0.01
R400	2017-06-22 14:44 PDT	8544 NBS19 Limestone	Chewbacca	NBS 19	90	9	9	1.83	0	0	5.43	0	0	36.45	0
R401	2017-06-22 21:04 PDT	88B Dolomitic Limestone	Chewbacca	SRM 88B	90	9	9	1.92	0	0	1.11	0	0	32.01	0
R402	2017-06-23 11:56 PDT	Bonedry DI H 6.6.17 DU	Chewbacca	Heated Gas	9	9	9	-37.43	0	0	0.26	0	0	31.12	0.01
R403	2017-06-23 14:03 PDT	ETH-1	Chewbacca	ETH-1-1	90	9	9	1.97	0	0	5.43	0	0	36.46	0.01
R404	2017-06-24 13:51 PDT	Evap DI+CM H 6.13.17 DU	Chewbacca	Heated Gas	9	9	9	2.08	0	0	-5.29	0	0	25.41	0
R405	2017-06-24 15:57 PDT	Carmel Chalk	Chewbacca	Carmel Chalk	90	9	9	-2.23	0	0	3.67	0	0	34.64	0
R406	2017-06-24 22:13 PDT	Carrara Marble	Chewbacca	Carrara Marble	90	9	9	1.96	0	0	6.15	0	0	37.2	0
R407	2017-06-25 12:06 PDT	Evap DI+CM UH 6.15.17 DU	Chewbacca	Unheated gas	9	9	9	2.13	0	0	-5.1	0	0	25.6	0
R6	2017-06-25 18:22 PDT	KP1SHC	Chewbacca	KP1SHC	90	9	9	-2.45	0	0	-4.78	0.01	0	25.94	0.01
R7	2017-06-25 20:25 PDT	KP1SHC	Chewbacca	KP1SHC	90	9	9	-2.5	0	0	-4.81	0.01	0	25.9	0.01
R408	2017-06-26 12:18 PDT	Bonedry DI UH 6.19.17 GJ	Chewbacca	Unheated gas	9	9	9	-37.48	0	0	2.16	0.01	0	33.09	0.01
R409	2017-06-26 14:30 PDT	Veinstrom	Chewbacca	Veinstrom	90	9	9	-6.19	0	0	-4.93	0.01	0	25.78	0.01
R1	2017-06-26 16:37 PDT	AY1W3B	Chewbacca	AY1W3B	90	9	9	-6.27	0	0	-5.74	0	0	24.94	0
R1	2017-06-26 18:43 PDT	AY2W3C	Chewbacca	AY2W3C	90	9	9	-4.51	0	0	-4.15	0	0	26.58	0
R410	2017-06-26 20:47 PDT	88B Dolomitic Limestone	Chewbacca	SRM 88B	90	9	9	1.91	0	0	1.18	0.01	0	32.08	0.01
R411	2017-06-27 16:57 PDT	Bonedry DI H 4.7.17 NH	Chewbacca	Heated Gas	10	8	8	-37.7	0	0	-6.97	0.01	0	23.68	0.01
R412	2017-06-27 19:45 PDT	88B Dolomitic Limestone	Chewbacca	SRM 88B	90	9	8	2.01	0	0	1.1	0.01	0	31.99	0.01
R413	2017-06-27 22:03 PDT	ETH-3	Chewbacca	ETH-3-1	90	9	8	1.71	0	0	5.77	0	0	36.81	0
R414	2017-06-28 00:14 PDT	ETH-4	Chewbacca	ETH-4-1	90	9	8	-10.15	0	0	-11.15	0.01	0	19.37	0.01
R415	2017-06-28 02:34 PDT	Carrara Marble-UCLA	Chewbacca	Carrara Marble	90	9	8	2.03	0	0	6.12	0	0	37.17	0
R416	2017-06-28 12:19 PDT	Bonedry DI H GJ 5/10/17	Chewbacca	Heated Gas	9	9	9	-38.04	0	0	-6.12	0	0	24.55	0
R417	2017-06-28 14:30 PDT	Carmel Chalk	Chewbacca	Carmel Chalk	90	9	9	-2.21	0	0	3.57	0.01	0	34.54	0.01
R1	2017-06-28 16:56 PDT	WA3W	Chewbacca	WA3W	90	9	9	-4.49	0	0	-5.11	0	0	25.59	0
R6	2017-06-28 19:16 PDT	AY2SHC	Chewbacca	AY2SHC	90	9	9	-4.21	0	0	-3.7	0	0	27.05	0
R418	2017-06-28 21:20 PDT	ETH-2	Chewbacca	ETH-2-1	90	9	9	-10.13	0	0	-11.13	0.01	0	19.38	0.01
R419	2017-06-29 10:50 PDT	EvapDI+CM H 6.15.17 DU	Chewbacca	Heated Gas	9	9	9	2.22	0	0	-5.97	0.01	0	24.71	0.01
R7	2017-06-29 15:10 PDT	KP1W	Chewbacca	KP1W	90	9	9	-4.31	0	0	-5.24	0.01	0	25.45	0.01
R8	2017-06-29 17:13 PDT	AY1SHC	Chewbacca	AY1SHC	90	9	9	-3.5	0	0	-4.86	0	0	25.85	0

S10 KP1W
S11 WA3SHC
S12 WA3W
S13 WA3W_mc_cs

0	5.332	0.003	0.001	12.161	0.008	0.003	17.225	0.026	0.009	-0.292	0.025	0.008	24.416	0.211	0.07	-0.053	0.216	0.072
0	4.994	0.003	0.001	9.871	0.003	0.001	14.989	0.044	0.015	0.081	0.042	0.014	19.473	0.193	0.064	-0.359	0.189	0.063
0	5.657	0.002	0.001	17.451	0.008	0.003	22.649	0.038	0.013	-0.433	0.036	0.012	35.929	0.202	0.067	0.698	0.192	0.064
0	-0.867	0.004	0.001	6.027	0.005	0.002	4.739	0.037	0.012	-0.287	0.038	0.013	11.23	0.151	0.05	-0.851	0.147	0.049
0	-0.588	0.002	0.001	7.474	0.006	0.002	6.404	0.037	0.012	-0.331	0.034	0.011	14.374	0.26	0.087	-0.621	0.254	0.085
0	1.627	0.002	0.001	14.975	0.006	0.002	16.21	0.017	0.006	-0.211	0.017	0.006	30.549	0.124	0.041	0.364	0.127	0.042
0	-31.749	0.003	0.001	5.811	0.006	0.002	-28.15	0.033	0.011	-0.947	0.034	0.011	10.431	0.267	0.089	-1.21	0.262	0.087
0	1.636	0.003	0.001	14.939	0.006	0.002	16.154	0.029	0.01	-0.241	0.033	0.011	30.407	0.242	0.081	0.296	0.234	0.078
0	-2.535	0.001	0	5.326	0.005	0.002	2.358	0.039	0.013	-0.249	0.035	0.012	9.687	0.268	0.089	-0.982	0.266	0.089
0	-2.547	0.002	0.001	5.316	0.005	0.002	2.311	0.037	0.012	-0.274	0.036	0.012	9.676	0.232	0.077	-0.975	0.226	0.075
0	-2.526	0.003	0.001	5.265	0.005	0.002	2.287	0.037	0.012	-0.268	0.038	0.013	9.756	0.093	0.031	-0.793	0.094	0.031
0	5.65	0.003	0.001	16.796	0.006	0.002	21.873	0.03	0.01	-0.552	0.026	0.009	34.526	0.148	0.049	0.63	0.143	0.048
0	-2.513	0.004	0.001	5.285	0.005	0.002	2.349	0.025	0.008	-0.24	0.022	0.007	9.853	0.168	0.056	-0.737	0.166	0.055
0	-6.382	0.003	0.001	-0.051	0.002	0.001	-7.318	0.04	0.013	-0.69	0.039	0.013	-2.202	0.185	0.062	-2.101	0.183	0.061
0	0.305	0.002	0.001	6.634	0.006	0.002	6.48	0.036	0.012	-0.355	0.037	0.012	12.417	0.147	0.049	-0.883	0.138	0.046
0	0.262	0.003	0.001	6.617	0.004	0.001	6.417	0.067	0.022	-0.358	0.065	0.022	12.458	0.25	0.083	-0.809	0.252	0.084
0	-0.619	0.002	0.001	7.426	0.005	0.002	6.357	0.041	0.014	-0.299	0.04	0.013	14.129	0.193	0.064	-0.767	0.192	0.064
0	-2.329	0.002	0.001	6.296	0.003	0.001	3.513	0.047	0.016	-0.259	0.048	0.016	11.964	0.165	0.055	-0.659	0.163	0.054
0	-0.617	0.004	0.001	7.43	0.004	0.001	6.367	0.032	0.011	-0.295	0.032	0.011	14.622	0.246	0.082	-0.289	0.239	0.08
0	4.488	0.002	0.001	8.878	0.005	0.002	13.497	0.034	0.011	0.097	0.032	0.011	17.336	0.175	0.058	-0.489	0.173	0.058
0	5.422	0.001	0	17.1	0.006	0.002	22.313	0.05	0.017	-0.182	0.047	0.016	35.091	0.158	0.053	0.579	0.159	0.053
0	-0.582	0.003	0.001	7.071	0.005	0.002	6.052	0.031	0.01	-0.292	0.028	0.009	13.393	0.164	0.055	-0.787	0.161	0.054
0	-0.559	0.003	0.001	7.099	0.005	0.002	6.093	0.04	0.013	-0.304	0.039	0.013	13.453	0.153	0.051	-0.784	0.152	0.051
0	-0.8	0.002	0.001	6.003	0.007	0.002	4.77	0.027	0.009	-0.301	0.032	0.011	11.314	0.19	0.063	-0.719	0.186	0.062
0	5.721	0.004	0.001	17.482	0.007	0.002	22.732	0.03	0.01	-0.448	0.026	0.009	36.228	0.129	0.043	0.926	0.122	0.041
0	-0.784	0.003	0.001	5.987	0.005	0.002	4.742	0.045	0.015	-0.329	0.045	0.015	11.583	0.222	0.074	-0.421	0.226	0.075
0	-0.738	0.002	0.001	6.073	0.008	0.003	4.892	0.034	0.011	-0.312	0.037	0.012	11.651	0.204	0.068	-0.526	0.204	0.068
0	5.079	0.004	0.001	14.451	0.01	0.003	18.83	0.039	0.013	-0.677	0.035	0.012	29.012	0.337	0.112	-0.096	0.31	0.103
0	1.592	0.002	0.001	14.951	0.005	0.002	16.127	0.045	0.015	-0.233	0.048	0.016	30.519	0.101	0.034	0.382	0.099	0.033
0	-0.781	0.003	0.001	6.993	0.006	0.002	5.784	0.037	0.012	-0.279	0.037	0.012	13.255	0.147	0.049	-0.768	0.148	0.049
0	-0.912	0.002	0.001	6.067	0.008	0.003	4.729	0.045	0.015	-0.289	0.039	0.013	11.364	0.19	0.063	-0.798	0.177	0.059
0	-32.218	0.003	0.001	10.368	0.006	0.002	-24.298	0.043	0.014	-0.933	0.042	0.014	20.345	0.212	0.071	-0.489	0.212	0.071
0	5.629	0.002	0.001	17.45	0.005	0.002	22.622	0.045	0.015	-0.431	0.044	0.015	35.807	0.196	0.065	0.581	0.187	0.062
0	-0.666	0.003	0.001	6.141	0.006	0.002	5.072	0.028	0.009	-0.272	0.027	0.009	11.451	0.192	0.064	-0.858	0.19	0.063
0	-0.961	0.003	0.001	6.03	0.006	0.002	4.645	0.049	0.016	-0.285	0.051	0.017	11.201	0.283	0.094	-0.884	0.278	0.093
0	5.65	0.002	0.001	16.863	0.006	0.002	21.924	0.041	0.014	-0.567	0.039	0.013	34.746	0.101	0.034	0.712	0.101	0.034
0	-0.934	0.002	0.001	6.018	0.002	0.001	4.646	0.046	0.015	-0.3	0.045	0.015	11.265	0.155	0.052	-0.797	0.152	0.051
0	-0.712	0.002	0.001	6.059	0.006	0.002	4.997	0.041	0.014	-0.22	0.04	0.013	11.664	0.299	0.1	-0.484	0.295	0.098
0	-0.687	0.001	0	6.059	0.003	0.001	5.141	0.03	0.01	-0.103	0.031	0.01	12.103	0.214	0.071	-0.05	0.212	0.071
0	-31.598	0.003	0.001	7.609	0.001	0	-25.528	0.049	0.016	-0.169	0.049	0.016	14.605	0.09	0.03	-0.661	0.089	0.03
0	1.595	0.002	0.001	15.036	0.006	0.002	16.232	0.051	0.017	-0.216	0.053	0.018	30.758	0.129	0.043	0.446	0.124	0.041
0	-2.533	0.002	0.001	5.371	0.007	0.002	2.408	0.035	0.012	-0.245	0.039	0.013	9.789	0.142	0.047	-0.971	0.135	0.045
0	1.028	0.002	0.001	6.402	0.006	0.002	7.047	0.037	0.012	-0.312	0.034	0.011	12.168	0.157	0.052	-0.668	0.158	0.053
0	-6.303	0.002	0.001	0.159	0.006	0.002	-7.052	0.038	0.013	-0.709	0.039	0.013	-1.433	0.136	0.045	-1.749	0.137	0.046
0	4.349	0.003	0.001	8.603	0.006	0.002	13.094	0.031	0.01	0.11	0.03	0.01	17.234	0.144	0.048	-0.045	0.142	0.047
0	5.333	0.003	0.001	17.203	0.006	0.002	22.37	0.064	0.021	-0.133	0.064	0.021	35.675	0.127	0.042	0.941	0.123	0.041
0	0.221	0.002	0.001	6.673	0.004	0.001	6.437	0.039	0.013	-0.351	0.041	0.014	12.801	0.24	0.08	-0.582	0.234	0.078
0	-0.91	0.004	0.001	6.861	0.007	0.002	5.505	0.068	0.023	-0.293	0.067	0.022	13.11	0.108	0.036	-0.649	0.109	0.036
0	-0.715	0.004	0.001	7.398	0.007	0.002	6.249	0.061	0.02	-0.28	0.063	0.021	14.344	0.277	0.092	-0.5	0.272	0.091
0	-6.324	0.003	0.001	0.11	0.004	0.001	-6.878	0.051	0.017	-0.465	0.05	0.017	-1.25	0.218	0.073	-1.47	0.216	0.072
0	-0.694	0.002	0.001	6.112	0.005	0.002	5.021	0.033	0.011	-0.268	0.031	0.01	11.947	0.186	0.062	-0.311	0.184	0.061
0	5.079	0.002	0.001	5.848	0.006	0.002	11.091	0.043	0.014	0.071	0.045	0.015	10.77	0.231	0.077	-0.949	0.234	0.078
0	-0.709	0.002	0.001	6.868	0.003	0.001	5.727	0.048	0.016	-0.287	0.047	0.016	13.053	0.346	0.115	-0.72	0.341	0.114
0	5.657	0.002	0.001	17.57	0.006	0.002	22.749	0.033	0.011	-0.45	0.03	0.01	36.262	0.16	0.053	0.786	0.152	0.051
0	-0.684	0.002	0.001	7.439	0.003	0.001	6.31	0.046	0.015	-0.291	0.048	0.016	14.399	0.187	0.062	-0.526	0.187	0.062
0	-0.75	0.002	0.001	7.389	0.004	0.001	6.215	0.064	0.021	-0.269	0.065	0.022	14.227	0.187	0.062	-0.598	0.179	0.06
0	6.519	0.002	0.001	6.854	0.003	0.001	12.745	0.048	0.016	-0.754	0.051	0.017	12.717	0.186	0.062	-1.023	0.18	0.06
0	5.421	0.003	0.001	12.47	0.008	0.003	17.671	0.03	0.01	-0.245	0.027	0.009	25.108	0.153	0.051	0.027	0.146	0.049
0	5.697	0.002	0.001	17.001	0.007	0.002	22.117	0.036	0.012	-0.559	0.037	0.012	35.016	0.197	0.066	0.701	0.186	0.062

119.482	2.171	0.724	87.026	2.111	0.704	-1.145	0.02	0.007	1.84	1.0093	-8.4	-8.06	22.55	0.004815638
127.419	5.767	1.922	100.01	5.633	1.878	-1.19	0.028	0.009	1.57		-1.44	-1.07	29.76	0.004815638
119.381	2.167	0.722	75.479	2.082	0.694	-1.133	0.017	0.006	2	1.007950954	-1.88	-1.51	29.3	0.004815638
124.732	2.428	0.809	112.555	2.41	0.803	-1.195	0.018	0.006	-4.58	1.007950954	-13.08	-12.77	17.7	0.004815638
123.432	1.345	0.448	107.807	1.329	0.443	-1.18	0.011	0.004	-4.34	1.007950954	-11.66	-11.34	19.17	0.004815638
120.078	1.257	0.419	85.952	1.213	0.404	-1.142	0.01	0.003	-2.24	1.007950954	-4.3	-3.94	26.79	0.004815638
129.555	1.695	0.565	155.876	1.742	0.581	-1.265	0.015	0.005	-37.71		-5.38	-5.03	25.68	0.004815638
121.445	2.73	0.91	87.342	2.653	0.884	-1.174	0.023	0.008	-2.22	1.007950954	-4.34	-3.98	26.76	0.004815638
125.315	2.66	0.887	116.646	2.643	0.881	-1.209	0.021	0.007	-6.35	1.007950954	-13.77	-13.46	16.99	0.004815638
125.756	2.525	0.842	117.119	2.507	0.836	-1.203	0.022	0.007	-6.36	1.007950954	-13.78	-13.47	16.98	0.004815638
124.956	1.903	0.634	116.412	1.893	0.631	-1.202	0.018	0.006	-6.33	1.007950954	-13.83	-13.52	16.93	0.004815638
122.031	2.71	0.903	79.398	2.615	0.872	-1.167	0.023	0.008	2.02	1.007950954	-2.52	-2.15	28.64	0.004784627
125.084	3.178	1.059	116.48	3.165	1.055	-1.203	0.025	0.008	-6.32	1.007950954	-13.81	-13.5	16.95	0.004815638
134.276	2.321	0.774	142.154	2.339	0.78	-1.294	0.021	0.007	-10.28	1.007950954	-19.04	-18.76	11.52	0.00486748
130.06	1.769	0.59	115.11	1.737	0.579	-1.257	0.014	0.005	-3.35	1.007950954	-12.49	-12.17	18.31	0.004815638
130.237	2.098	0.699	115.371	2.072	0.691	-1.252	0.021	0.007	-3.39	1.007950954	-12.51	-12.19	18.3	0.004815638
129.713	3.305	1.102	114.141	3.288	1.089	-1.245	0.028	0.009	-4.37	1.007950954	-11.71	-11.39	19.12	0.004815638
131.709	1.812	0.604	120.617	1.798	0.599	-1.255	0.017	0.006	-6.16	1.007950954	-12.82	-12.5	17.97	0.004815638
133.059	2.125	0.708	117.429	2.094	0.698	-1.269	0.02	0.007	-4.37	1.007950954	-11.71	-11.38	19.12	0.004815638
124.414	5.369	1.79	99.792	5.257	1.752	-1.197	0.03	0.01	1.06		-2.43	-2.06	28.74	0.004815638
117.442	2.776	0.925	74.612	2.672	0.891	-1.142	0.025	0.008	1.76	1.007950954	-2.22	-1.86	28.95	0.004815638
121.599	2.911	0.97	106.863	2.872	0.957	-1.182	0.026	0.009	-4.32	1.007950954	-12.06	-11.74	18.76	0.004815638
122.923	2.515	0.838	108.081	2.478	0.826	-1.192	0.021	0.007	-4.29	1.007950954	-12.03	-11.71	18.79	0.004815638
122.729	1.104	0.368	110.547	1.104	0.368	-1.187	0.01	0.003	-4.51	1.007950954	-13.11	-12.79	17.67	0.004815638
116.102	2.314	0.771	72.191	2.235	0.745	-1.137	0.019	0.006	2.07	1.007950954	-1.85	-1.48	29.34	0.004815638
123.063	1.569	0.523	110.895	1.553	0.518	-1.191	0.014	0.005	-4.49	1.007950954	-13.12	-12.81	17.66	0.004815638
123.458	1.757	0.586	111.043	1.733	0.578	-1.191	0.017	0.006	-4.44	1.007950954	-13.04	-12.72	17.74	0.004815638
125.225	3.1	1.033	88.052	2.98	0.993	-1.153	0.018	0.006	1.49		3.09	3.49	34.45	0.004815638
118.859	3.189	1.063	84.861	3.093	1.031	-1.121	0.026	0.009	-2.27	1.007950954	-4.33	-3.97	26.77	0.004815638
119.943	2.137	0.712	105.631	2.107	0.702	-1.145	0.018	0.006	-4.52	1.007950954	-12.14	-11.82	18.68	0.004815638
120.655	1.225	0.408	108.489	1.207	0.402	-1.154	0.012	0.004	-4.63	1.007950954	-13.04	-12.73	17.74	0.004815638
127.978	2.686	0.895	144.653	2.734	0.911	-1.259	0.023	0.008	-38.38		-0.87	-0.49	30.35	0.004815638
120.049	2.037	0.679	76.154	1.961	0.654	-1.169	0.018	0.006	1.97	1.007950954	-1.88	-1.51	29.3	0.004815638
124.941	2.05	0.683	112.278	2.026	0.675	-1.221	0.02	0.007	-4.37	1.007950954	-12.97	-12.66	17.81	0.004815638
125.7	1.822	0.607	113.619	1.799	0.6	-1.212	0.018	0.006	-4.68	1.007950954	-13.08	-12.77	17.7	0.004815638
119.844	1.635	0.545	77.155	1.573	0.524	-1.165	0.016	0.005	2.01	1.007950954	-2.46	-2.09	28.71	0.004832384
122.599	2.322	0.774	110.546	2.298	0.766	-1.2	0.018	0.006	-4.65	1.007950954	-13.09	-12.78	17.69	0.004815638
112.894	1.809	0.603	100.596	1.788	0.596	-1.093	0.017	0.006	-4.42	1.007950954	-13.05	-12.74	17.73	0.004815638
97.134	2.532	0.844	84.981	2.505	0.835	-0.943	0.024	0.008	-4.39	1.007950954	-13.05	-12.74	17.73	0.004815638
134.217	2.996	0.999	156.39	3.056	1.019	-1.286	0.01	0.003	-37.62		-3.6	-3.24	27.52	0.004815638
119.939	2.135	0.712	85.724	2.078	0.693	-1.175	0.018	0.006	-2.27	1.007950954	-4.24	-3.88	26.86	0.004815638
124.324	2.312	0.771	115.562	2.295	0.765	-1.213	0.02	0.007	-6.35	1.007950954	-13.72	-13.41	17.03	0.004815638
121.055	2.859	0.953	105.872	2.824	0.941	-1.187	0.024	0.008	-2.56	1.007950954	-12.72	-12.4	18.07	0.004815638
126.244	1.931	0.644	133.505	1.944	0.648	-1.234	0.016	0.005	-10.2	1.007950954	-18.83	-18.55	11.74	0.004780242
115.28	1.903	0.634	91.603	1.868	0.623	-1.148	0.022	0.007	0.92		-2.7	-2.33	28.46	0.004815638
113.552	1.976	0.659	70.759	1.908	0.636	-1.119	0.018	0.006	1.66	1.007950954	-2.12	-1.75	29.05	0.004815638
118.1	2.487	0.829	103.321	2.449	0.816	-1.161	0.022	0.007	-3.44	1.007950954	-12.45	-12.13	18.35	0.004815638
116.536	2.006	0.669	102.704	1.987	0.662	-1.155	0.016	0.005	-4.66	1.007950954	-12.26	-11.95	18.55	0.004815638
115.666	1.726	0.575	100.459	1.707	0.569	-1.146	0.015	0.005	-4.47	1.007950954	-11.74	-11.42	19.09	0.004815638
117.894	1.401	0.467	125.234	1.414	0.471	-1.17	0.009	0.003	-10.22	1.007950954	-18.88	-18.59	11.69	0.004815638
116.209	1.969	0.656	103.737	1.948	0.649	-1.142	0.02	0.007	-4.4	1.007950954	-13	-12.68	17.78	0.004815638
116.789	1.745	0.582	98.122	1.72	0.573	-1.16	0.019	0.006	1.8		-5.43	-5.07	25.63	0.004815638
116.902	3.081	1.027	102.812	3.045	1.015	-1.152	0.025	0.008	-4.44	1.007950954	-12.26	-11.94	18.55	0.004815638
111.142	1.826	0.609	67.318	1.764	0.588	-1.101	0.016	0.005	1.99	1.007950954	-1.76	-1.39	29.43	0.004815638
116.534	1.959	0.653	101.192	1.935	0.645	-1.145	0.016	0.005	-4.44	1.007950954	-11.7	-11.38	19.13	0.004815638
115.186	2.173	0.724	100.047	2.152	0.717	-1.138	0.018	0.006	-4.51	1.007950954	-11.75	-11.42	19.08	0.004815638
119.344	1.091	0.364	96.8	1.066	0.355	-1.187	0.01	0.003	3.31		-4.43	-4.08	22.66	0.004815638
120.077	1.706	0.569	86.85	1.654	0.551	-1.171	0.016	0.005	1.93	1.0093	-8.1	-7.76	26.86	0.004815638
114.388	2.264	0.755	71.568	2.183	0.728	-1.125	0.017	0.006	2.06	1.007950954	-2.32	-1.95	28.85	0.004809932
									-3.82			-12.29	18.19	
									-6.34			-13.44	17.01	
									-5.72			-12.05	18.44	
									-4.37			-11.31	19.2	
									-5.44			-12.12	18.37	
									-4.47			-11.78	18.72	
									-2.54			-12.39	18.09	

-4.41
-6.59
-4.57

-13.09
-13.61
-12.75

17.37
16.83
17.72

D47 Nonlinearity Intercepts	D47 WG (HG)	ETF Slope	ETF Intercept	D47 CDES (ETF)	Clumped AFF	D47 CDES (Final)	D48 WG (HG)
1=-0.0423376244908604,2=-0.8186394497140147,3=-0.640038353887165	0.012	1.198545765	0.963885195	0.978		0.978	-6.762
1=-0.04352724327289068,2=-0.8202496720331918,3=-0.635586534989798	-0.014	1.198545765	0.963885195	0.948		0.948	8.005
1=-0.037279822539806544,2=-0.8195690953530168,3=-0.6374681410822151	-0.288	1.198545765	0.963885195	0.618	0.082	0.7	0.023
1=-0.037279822539806544,2=-0.8195690953530168,3=-0.6374681410822151	-0.553	1.197882141	0.963694929	0.302	0.082	0.384	4.196
1=-0.037279822539806544,2=-0.8195690953530168,3=-0.6374681410822151	-0.296	1.201966063	0.96587366	0.61	0.082	0.692	3.429
1=-0.0372798225398067,2=-0.8195690953530167,3=-0.6374681410822147	-0.273	1.198545765	0.963885195	0.636	0.082	0.718	0.169
1=-0.037279822539806544,2=-0.8195690953530168,3=-0.6374681410822151	-0.441	1.19891266	0.963806341	0.435	0.082	0.517	-2.098
1=-0.037279822539806544,2=-0.8195690953530168,3=-0.6374681410822151	-0.562	1.202787751	0.965101405	0.289	0.082	0.371	3.988
1=-0.037279822539806544,2=-0.8195690953530168,3=-0.6374681410822151	-0.267	1.19865373	0.963942808	0.644	0.082	0.726	0.33
1=-0.03727982253980647,2=-0.8195690953530167,3=-0.6374681410822146	-0.252	1.198545765	0.963885195	0.662	0.082	0.744	-0.361
1=-0.037279822539806544,2=-0.8195690953530168,3=-0.6374681410822151	-0.292	1.196000522	0.962477241	0.613	0.082	0.695	3.469
1=-0.037279822539806544,2=-0.8195690953530168,3=-0.6374681410822151	-0.464	1.201023363	0.963352702	0.406	0.082	0.488	-2.572
1=-0.039540344457958246,2=-0.81914115538658865,3=-0.6386501749226037	-0.015	1.198545765	0.963885195	0.946		0.946	-7.752
1=-0.037279822539806544,2=-0.8195690953530168,3=-0.6374681410822151	-0.293	1.185935291	0.957156008	0.609	0.082	0.691	0.031
1=-0.0429101130665148206,2=-0.873573860492631,3=-0.632085167133571	-0.717	1.198545765	0.963885195	0.104		0.104	5.202
1=-0.037279822539806544,2=-0.8195690953530168,3=-0.6374681410822151	-0.561	1.202171565	0.96492474	0.29	0.082	0.372	4.049
1=-0.037279822539806544,2=-0.8195690953530168,3=-0.6374681410822151	-0.301	1.20033545	0.964925668	0.604	0.082	0.686	3.331
1=-0.037279822539806544,2=-0.819569095353017,3=-0.6374681410822146	-0.345	1.198545765	0.963885195	0.55	0.082	0.632	0.153
1=-0.037279822539806544,2=-0.8195690953530169,3=-0.6374681410822148	-0.344	1.198545765	0.963885195	0.552	0.082	0.634	0.216
1=-0.03727982253980653,2=-0.8195690953530169,3=-0.6374681410822146	-0.319	1.198545765	0.963885195	0.581	0.082	0.663	0.396
1=-0.03728576522440252,2=-0.8195711504035579,3=-0.6264277773718168	-0.648	1.195735117	0.96294153	0.188	0.082	0.27	3.676
1=-0.037279822539806544,2=-0.8195690953530168,3=-0.6374681410822151	-0.55	1.19652777	0.963306621	0.305	0.082	0.387	4.161
1=-0.037279822539806544,2=-0.8195690953530168,3=-0.6374681410822151	-0.24	1.211727914	0.970919439	0.68	0.082	0.762	0.277
1=-0.037279822539806544,2=-0.8195690953530168,3=-0.6374681410822151	-0.437	1.198520913	0.963890537	0.44	0.082	0.522	-2.286
1=-0.02471032935779584,2=-0.8185326176255691,3=-0.640333715033588	-0.092	1.198545765	0.963885195	0.854		0.854	6.731
1=-0.037279822539806544,2=-0.819569095353017,3=-0.6374681410822151	-0.352	1.198545765	0.963885195	0.542	0.082	0.624	0.354
1=-0.044500962334719264,2=-0.8182195905644611,3=-0.6411991481911284	0.033	1.198545765	0.963885195	1.004		1.004	-7.59
1=-0.037279822539806544,2=-0.8195690953530168,3=-0.6374681410822151	-0.569	1.206184286	0.966075217	0.29	0.082	0.362	4.301
1=-0.037279822539806544,2=-0.8195690953530168,3=-0.6374681410822151	-0.295	1.202353628	0.966098979	0.611	0.082	0.693	3.225
1=-0.046466747039259994,2=-0.7752770685037907,3=-0.6286847621382454	-0.918	1.198545765	0.963885195	-0.136		-0.136	-7.087
1=-0.037279822539806544,2=-0.8195690953530168,3=-0.6374681410822151	-0.252	1.212850318	0.971798057	0.666	0.082	0.748	4.037
1=-0.037279822539806544,2=-0.8195690953530168,3=-0.6374681410822151	-0.434	1.198279356	0.963942453	0.444	0.082	0.526	-2.143
1=-0.036131717001600526,2=-0.8057251589183565,3=-0.6385658148478295	-0.846	1.198545765	0.963885195	-0.05		-0.05	3.082
1=-0.03728576522440239,2=-0.8195711504035579,3=-0.6484971415010666	-0.626	1.175654963	0.956196991	0.22	0.082	0.302	4.086
1=-0.037279822539806544,2=-0.8195690953530168,3=-0.6374681410822151	-0.312	1.196509257	0.962701228	0.589	0.082	0.671	3.346
1=-0.037279822539806544,2=-0.8195690953530168,3=-0.6374681410822151	-0.29	1.187718542	0.958107585	0.614	0.082	0.696	0.335
1=-0.037279822539806544,2=-0.8195690953530168,3=-0.6374681410822151	-0.308	1.198054808	0.963599767	0.595	0.082	0.677	3.379
1=-0.028330632797807884,2=-0.8200280310210829,3=-0.6361993110235088	-0.1	1.198545765	0.963885195	0.844		0.844	0.949
1=-0.030080524496644934,2=-0.8188482191312032,3=-0.6394611642497066	-0.066	1.198545765	0.963885195	0.885		0.885	6.509
2=-0.8408376034211004	-0.984	1.214929236	1.207846531	0.012		0.012	-0.493
2=-0.8408376034211004	-0.283	1.214929236	1.207846531	0.864		0.864	-0.299
2=-0.8408376034211004	-0.674	1.196111705	1.190538247	0.385	0.082	0.467	-0.234
2=-0.8408376034211004	-0.494	1.214929236	1.207846531	0.607	0.082	0.689	-0.311
2=-0.8408376034211004	-0.506	1.214929236	1.207846531	0.593	0.082	0.675	-0.297
2=-0.8408376034211004	-0.758	1.214929236	1.207846531	0.287	0.082	0.369	-0.376
2=-0.8408376034211004	-0.55	1.214929236	1.207846531	0.539	0.082	0.621	-0.219
2=-0.8408376034211004	-0.321	1.214929236	1.207846531	0.818		0.818	-0.601
2=-0.8408376034211004	-0.286	1.214929236	1.207846531	0.86		0.86	-0.336
2=-0.8408376034211004	-1.104	1.214929236	1.207846531	-0.134		-0.134	-0.76
2=-0.8408376034211004	-1.026	1.214929236	1.207846531	-0.039		-0.039	-0.581
2=-0.8408376034211004	-0.267	1.214929236	1.207846531	0.883		0.883	-0.454
2=-0.8408376034211004	-0.649	1.207110997	1.200655349	0.417	0.082	0.499	-0.228
2=-0.8408376034211004	-0.117	1.214929236	1.207846531	1.066		1.066	-0.185
2=-0.8408376034211004	-0.612	1.214929236	1.207846531	0.464	0.082	0.546	-0.388
2=-0.8408376034211004	-0.469	1.214929236	1.207846531	0.639	0.082	0.721	-0.297
2=-0.8408376034211004	-0.744	1.214929236	1.207846531	0.304	0.082	0.386	-0.426
2=-0.8408376034211004	-0.08	1.214929236	1.207846531	1.111		1.111	4.141
2=-0.8408376034211004	-0.541	1.214929236	1.207846531	0.551	0.082	0.633	17.813
2=-0.8434232886398524	-0.821	1.202590408	1.200804281	0.213	0.082	0.295	-0.35
2=-0.8408376034211004	-1.053	1.214929236	1.207846531	-0.071		-0.071	-0.614
2=-0.8408376034211004	-0.241	1.214929236	1.207846531	0.915		0.915	-0.501
2=-0.8408376034211004	-0.373	1.214929236	1.207846531	0.755	0.082	0.837	-0.223
2=-0.8408376034211004	-0.2	1.214929236	1.207846531	0.965		0.965	-0.316
2=-0.8331060524052312	-0.888	1.242427788	1.223599423	0.12	0.082	0.202	-0.468
2=-0.8408376034211004	-0.144	1.214929236	1.207846531	1.033		1.033	-0.227

2=-.8408376034211004	-0.475	1.214929236	1.207846531	0.63	0.082	0.712	-0.275
2=-.8408376034211004	-0.448	1.214929236	1.207846531	0.664	0.082	0.746	-0.295
2=-.8361028989348617	-0.877	1.236385668	1.220092553	0.136	0.082	0.218	-0.307
2=-.8408376034211004	-0.5	1.214929236	1.207846531	0.6	0.082	0.682	-0.245
2=-.8408376034211004	-0.255	1.214929236	1.207846531	0.898		0.898	-0.343
2=-.8408376034211004	-0.812	1.214929236	1.207846531	0.222	0.082	0.304	-0.465
2=-.8408376034211004	-0.48	1.214929236	1.207846531	0.624	0.082	0.706	-0.322
2=-.8408376034211004	-0.649	1.207011463	1.200563798	0.417	0.082	0.499	-0.274
2=-.8408376034211004	-1.036	1.214929236	1.207846531	-0.051		-0.051	-0.607
2=-.8408376034211004	-1.107	1.214929236	1.207846531	-0.136		-0.136	-0.543
2=-.8408376034211004	-0.335	1.214929236	1.207846531	0.8		0.8	-0.477
2=-.8408376034211003	-0.461	1.214929236	1.207846531	0.648	0.082	0.73	-0.211
2=-.8408376034211004	-0.694	1.214929236	1.207846531	0.365	0.082	0.447	-0.385
2=-.8408376034211003	-0.463	1.214929236	1.207846531	0.646	0.082	0.728	-0.199
2=-.8408376034211003	-0.457	1.214929236	1.207846531	0.653	0.082	0.735	-0.165
2=-.8439464125741222	-0.822	1.201945226	1.200408478	0.213	0.082	0.295	-0.395
2=-.8408376034211004	-0.194	1.214929236	1.207846531	0.972		0.972	-0.268
2=-.8404727519320679	-0.844	1.215968852	1.208439881	0.183	0.082	0.265	-0.326
2=-.8408376034211003	-0.511	1.214929236	1.207846531	0.587	0.082	0.669	-0.195
2=-.8408376034211004	-0.48	1.214929236	1.207846531	0.625	0.082	0.707	-0.211
2=-.8408376034211	-1.358	1.214929236	1.207846531	-0.442	0.082	-0.36	-0.599
2=-.8408376034211004	-1.038	1.214929236	1.207846531	-0.054		-0.054	-0.534
2=-.8408376034211004	-0.451	1.214929236	1.207846531	0.66	0.082	0.742	-0.244
2=-.8408376034211004	-0.543	1.214929236	1.207846531	0.548	0.082	0.63	-0.331
2=-.8408376034211004	-0.502	1.214929236	1.207846531	0.598	0.082	0.68	-0.378
2=-.8408376034211004	-0.698	1.214929236	1.207846531	0.36	0.082	0.442	-0.322
2=-.8408376034211003	-2.128	1.214929236	1.207846531	-1.378	0.082	-1.296	-0.93
2=-.8408376034211003	-1.242	1.214929236	1.207846531	-0.301	0.082	-0.219	-0.535
2=-.8408376034211	-0.525	1.214929236	1.207846531	0.57	0.082	0.652	-0.285
2=-.8408376034211004	-0.423	1.214929236	1.207846531	0.694	0.082	0.776	-0.208
2=-.8408376034211	-0.543	1.214929236	1.207846531	0.548	0.082	0.63	-0.23
2=-.8408376034211004	-0.594	1.214929236	1.207846531	0.486	0.082	0.568	-0.304
2=-.8408376034211003	-0.532	1.214929236	1.207846531	0.562	0.082	0.644	-0.266
2=-.8408376034211004	-0.299	1.214929236	1.207846531	0.844		0.844	-0.326
2=-.8408376034211004	-0.618	1.214929236	1.207846531	0.458	0.082	0.54	-0.33
2=-.8408376034211004	-0.408	1.214929236	1.207846531	0.712		0.712	-0.43
2=-.8408376034211003	-0.599	1.214929236	1.207846531	0.48	0.082	0.562	-0.305
2=-.8408376034211004	-0.51	1.214929236	1.207846531	0.588	0.082	0.67	-0.277
2=-.8408376034211003	-1.858	1.214929236	1.207846531	-1.049	0.082	-0.967	-0.758
2=-.8408376034211004	-1.13	1.214929236	1.207846531	-0.165		-0.165	-0.616
2=-.8408376034211004	-0.224	1.214929236	1.207846531	0.935		0.935	-0.272
2=-.8408376034211004	-0.563	1.214929236	1.207846531	0.524	0.062	0.586	-0.356
2=-.8408376034211004	-0.247	1.214929236	1.207846531	0.908		0.908	-0.309
2=-.8408376034211004	-0.264	1.214929236	1.207846531	0.887		0.887	-0.314
2=-.8408376034211004	-0.911	1.214929236	1.207846531	0.101		0.101	-0.45
2=-.8408376034211	-0.563	1.214929236	1.207846531	0.523	0.082	0.605	-0.19
2=-.8408376034211003	-1.834	1.214929236	1.207846531	-1.021	0.082	-0.939	-0.687
2=-.8408376034211004	-1.014	1.214929236	1.207846531	-0.024		-0.024	-0.49
2=-.8408376034211004	-0.462	1.247247789	1.23367583	0.657	0.082	0.739	-0.277
2=-.8408376034211004	-0.429	1.214929236	1.207846531	0.687	0.082	0.769	-0.171
2=-.8408376034211004	-0.596	1.231706171	1.223277884	0.489	0.082	0.571	-0.174
2=-.8408376034211004	-0.687	1.214929236	1.207846531	0.373	0.082	0.455	-0.28
2=-.8454278937496892	-0.813	1.196637007	1.197367598	0.225	0.082	0.307	-0.392
2=-.8408376034211004	-0.186	1.214929236	1.207846531	0.982		0.982	-0.199
2=-.8408376034211004	-0.21	1.214929236	1.207846531	0.953		0.953	-0.18
2=-.8408376034211004	-0.49	1.214929236	1.207846531	0.612	0.082	0.694	-0.249
2=-.8408376034211004	-0.459	1.214929236	1.207846531	0.65	0.082	0.732	-0.26
2=-.8408376034211004	-0.688	1.214929236	1.207846531	0.372	0.082	0.454	-0.4
2=-.8408376034211004	-0.44	1.214929236	1.207846531	0.674	0.082	0.756	-0.21
2=-.8408376034211004	-0.967	1.214929236	1.207846531	0.033		0.033	-0.523
2=-.8408376034211004	-1.017	1.214929236	1.207846531	-0.028		-0.028	-0.439
2=-.8445847072117015	-0.812	1.197367469	1.197823346	0.225	0.082	0.307	-0.256
2=-.8408376034211004	-0.247	1.214929236	1.207846531	0.908		0.908	-0.277
2=-.8408376034211004	-0.148	1.214929236	1.207846531	1.028		1.028	-0.174
2=-.8408376034211004	-0.624	1.218569936	1.211195232	0.451	0.082	0.533	-0.302
2=-.8408376034211004	-0.485	1.21185338	1.205388278	0.618	0.082	0.7	-0.264
2=-.8408376034211004	-0.196	1.214929236	1.207846531	0.97		0.97	-0.267
2=-.8408376034211004	-0.412	1.214929236	1.207846531	0.707	0.082	0.789	-0.21

2=-0.8408376034211004	-0.423	1.214929236	1.207846531	0.694	0.082	0.776	-0.184
2=-0.8408376034211004	-0.168	1.214929236	1.207846531	1.004		1.004	-0.17
2=-0.8408376034211004	-0.799	1.214929236	1.207846531	0.238	0.082	0.32	-0.388
2=-0.8408376034211004	-0.614	1.214929236	1.207846531	0.462	0.082	0.544	-0.347
2=-0.8408376034211004	-0.44	1.214929236	1.207846531	0.673	0.082	0.755	-0.218
2=-0.8408376034211004	-0.696	1.214929236	1.207846531	0.362	0.082	0.444	-0.247
2=-0.8408376034211004	-0.193	1.214929236	1.207846531	0.973		0.973	-0.304
2=-0.8408376034211004	-0.239	1.214929236	1.207846531	0.917		0.917	-0.278
2=-0.8396205920699701	-0.85	1.219895805	1.210681146	0.174	0.082	0.256	-0.335
2=-0.8408376034211004	-0.5	1.214929236	1.207846531	0.6	0.082	0.682	-0.275
2=-0.8408376034211004	-0.769	1.214929236	1.207846531	0.274	0.082	0.356	-0.418
2=-0.8408376034211004	-0.939	1.214929236	1.207846531	0.068		0.068	-0.434
2=-0.8408376034211004	-1.004	1.214929236	1.207846531	-0.012		-0.012	-0.46
2=-0.8408376034211004	-0.857	1.214929236	1.207846531	0.167	0.082	0.249	-0.508
2=-0.8408376034211004	-0.201	1.214929236	1.207846531	0.963		0.963	-0.188
2=-0.8408376034211004	-0.522	1.214929236	1.207846531	0.573	0.082	0.655	-0.281
2=-0.8408376034211004	-1.08	1.214929236	1.207846531	-0.105		-0.105	-0.546
2=-0.8408376034211004	-0.47	1.214929236	1.207846531	0.636	0.082	0.718	-0.206
2=-0.8408376034211004	-0.775	1.214929236	1.207846531	0.266	0.082	0.348	-0.368
2=-0.8408376034211004	-0.494	1.214929236	1.207846531	0.607	0.082	0.689	-0.248
2=-0.8408376034211004	-0.819	1.214929236	1.207846531	0.213	0.082	0.295	-0.344
2=-0.8408376034211004	-0.256	1.214929236	1.207846531	0.897		0.897	-0.23
2=-0.8408376034211004	-1.136	1.214929236	1.207846531	-0.172		-0.172	-0.616
2=-0.8408376034211004	-0.442	1.214929236	1.207846531	0.671	0.082	0.753	-0.245
1=-0.028724886454931858,2=-0.737505060926956,3=-0.6186269516721761	-0.757	1.258386047	0.963092356	0.011		0.011	2.395
1=-0.03130070809473073,2=-0.7412956094142923,3=-0.6192509823116246	-0.377	1.257272451	0.965664492	0.491	0.082	0.573	-0.715
1=-0.015088345973302133,2=-0.7412632707813939,3=-0.6195828403735599	-0.085	1.258386047	0.963092356	0.856		0.856	0.688
1=-0.02942911284203014,2=-0.7383093152837943,3=-0.6187975608618294	-0.753	1.258386047	0.963092356	0.015		0.015	2.286
1=-0.03130070809473073,2=-0.7412956094142923,3=-0.6192509823116246	-0.281	1.258386047	0.963092356	0.61	0.082	0.692	0.514
1=-0.04135276437415358,2=-0.7413245448262279,3=-0.6189540479991427	0.004	1.258386047	0.963092356	0.968		0.968	0.528
1=-0.03130070809473073,2=-0.7412956094142923,3=-0.6192509823116246	-0.232	1.258386047	0.963092356	0.671	0.082	0.753	0.51
1=-0.03130070809473073,2=-0.7412956094142923,3=-0.6192509823116246	-0.239	1.267667562	0.968154178	0.666	0.082	0.748	0.124
1=-0.02546537460029194,2=-0.7489712678989594,3=-0.6178372870325464	-0.711	1.258386047	0.963092356	0.068		0.068	1.021
1=-0.03161199450966029,2=-0.7412882605609945,3=-0.6169120360014355	-0.627	1.26582648	0.965377083	0.172	0.082	0.254	-0.759
1=-0.03130070809473073,2=-0.7412956094142923,3=-0.6192509823116246	-0.428	1.258755763	0.962238402	0.423	0.082	0.505	-0.682
1=-0.03336337466978,2=-0.7485724299416187,3=-0.6197506935967189	-0.712	1.258386047	0.963092356	0.067		0.067	0.887
1=-0.03130070809473073,2=-0.7412956094142923,3=-0.6192509823116246	-0.291	1.258386976	0.963092904	0.597	0.082	0.679	0.938
1=-0.03130070809473073,2=-0.7412956094142923,3=-0.6192509823116246	-0.309	1.258386047	0.963092356	0.575	0.082	0.657	0.428
1=-0.039267516112924124,2=-0.7310717349768161,3=-0.6211810586123837	-0.781	1.258386047	0.963092356	-0.02		-0.02	-0.431
1=-0.03115135229454417,2=-0.7412991354077573,3=-0.6203986148635968	-0.616	1.256001861	0.962360247	0.189	0.082	0.271	-0.74
1=-0.03130070809473073,2=-0.7412956094142923,3=-0.6192509823116246	-0.27	1.259494263	0.963717212	0.624	0.082	0.706	1.251
1=-0.04981529531020579,2=-0.7412574614338457,3=-0.6196424557204606	0.018	1.258386047	0.963092356	0.985		0.985	1.88
1=-0.03130070809473073,2=-0.7412956094142923,3=-0.6192509823116246	-0.393	1.257727432	0.964613597	0.47	0.082	0.552	-0.839
1=-0.03130070809473073,2=-0.7412956094142923,3=-0.6192509823116246	-0.266	1.258386047	0.963092356	0.628	0.082	0.71	0.04
1=-0.03130070809473073,2=-0.7412956094142923,3=-0.6192509823116246	-0.259	1.258386047	0.963092356	0.637	0.082	0.719	0.486
1=-0.03130070809473098,2=-0.7412956094142924,3=-0.6192509823116246	-0.263	1.258386047	0.963092356	0.632	0.082	0.714	0.109
1=-0.03130070809473128,2=-0.7412956094142922,3=-0.6192509823116246	-0.28	1.258386047	0.963092356	0.61	0.082	0.692	0.182
1=-0.03130070809473073,2=-0.7412956094142923,3=-0.6192509823116246	-0.547	1.267728962	0.965238336	0.272	0.082	0.354	1.273
1=-0.031300708094730845,2=-0.7412956094142922,3=-0.6192509823116248	-0.256	1.258386047	0.963092356	0.641	0.082	0.723	0.172
1=-0.03130070809473086,2=-0.7412956094142923,3=-0.6192509823116247	-0.259	1.258386047	0.963092356	0.637	0.082	0.719	0.209
1=-0.03130070809473073,2=-0.7412956094142923,3=-0.6192509823116246	-0.254	1.258386312	0.963092501	0.644	0.082	0.726	-0.047
1=-0.01982826307690555,2=-0.7413181927180071,3=-0.6190192331394678	-0.062	1.258386047	0.963092356	0.885		0.885	1.895
1=-0.03075991906653638,2=-0.7413083763679493,3=-0.6177070475278551	-0.623	1.26151411	0.964055251	0.178	0.082	0.26	1.09
1=-0.030983260584106175,2=-0.7413031037188091,3=-0.6216609430159012	-0.612	1.252481188	0.961279158	0.195	0.082	0.277	-0.871
1=-0.03130070809473073,2=-0.7412956094142923,3=-0.6192509823116246	-0.307	1.251306052	0.958919727	0.575	0.082	0.657	0.962
1=-0.03130070809473073,2=-0.7412956094142923,3=-0.6192509823116246	-0.289	1.258386047	0.963092356	0.6	0.082	0.682	0.426
1=-0.03130070809473073,2=-0.7412956094142923,3=-0.6192509823116246	-0.279	1.254434783	0.960864479	0.611	0.082	0.693	1.197
1=-0.03130070809473073,2=-0.7412956094142923,3=-0.6192509823116246	-0.529	1.259164293	0.963271112	0.298	0.082	0.38	1.163
1=-0.03130070809473073,2=-0.7412956094142923,3=-0.6192509823116246	-0.254	1.258178986	0.962979432	0.644	0.082	0.726	0.112
1=-0.03130070809473073,2=-0.7412956094142924,3=-0.6192509823116246	-0.29	1.248967456	0.957781786	0.596	0.082	0.678	1.361
1=-0.033210926619664086,2=-0.6992549799272896,3=-0.6060881915259552	-0.024	1.334929305	0.991069994	0.959		0.959	1.303
1=-0.032534200280603436,2=-0.6993131094671332,3=-0.6060459140094878	-0.242	1.338959593	0.993217112	0.669	0.082	0.751	0.086
1=-0.032534200280603436,2=-0.6993131094671332,3=-0.6060459140094878	-0.251	1.334929305	0.991069994	0.656	0.082	0.738	0.5
1=-0.03253420028060354,2=-0.699313109467133,3=-0.6060459140094879	-0.298	1.334929305	0.991069994	0.593	0.082	0.675	0.084
1=-0.032534200280603436,2=-0.6993131094671332,3=-0.6060459140094878	-0.516	1.334588003	0.990986464	0.302	0.082	0.384	1.084
1=-0.03253420028060359,2=-0.699313109467133,3=-0.6060459140094878	-0.328	1.334929305	0.991069994	0.553	0.082	0.635	0.178
1=-0.03253420028060361,2=-0.6993131094671331,3=-0.6060459140094882	-0.272	1.334929305	0.991069994	0.628	0.082	0.71	-0.068
1=-0.03253420028060365,2=-0.699313109467133,3=-0.6060459140094878	-0.356	1.334929305	0.991069994	0.516	0.082	0.598	-0.02

1=-0.011573931534369107,2=-0.7990440324271278,3=-0.6725589246787634	-0.01	1.156359881	0.964607687	0.953		0.953	0.998
1=-0.011525287252707387,2=-0.79866868684345213,3=-0.6757876476706304	-0.646	1.14856308	0.961890561	0.22	0.082	0.302	-1.737
1=-0.011493036719517097,2=-0.7989850512778055,3=-0.6723170616148557	-0.675	1.156119802	0.964523748	0.184	0.082	0.266	0.508
1=-0.010214914467418701,2=-0.7985974940170997,3=-0.6727983203369157	-0.033	1.156359881	0.964607687	0.927		0.927	0.906
1=-0.01142371092169186,2=-0.7958695508390884,3=-0.672259355102159	-0.857	1.156359881	0.964607687	-0.026		-0.026	-0.938
1=-0.011489832635193651,2=-0.7990164838529651,3=-0.6725736938652319	-0.311	1.156359881	0.964607687	0.606	0.082	0.688	-0.785
1=-0.011489832635193853,2=-0.799016483852965,3=-0.6725736938652316	-0.405	1.156359881	0.964607687	0.496	0.082	0.578	-0.667
1=-0.01149055280467388,2=-0.7990093945882694,3=-0.6726380278148238	-0.672	1.155769359	0.964401895	0.188	0.082	0.27	-1.739
1=-0.01148983263519376,2=-0.7990164838529653,3=-0.6725736938652316	-0.387	1.156359881	0.964607687	0.517	0.082	0.599	-0.684
1=-0.011489832635193783,2=-0.7990164838529654,3=-0.6725736938652318	-0.401	1.156359881	0.964607687	0.5	0.082	0.582	-0.736
1=-0.01153210634494368,2=-0.7976573129994109,3=-0.6727960268173657	-0.813	1.156359881	0.964607687	0.025		0.025	0.27
1=-0.010562489414019067,2=-0.7993288642302482,3=-0.6724062222562187	-0.026	1.156359881	0.964607687	0.935		0.935	-0.181
1=-0.011489832635193651,2=-0.7990164838529651,3=-0.6725736938652319	-0.268	1.15892153	0.966157287	0.655	0.082	0.737	-0.765
1=-0.012273087203189557,2=-0.7991469076180878,3=-0.6725037718106238	0.001	1.156359881	0.964607687	0.966		0.966	-0.465
1=-0.011471321827294701,2=-0.7981513438084313,3=-0.6724763387338542	-0.815	1.156359881	0.964607687	0.022		0.022	-0.806
1=-0.011489832635193651,2=-0.7990164838529651,3=-0.6725736938652319	-0.252	1.156359881	0.964607687	0.673	0.082	0.755	-0.266
1=-0.012376170322919515,2=-0.7991657456102431,3=-0.672493672492337	0.003	1.156359881	0.964607687	0.968		0.968	-0.471
1=-0.01149196955659965,2=-0.798995520315203,3=-0.6724047813032936	-0.674	1.155886253	0.964442092	0.185	0.082	0.267	0.294
1=-0.010563851423680047,2=-0.7993252350195568,3=-0.6724081679282203	-0.026	1.156359881	0.964607687	0.935		0.935	-0.244
1=-0.011489832635193651,2=-0.7990164838529651,3=-0.6725736938652319	-0.281	1.160371648	0.967090118	0.641	0.082	0.723	0.795
1=-0.012087064056943403,2=-0.7991128755649036,3=-0.6725220168833601	-0.002	1.156359881	0.964607687	0.963		0.963	-0.604
3=-0.666900519144065	-0.034	1.149339772	0.947509318	0.909		0.909	-0.447
3=-0.6675451723479657	-0.636	1.145691604	0.946309301	0.218	0.082	0.3	0.668
3=-0.666900519144065	-0.282	1.147158981	0.946203465	0.623	0.082	0.705	-0.757
3=-0.666900519144065	0.005	1.149339772	0.947509318	0.953		0.953	0.57
3=-0.666900519144065	-0.798	1.149339772	0.947509318	0.03		0.03	-1.125
3=-0.666900519144065	-0.539	1.14785045	0.947219516	0.329	0.082	0.411	0.746
3=-0.666900519144065	-0.289	1.1508544	0.948469998	0.616	0.082	0.698	0.646
3=-0.666900519144065	-0.804	1.149339772	0.947509318	0.023		0.023	-1.291
3=-0.666900519144065	-0.262	1.149630145	0.947683193	0.647	0.082	0.729	-0.324
3=-0.666900519144065	-0.385	1.149339772	0.947509318	0.505	0.082	0.587	0.308
3=-0.666900519144065	0.019	1.149339772	0.947509318	0.969		0.969	-0.447
3=-0.666900519144065	-0.305	1.147032285	0.946092239	0.596	0.082	0.678	0.922
3=-0.666900519144065	-0.775	1.149339772	0.947509318	0.057		0.057	0.208
3=-0.666900519144065	-0.451	1.149216509	0.947291593	0.428	0.082	0.51	-1.576
3=-0.666900519144065	-0.582	1.150473081	0.947729844	0.278	0.082	0.36	0.843
3=-0.666900519144065	0.038	1.149339772	0.947509318	0.991		0.991	-0.487
3=-0.666900519144065	-0.3	1.149824817	0.947816966	0.603	0.082	0.685	0.63
3=-0.666900519144065	-0.394	1.149339772	0.947509318	0.495	0.082	0.577	-0.115
3=-0.666900519144065	-0.821	1.149339772	0.947509318	0.004		0.004	-1.071
3=-0.666900519144065	-0.352	1.149339772	0.947509318	0.543	0.082	0.625	-0.04
3=-0.666451614101533	-0.689	1.152273394	0.948474294	0.155	0.082	0.237	0.372
3=-0.666900519144065	0.004	1.149339772	0.947509318	0.952		0.952	-0.353
3=-0.666900519144065	-0.553	1.14869317	0.947383498	0.312	0.082	0.394	0.866
3=-0.6640417557013011	-0.698	1.153628121	0.948914965	0.143	0.082	0.225	0.748
3=-0.666900519144065	-0.814	1.149339772	0.947509318	0.012		0.012	-1.425
3=-0.666900519144065	-0.28	1.149833753	0.947812682	0.626	0.082	0.708	-0.191
3=-0.666900519144065	-0.441	1.149342759	0.947514593	0.44	0.082	0.522	-1.637
3=-0.666900519144065	-0.003	1.149339772	0.947509318	0.944		0.944	-0.254
3=-0.666900519144065	-0.278	1.147665923	0.94650702	0.628	0.082	0.71	-0.805
3=-0.666900519144065	-0.335	1.146516321	0.945718492	0.562	0.082	0.644	-0.106
3=-0.6661769168581735	-0.702	1.153872759	0.949000384	0.139	0.082	0.221	-0.033
3=-0.666900519144065	-0.611	1.152240459	0.948073752	0.244	0.082	0.326	-0.495
3=-0.666900519144065	0.036	1.149339772	0.947509318	0.989		0.989	0.591
3=-0.666900519144065	-0.093	1.149339772	0.947509318	0.841	0.082	0.923	1.561
3=-0.6680714984302639	-0.654	1.148187433	0.947131601	0.196	0.082	0.278	-1.496
3=-0.666900519144065	-0.822	1.149339772	0.947509318	0.003		0.003	-0.143
3=-0.666900519144065	-0.027	1.149339772	0.947509318	0.916		0.916	0.361
3=-0.666900519144065	-0.272	1.148350912	0.94691719	0.634	0.082	0.716	-0.776
3=-0.666900519144065	-0.298	1.150018595	0.947939874	0.605	0.082	0.687	0.55
3=-0.666900519144065	-0.844	1.149339772	0.947509318	-0.023		-0.023	-1.064
3=-0.6668543724548371	-0.669	1.149827128	0.947669627	0.178	0.082	0.26	0.831
3=-0.6677056723187157	-0.658	1.148686278	0.947295114	0.191	0.082	0.273	-1.74
3=-0.666900519144065	-0.007	1.149339772	0.947509318	0.94		0.94	-0.702
3=-0.666900519144065	-0.294	1.15043172	0.948201906	0.611	0.082	0.693	-0.159
3=-0.6668859712917137	-0.668	1.149641895	0.947608697	0.18	0.082	0.262	-0.067
3=-0.664494532550945	-0.693	1.152996564	0.948707952	0.15	0.082	0.232	-1.616
3=-0.666900519144065	-0.38	1.149339772	0.947509318	0.511	0.082	0.593	-0.444

3=-0.666900519144065	-0.811	1.149339772	0.947509318	0.015		0.015	-0.299
3=-0.666900519144065	-0.285	1.149254553	0.947456983	0.62	0.082	0.702	0.452
3=-0.666900519144065	-0.446	1.149285445	0.947413358	0.435	0.082	0.517	-1.735
3=-0.666900519144065	0.037	1.149339772	0.947509318	0.99		0.99	-0.901
3=-0.666900519144065	-0.563	1.149340087	0.947509379	0.3	0.082	0.382	0.436
3=-0.666900519144065	0.006	1.149339772	0.947509318	0.955		0.955	-1.118
3=-0.666900519144065	-0.393	1.149339772	0.947509318	0.496	0.082	0.578	-1.113
3=-0.6668686104344863	-0.668	1.149741226	0.947641371	0.179	0.082	0.261	-0.492
3=-0.666900519144065	-0.29	1.146152542	0.945600811	0.613	0.082	0.695	-1.358
3=-0.666900519144065	-0.76	1.149339772	0.947509318	0.074		0.074	-1.392
3=-0.666900519144065	-0.305	1.149313196	0.947492461	0.597	0.082	0.679	-0.308
3=-0.666900519144065	-0.804	1.149339772	0.947509318	0.024		0.024	-0.901
3=-0.666900519144065	-0.562	1.149282014	0.947498079	0.301	0.082	0.383	0.02
3=-0.666900519144065	-0.388	1.149339772	0.947509318	0.502	0.082	0.584	-0.301
3=-0.666900519144065	0.042	1.149339772	0.947509318	0.996		0.996	-0.29
3=-0.6672668622780997	-0.649	1.147387927	0.946867284	0.202	0.082	0.284	-0.037
3=-0.668211826270766	-0.653	1.147998679	0.947069731	0.198	0.082	0.28	-1.884
3=-0.666900519144065	0.017	1.149339772	0.947509318	0.967		0.967	-0.864
3=-0.666900519144065	-0.286	1.149118798	0.947373613	0.619	0.082	0.701	0.248
3=-0.666900519144065	-0.437	1.149397514	0.94761131	0.445	0.082	0.527	-1.802
3=-0.666900519144065	-0.758	1.149339772	0.947509318	0.077		0.077	-1.092
3=-0.666900519144065	-0.258	1.150068389	0.947945612	0.651	0.082	0.733	-0.925
3=-0.666900519144065	-0.33	1.146982092	0.946013916	0.568	0.082	0.65	-0.076
3=-0.666900519144065	-0.817	1.149339772	0.947509318	0.009		0.009	-1.032
3=-0.666900519144065	-0.556	1.148889527	0.947421706	0.309	0.082	0.391	0.295
3=-0.666900519144065	-0.649	1.149339772	0.947509318	0.201	0.082	0.283	1.228
3=-0.666900519144065	-0.034	1.149339772	0.947509318	0.908		0.908	-0.822
3=-0.6666346347098115	-0.68	1.151128305	0.948097632	0.166	0.082	0.248	0.135
3=-0.6647083292635076	-0.691	1.152700251	0.948610825	0.152	0.082	0.234	-1.868
3=-0.666900519144065	0.027	1.149339772	0.947509318	0.979		0.979	-0.01
3=-0.666900519144065	-0.298	1.147796151	0.946561346	0.604	0.082	0.686	0.445
3=-0.666900519144065	-0.438	1.149379206	0.947578972	0.444	0.082	0.526	-1.828
3=-0.666900519144065	-0.767	1.149339772	0.947509318	0.066		0.066	-1.311
3=-0.666900519144065	-0.269	1.149339772	0.947509318	0.638	0.082	0.72	-0.295
3=-0.666900519144065	-0.26	1.149876865	0.947830928	0.649	0.082	0.731	-0.979
3=-0.666900519144065	-0.79	1.149339772	0.947509318	0.039		0.039	-1.137
3=-0.666900519144065	-0.285	1.151253381	0.94872306	0.621	0.082	0.703	0.031
3=-0.666900519144065	-0.023	1.149339772	0.947509318	0.921		0.921	-1.087
3=-0.666900519144065	-0.533	1.149339772	0.947509318	0.335	0.082	0.417	0.238
3=-0.666900519144065	-0.004	1.149339772	0.947509318	0.943		0.943	-0.078
3=-0.666900519144065	-0.57	1.149339772	0.947509318	0.293	0.082	0.375	0.298
3=-0.666900519144065	-0.365	1.149339772	0.947509318	0.528	0.082	0.61	-0.261
3=-0.666900519144065	-0.78	1.149339772	0.947509318	0.052		0.052	-0.698
3=-0.6672761591349027	-0.649	1.147332069	0.94684891	0.202	0.082	0.284	0.194
3=-0.666900519144065	-0.802	1.149339772	0.947509318	0.025		0.025	-1.207
3=-0.666900519144065	-0.314	1.148510486	0.946983328	0.587	0.082	0.669	0.02
3=-0.666900519144065	-0.553	1.148698559	0.947384547	0.312	0.082	0.394	0.562
3=-0.666900519144065	0	1.149339772	0.947509318	0.948		0.948	-0.907
3=-0.666900519144065	-0.361	1.149339772	0.947509318	0.533	0.082	0.615	-0.873
3=-0.6669005191440648	-0.389	1.149339772	0.947509318	0.5	0.082	0.582	-1.078
3=-0.666900519144065	0.014	1.149339772	0.947509318	0.963		0.963	0.129
3=-0.666900519144065	-0.268	1.148847818	0.947214737	0.639	0.082	0.721	-0.838
3=-0.6669005191440649	-0.256	1.149339772	0.947509318	0.654	0.082	0.736	-1.028
3=-0.666900519144065	-0.329	1.149339772	0.947509318	0.57	0.082	0.652	-0.845
3=-0.666900519144065	-0.37	1.149339772	0.947509318	0.523	0.082	0.605	-0.184
3=-0.666900519144065	-0.749	1.149339772	0.947509318	0.087		0.087	-1.398
3=-0.666900519144065	-0.39	1.149339772	0.947509318	0.499	0.082	0.581	-0.042
3=-0.666900519144065	-0.264	1.151543023	0.948862383	0.645	0.082	0.727	0.576
3=-0.666900519144065	-0.41	1.149731409	0.948201081	0.477	0.082	0.559	-1.777
3=-0.666900519144065	-0.561	1.149214791	0.947484998	0.302	0.082	0.384	0.46
3=-0.666900519144065	-0.808	1.149339772	0.947509318	0.019		0.019	-1.197
3=-0.666900519144065	-0.291	1.150643145	0.948336006	0.613	0.082	0.695	0.472
3=-0.6669005191440649	-0.317	1.149339772	0.947509318	0.583	0.082	0.665	-0.658
3=-0.6669005191440649	-0.328	1.149339772	0.947509318	0.57	0.082	0.652	-0.615
3=-0.6707188642073036	-0.625	1.144670106	0.945978682	0.23	0.082	0.312	-1.865
3=-0.666900519144065	-0.796	1.149339772	0.947509318	0.032		0.032	-1.198
3=-0.6669005191440651	-0.297	1.149339772	0.947509318	0.606	0.082	0.688	-0.822
3=-0.6669005191440649	-0.392	1.149339772	0.947509318	0.497	0.082	0.579	-0.791

0.722
0.491
0.659